

AD-A062 344

AIR FORCE GLOBAL WEATHER CENTRAL OFFUTT AFB NEBR
JET-STREAM ANALYSIS AND TURBULENCE FORECASTING.(U)
MAR 76 M C HOLCOMB
AFGWC-TM-76-1

F/G 4/2

UNCLASSIFIED

NL

1 OF 2
AD A062344



LEVEL II

AFGI



AD A062344

DDC FILE COPY



JET-STREAM ANALYSIS AND TURBULENCE FORECAST

by
Michael C. Holcomb, Captain

MARCH 1976

Approved for Public Release; Distribution Unlimited

**UNITED STATES AIR FORCE
AIR WEATHER SERVICE (M)
AIR FORCE GLOBAL WEATHER
OFFUTT, AIR FORCE BASE, NEBRASKA**

78 12 18

Review and Approval Statement

This report approved for public release. There is no objection to unlimited distribution of this report to the public at large, or by Defense Documentation Center (DDC) to the National Technical Information Service (NTIS).

This technical report has been reviewed and is approved for publication.

FOR THE COMMANDER

Donald C. Hansen

DONALD C. HANSEN, Colonel, USAF
Chief, Studies and Analysis

JET-STREAM ANALYSIS
AND
TURBULENCE FORECASTING

Michael E. Heacock, Capt, USAF

MARCH 1976

Approved for Public Release; Distribution Unlimited

AIR FORCE GLOBAL WEATHER CENTRAL
AIR WEATHER SERVICE (AWS)
UNITED STATES AIR FORCE

88-12 13 014

143300AQA

DDC LIFE COLA

UNCLASSIFIED

SECURITY CLASSIFICATION OF THIS PAGE (When Data Entered)

REPORT DOCUMENTATION PAGE		READ INSTRUCTIONS BEFORE COMPLETING FORM
1. REPORT NUMBER (14) AFGWC-TM-76-1	2. GOVT ACCESSION NO.	3. RECIPIENT'S CATALOG NUMBER
4. TITLE (and Subtitle) (16) Jet-Stream Analysis and Turbulence Forecasting		5. TYPE OF REPORT & PERIOD COVERED (9) Final Repts
7. AUTHOR(s) (10) Michael C. Holcomb, Capt, USAF		6. PERFORMING ORG. REPORT NUMBER
9. PERFORMING ORGANIZATION NAME AND ADDRESS Air Force Global Weather Central Offutt AFB, Nebraska 68113		8. CONTRACT OR GRANT NUMBER(s)
11. CONTROLLING OFFICE NAME AND ADDRESS Air Force Global Weather Central Offutt AFB, Nebraska 68113		10. PROGRAM ELEMENT, PROJECT, TASK AREA & WORK UNIT NUMBERS
14. MONITORING AGENCY NAME & ADDRESS (if different from Controlling Office)		12. REPORT DATE (11) Mar 76
		13. NUMBER OF PAGES 101
		15. SECURITY CLASS. (of this report) Unclassified
		15a. DECLASSIFICATION/DOWNGRADING SCHEDULE
16. DISTRIBUTION STATEMENT (of this Report) Approved for public release; distribution unlimited (12) 108 p.		
17. DISTRIBUTION STATEMENT (of the abstract entered in Block 20, if different from Report)		
18. SUPPLEMENTARY NOTES		
19. KEY WORDS (Continue on reverse side if necessary and identify by block number) Meteorology Atmospheric turbulence Jet streams		
20. ABSTRACT (Continue on reverse side if necessary and identify by block number) This Technical Memorandum summarizes the synoptic techniques available to USAF weather officers and technicians to forecast turbulence. The report is based on the classification scheme of Sorensen along with some later studies.		

DD FORM 1 JAN 73 1473

EDITION OF 1 NOV 65 IS OBSOLETE

UNCLASSIFIED

111 SECURITY CLASSIFICATION OF THIS PAGE (When Data Entered)

403 677

REPORT DOCUMENTATION PAGE	
1. REPORT NUMBER	2. GOVT ACCESSION NO.
3. REPORT TYPE AND DATES COVERED	4. AUTHOR(s)
5. PERFORMING ORG. REPORT NUMBER	6. CONTRACT OR GRANT NUMBER(s)
7. AUTHORING ORG. NAME AND ADDRESS	8. PERFORMING ORG. NAME AND ADDRESS
9. CONTROLLING ORG. NAME AND ADDRESS	10. PROGRAM ELEMENT PROJECT TASK AREA & WORK UNIT NUMBERS
11. MONITORING AGENCY NAME & ADDRESS (if different from Controlling Office)	12. SECURITY CLASS. (if this report)
13. DISTRIBUTION STATEMENT (of this Report)	
14. DISTRIBUTION STATEMENT (of the abstract entered in Block 20, if different from Report)	
15. SUPPLEMENTARY NOTES	
16. KEY WORDS (Continue on reverse side if necessary; use block numbering)	
17. ABSTRACT (Continue on reverse side if necessary; use block numbering)	

TABLE OF CONTENTS

	Page
Chapter 1. Introduction.	1
Chapter 2. The Descriptive Side of Turbulence.	2
2.1. Resolving Turbulent Motions	2
2.2. Dimensions of Turbulent Motions	3
2.3. Turbulence Intensity Estimates.	5
2.4. The Distribution of Turbulence Reports.	5
Continental United States	6
Overseas Routes with a High Density of Reports.	7
Data-Poor Areas	7
Data Voids.	7
2.5. The Probability of Turbulence Occurring in Flight	7
2.6. Pilot Reports and Actual Conditions	8
Data Coverage	8
Aircraft Type and Mission	8
Subjectivity.	8
Avoidance	8
The Nature of the Turbulence Field.	8
Chapter 3. Fundamental Concepts for Jet Analysis	10
3.1. Introduction.	10
3.2. The Definition of a Jet Stream.	10
3.3. Depicting a Jet Stream.	10
3.4. Divergence.	11
3.5. Vorticity	12
3.6. Gradient Flow	12
3.7. Stability	14
3.8. Energy.	14
Internal Energy	14
Kinetic Energy.	14
Potential Energy.	15
Latent Heat	15
3.9. Isentropic Analysis	15
Chapter 4. The Role of Jet Streams in the General Circulation.	17
4.1. Introduction.	17
4.2. The Hemispheric Meridional Circulation.	17
4.3. Criteria to Identify the Major Jet Streams.	19
The Polar Jet Stream.	20
The Subtropical Jet Stream.	21
4.4. Interacting Polar and Subtropical Jet Streams	23
Converging Polar and Possible Subtropical Jet Stream Ahead of Trailing Long-Wave Trough.	26
Converging Jet Streams Over a Low-Level Trough.	28
A Double Polar Jet Stream	28
Chapter 5. A Hemispheric Analysis of Jet-Stream Flow	34
5.1. Hemispheric Analysis.	34
5.2. A Closer Look at Portions of the Hemisphere	40
Chapter 6. Jet Development and Turbulence.	48
6.1. Introduction.	48
6.2. Divergence Fields	48
6.3. Vorticity Fields.	53
6.4. Energy Transformations.	56
6.5. The Initiation and Maintenance of Turbulence	57
6.6. Gravity Waves	60
6.7. Characteristics of Kelvin-Helmholtz Waves	61
6.8. Billow Clouds on Satellite Pictures	63
Chapter 7. Synoptic Patterns with High Turbulence Potential.	68
7.1. Introduction.	68
7.2. Increasing Horizontal Temperature Gradient Through Cold-Air Advection in Cyclone-Scale Waves.	69
7.3. Increasing Horizontal Temperature Gradient Through Warm-Air Advection in Cyclone-Scale Waves.	73
7.4. Increasing Horizontal Temperature Gradients with Short Waves.	76
7.5. Decreasing Stability in the Vicinity of the Jet Exit.	81
7.6. Turbulence Potential Within Tilting Troughs and Ridges.	87

TABLE OF CONTENTS (Cont'd)

	Page
7.7. Turbulence in Polar and Subtropical Jet-Stream Interactions	91
7.8. Turbulence in Sharp Anticyclonic Curvature.	94
7.9. Examples of Low-Level Turbulence in Possible Lee Waves.	95
Frontal Systems and Anticyclones.	95
Warm-Air Advection at Low Levels.	95
Turbulence on the Lee of Major Ranges in the Absence of Strong Flow	96
Chapter 8. Conclusion.	98
REFERENCES AND BIBLIOGRAPHY.	99

LIST OF ILLUSTRATIONS

Figure 1. Commonly-Observed Turbulent Motions	1
Figure 2. Examples of the Relation Between Horizontal Eddy Diameter and Wavelength to Derive a Mean Wavelength.	3
Figure 3. Frequency Ranges of Turbulence Important to Aircraft Design and Physiology.	4
Figure 4. Dimensions of Turbulent Components Important to Aviation.	4
Figure 5. Frequency of Civil Airline Flights During the Day, taken from AFGWC Records	6
Figure 6. Jet-Stream Depictions and Velocity Profiles	11
Figure 7. Total Divergence and Its Components	12
Figure 8. Gradient Balance and Its Applications	13
Figure 9. A Northern Hemisphere Meridional Circulation Model for Winter	17
Figure 10. Mean January Meridional Temperature Field for 147.5°E	18
Figure 11. Mean July Meridional Temperature Field for 147.5°E.	20
Figure 12. The Normal Relationship of Jet Streams to Tropopause Leafs, Including Leaf Temperature Ranges	20
Figure 13. Polar Jet Stream.	21
Figure 14. Cross Section of Polar Jet Stream, 0000 GMT, 28 Nov 73.	22
Figure 15. Subtropical Jet Stream.	22
Figure 16. Cross Section of Subtropical Jet Stream, 1200 GMT, 21 Mar 74.	23
Figure 17. Average Winter Tracks of the Polar and Subtropical Jet Streams	24
Figure 18. Basic Polar-Subtropical Jet-Stream Intersections.	24
Figure 19. Polar Jet Stream Ahead of a "Trailing Trough"	25
Figure 20. Cross Section of Polar Jet Stream, 1200 GMT, 1 Apr 74	26
Figure 21. Lapse Rate and Speed Profile for Sendai, Japan, the Station Under the Polar Jet Core.	27
Figure 22. Subtropical Jet Stream Overlying a "Short" Long-Wave Trough	27
Figure 23. Cross Section of Subtropical Jet Stream, 1200 GMT, 18 Feb 75.	28
Figure 24. Lapse Rate and Speed Profile for Kagoshima, Japan, Under the Subtropical Jet-Stream Core and Jet Front	29
Figure 25. Lapse Rate and Speed Profile for Naha, Okinawa, Showing Low- Level Inversion	29
Figure 26. Double Polar Jet Stream, 300 mb	30
Figure 27. Isotach Analysis of Double Polar Jet Stream	30
Figure 28. Double Polar Jet Stream, 200 mb	31
Figure 29. Cross Section of Double Polar Jet Stream.	32
Figure 30. Polar Jet Stream with Multiple Tropopause	32
Figure 31. Cross Section of Polar Jet Stream with Multiple Tropopause.	33
Figure 32. Lapse Rate and Speed Profile for Monett, Missouri, Under the Multiple Tropopause	33
Figure 33. Surface and 300-mb Analysis Composite	34
Figure 34. Maximum Wind Analysis	35
Figure 35. An Example of the Thermal Wind Relationship	36
Figure 36. Identifying Jet Streams from the 200-mb Temperature Field	37
Figure 37. Relating Fronts and Maximum Wind Lines.	38
Figure 38. Relating Maximum Wind Lines to Split Flow and Frontal Systems	39

LIST OF ILLUSTRATIONS (Cont'd)

		Page
Figure 39.	300-mb Wind Analysis, Western United States	40
Figure 40.	Cross Section Through International Falls, Minnesota to Grand Junction, Colorado.	41
Figure 41.	Cross Section Through Peoria, Illinois to Del Rio, Texas.	41
Figure 42.	300-mb Wind Analysis, Eastern United States	42
Figure 43.	Cross Section Through Dayton, Ohio to Key West, Florida	42
Figure 44.	300-mb Wind Analysis, North Atlantic-Europe	43
Figure 45.	Cross Section Through Stavanger, Norway to Petrozavodsk, Russia.	44
Figure 46.	Cross Section Through Poznan, Poland to Moscow, Russia.	44
Figure 47.	300-mb Wind Analysis, Western Pacific-Japan	45
Figure 48.	Cross Section Through Teng Kou Nau Pao, China to Yulin, China	46
Figure 49.	Cross Section Through Harbin, China to Minamidaitojima, Japan	46
Figure 50.	Cross Section Through Aleksandrovsk, Sakhalin to Tatenno, Japan	47
Figure 51.	Schemes for Divergence and Vertical Velocity Circulations	49
Figure 52.	Upper-Level Analysis of Synoptic Pattern Used in Divergence and Vorticity Calculations in Sections 6.3 and 6.4 with Surface Fronts Included.	50
Figure 53.	Lower Tropospheric Divergence Field	51
Figure 54.	Upper Tropospheric Divergence Field	52
Figure 55.	Jet-Stream Divergence Pattern and Possible Meridional Circulation at the Jet Entrance and Exit	53
Figure 56.	Middle Tropospheric Vorticity Field	54
Figure 57.	Mean January Meridional Temperature Field for 147.5°E with Corresponding Potential Temperature Field	55
Figure 58.	Mean July Meridional Temperature Field for 147.5°E with Corresponding Potential Temperature Field.	55
Figure 59.	Turbulence Potential Nomogram	59
Figure 60.	Areas of High Turbulence Potential in Lee Waves and Jet Streams	59
Figure 61.	Scheme of Scorer's Demonstration.	60
Figure 62.	Kelvin-Helmholtz Waves Superimposed on Stable Gravity Waves in a Shear Zone	63
Figure 63.	Warm Occlusion in Northeast China	63
Figure 64.	Two Schematics of the Northeast China Occlusion	64
Figure 65.	Detail of Billow Clouds in the Northeast China Occlusion.	65
Figure 66.	Cloud Billows East of an Upper-Level Low.	66
Figure 67.	Cloud Billows in an Anticyclonically-Curved Cirrus Middle-Cloud Shield.	66
Figure 68.	Transverse Banding in Thin Cirrus	67
Figure 69.	Jet Cirrus Shield Over Japan with a Magnified View Showing Small Kelvin-Helmholtz Waves.	67
Figure 70.	The Effect of Superimposing a Warm or Cold Pool of Air on a Zonal Temperature Gradient.	69
Figure 71.	300-mb Analysis of Trough with Turbulence in Georgia Associated with Cold-Air Advection.	70
Figure 72.	Composite of Horizontal Temperature Gradient Over Georgia	71
Figure 73.	Cross Section of Polar Jet Stream in Cold-Air Advection	72
Figure 74.	300-mb Analysis of Ridge with Turbulence Over the Northeast Associated with Warm-Air Advection.	73
Figure 75.	Composite of Horizontal Temperature Gradient Over the Northeast.	74
Figure 76.	Cross Section of Polar Jet Stream in Warm-Air Advection, Dayton, Ohio to Cape Hatteras, North Carolina	75
Figure 77.	Cross Section of Polar Jet Stream in Warm-Air Advection, Maniwaki, Quebec to Ocean Station Vessel Hotel.	75
Figure 78.	250-mb Analysis Approximating the Jet Core.	76
Figure 79.	200-mb Thermal Field.	77
Figure 80.	500-mb Analysis with Cold-Air Advection into a Refueling Area	78
Figure 81.	300-mb Analysis Showing Maximum Wind Line Over Refueling Area	78
Figure 82.	Cross Section Through Refueling Area.	79
Figure 83.	500-mb Analysis of Warm-Air Advection with a Short-Wave Ridge	79

LIST OF ILLUSTRATIONS (Cont'd)

	Page
Figure 84. 300-mb Maximum Wind Analysis.	80
Figure 85. Reports of Turbulence in a Short-Wave Ridge	80
Figure 86. Cross Section Through Short-Wave Ridge.	81
Figure 87. 300-mb Analysis of Jet-Exit Region.	82
Figure 88. 300-mb Analysis of Jet Exit 24 Hours Later.	83
Figure 89. 200-mb Analysis of Jet-Exit Region.	84
Figure 90. Turbulence Reports Near the Tropopause and Jet Exit	85
Figure 91. Cross Section Through Polar Jet Streak.	86
Figure 92. Sounding Through Strong Jet Streak.	87
Figure 93. 300-mb Analysis of Tilted Trough Case	88
Figure 94. 200-mb Analysis of Tilted Trough Case	89
Figure 95. Turbulence Reports Above 26,000 Feet Near the Confluence of Two Jet Streams	89
Figure 96. 300-mb Analysis of Tilted Ridge and Shear Line.	90
Figure 97. 200-mb Analysis of Tilted Ridge Case.	90
Figure 98. Turbulence Reports in a Tilted Ridge Case	91
Figure 99. Turbulence Reports in an Area of Polar-Subtropical Jet Stream Intersection Near Hawaii.	92
Figure 100. 300-mb Analysis of Polar-Subtropical Jet Stream Intersection in the Caribbean.	93
Figure 101. 200-mb Analysis of Polar-Subtropical Jet Stream Intersection in the Caribbean.	93
Figure 102. An Example of Turbulence in a Ridge with Sharp Anticyclonic Curvature	94
Figure 103. Turbulence in Low-Level Jet Flow Over Rough Terrain	95
Figure 104. 850-mb Analysis of Warm Tongue of Air in the Lee of the Rockies	96
Figure 105. 700-mb Analysis of Turbulence in the Lee of the Rockies	97

LIST OF TABLES

Table 1. Turbulence Intensity Criteria	5
Table 2. Turbulence Reports Over Georgia from 0900 GMT 8 December 1973 to 0300 GMT 9 December 1973	72
Table 3. Turbulence Reports Over the Northeast from 0900 GMT 8 Decem- ber 1973 to 0300 GMT 9 December 1973.	74
Table 4. Reports of Turbulence Within a Jet Front.	77

ACCESSION for	
NTIS	White Section <input checked="" type="checkbox"/>
DDC	Buff Section <input type="checkbox"/>
UNANNOUNCED	<input type="checkbox"/>
JUSTIFICATION	
BY	
DISTRIBUTION/AVAILABILITY	
Dist.	COPIES
A	

Chapter 1

INTRODUCTION

Those few forecasters who predict clear-air turbulence (CAT) work within the confines of a small, specialized, and somewhat obscure field of meteorology. This field's primary application is towards safe aircraft operations, not the general public, and is outside the realm of popular forecasting.

CAT forecasting is barely out of its primitive stages. It, like so many other forecasting objectives, could not be seriously pursued until the global upper-air reporting network was established after World War II. Unfortunately, while many areas of forecasting benefited from the accumulating data, CAT failed to directly reveal itself, being a secondary phenomenon too small to show up in a coarse data array. For years the CAT study routine was to note pilot reports in certain synoptic patterns and possibly follow up on them with aircraft penetrations, an effective though risky method of limited scope. By 1960 there were still too few findings to support a thorough discussion of CAT forecasting and pioneering works feel short of being comprehensive.

In 1964, Sorenson [44] of United Air Lines was the first to present a thorough classification of turbulence-prone synoptic features. He compiled enough case studies of CAT in certain patterns to discern trends. His report classified them and presented case studies of each, along with meteorological explanations and verifications. This work has withstood the severe tests of time and it serves as the nucleus of this report. What must be added to it to provide a training text is to treat the nature of CAT itself and to discuss how it fits into the nature of things.

Air Force Global Weather Central (AFGWC) has the mission to forecast CAT over the entire Northern Hemisphere. A thorough training program is essential to indoctrinate incoming forecasters into this branch of forecasting. In view of the absence of any CAT forecasting text upon which to base a training program, this report is offered to fill the need. It is written with three objectives in mind.

First, the interactions of Man with CAT must be introduced to show how the customer (pilot) experiences and views turbulence (Chapter 2). Second, CAT must be discussed at length from its role in the earth's general circulation to its physical structure and that of its preferred environment. This requires a study of jet streams and their developmental processes, a topic in itself (Chapters 3 to 6). Last, Sorenson's pattern classification must be presented, modified as necessary, and tested with case studies (Chapter 7). It is here that the forecaster can apply what he has learned.

The text is deliberately detailed to hopefully answer all questions and has been kept nontechnical where possible in order to be meaningful to all. This work should serve as the basis upon which to develop an effective, personal forecast routine.

THE DESCRIPTIVE SIDE OF TURBULENCE

2.1. Resolving Turbulent Motions. Laboratory pictures of turbulent flow show a field of eddy-like motions that may be superimposed on an undulating basic flow. This suggests two components to turbulence that might have meaning in forecasting, eddies and waves. Figure 1 shows how these components might appear when waves are generated within a fluid and how they may be resolved in certain kinds of atmospheric conditions.

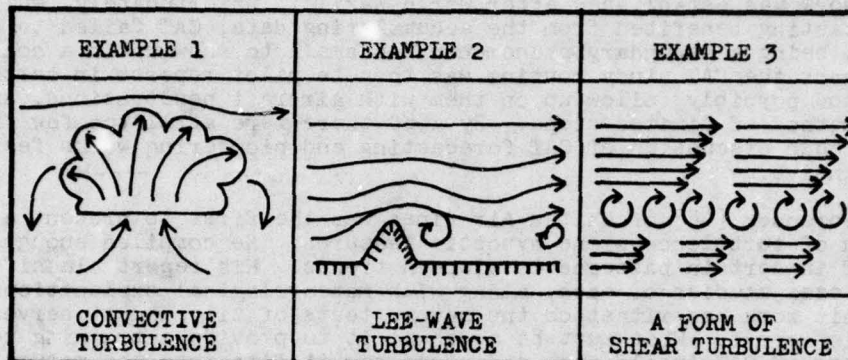


Figure 1. Commonly-Observed Turbulent Motions.

Example 1 of the figure is a model of convective turbulence which is seen in weather as ascending dry thermals, cumuliiform clouds, and certain high-cloud layers cooled to the point of instability by radiational heat losses. Convection is most common in weak flow, so only the eddy component is usually prominent. Convection occurs because of unequal surface heating and the subsequent redistributions of heat to restore thermal equilibrium. It is typically very widespread over vast areas of the lower atmosphere in fair weather, so much so that it is familiar to pilots and forecasters alike, and the need for operational forecasting is slight. However, convection in association with thunderstorms is of critical importance. At AFGWC moderate or greater turbulence is expressly implied in and about all forecast thunderstorms, but is not forecast separately.

Example 2 depicts lee turbulence caused through the interactions of wind and terrain. Both eddy and wave components are likely to be important. Eddies frequent the areas near rough terrain and form rotors in the lee of larger mountains, while waves occur aloft over mountains and constitute the oscillating flow on the lee side and some distance downwind. Numerical simulations of flow over mountain ranges in computer analysis have shown certain parameters to be critical to the development of strong lee-wave regimes. They include tall, narrow cross-sectional mountain profiles, perhaps steepest on the lee side, a flow approximately normal to the ranges, and synoptic conditions with increasing wind speed and decreasing stability with height. Lee turbulence is typically a forecast problem below 20,000 feet in moderate flow over mountains, but if wave energy can be propagated upward, waves will build into the better-known mountain-wave regime. In general, the potential for lee turbulence will be increased whenever there is jet flow over mountainous areas or when intense storms approach the windward side of the ranges.

Lee-turbulence forecasting requires two basic decisions, a choice of "yes-no" for potential and between the simple lee wave or the dangerous mountain-wave regimes. The energy processes which govern wave development are too complex for turbulence forecasters to efficiently discern over the world without aid, and at AFGWC they

follow Standard Operating Procedures to insure effective forecasting. An automated turbulence potential program is provided for the Northern Hemisphere and specific procedures are set up to use synoptic maps and observations correctly when estimating mountain-wave potential. Lee turbulence is typically a problem of the winter months.

Example 3 shows a major form of shear turbulence which develops in flow, changing speed so rapidly in a given direction that smooth flow is no longer dynamically possible. Shearing, in general, occurs both vertically and horizontally, including both speed and directional changes in the wind. Although turbulence potential may be significant in any combination of the above factors, the overwhelmingly important form in forecasting is vertical speed shear (shown in the example). Turbulence caused by vertical speed shear is a major forecast problem in jet-stream flow both below the jet core and above, in the vicinity of the tropopause. This type of trigger generates most of the forecasts above 10,000 feet at AFGWC.

2.2. Dimensions of Turbulent Motions. Limits to the size of turbulent eddies and waves that are of interest to forecasting cannot be specifically determined because their dimensions depend upon aircraft operations, including such variables as airplane speed and design, as well as a pilot's interpretation of turbulence. Nevertheless, it is possible to deduce the extent of a useful range of sizes by referencing studies that equate dimensions to aircraft and human responses. However, in order to do this it will be necessary to assume that fields of turbulence have an orderly structure so that eddy diameters and wavelengths of interest may be averaged and measurements taken. Atmospheric turbulence fields are not orderly. This assumption is acceptable because it defines a useful range of sizes and is not a prerequisite for actual forecasting.

Figure 2 shows how eddy diameters and wavelengths may be measured. The interrelationship between eddies and waves shown in Figure 1 may be used to approximate a mean turbulence wavelength which can then be applied to calculations to determine those wavelengths affecting man and machine. Of particular interest is the number of turbulence cycles, or "jolts" experienced in a given period of time, the definition of frequency. This quantity must be known before wavelength ranges can be determined. Frequency is often implied in pilot reports through such terms as gusts, drafts (including updrafts and downdrafts), waves, chop, and vibrations. Note that these terms apply consecutively to turbulence with increasing frequency but decreasing wavelength.

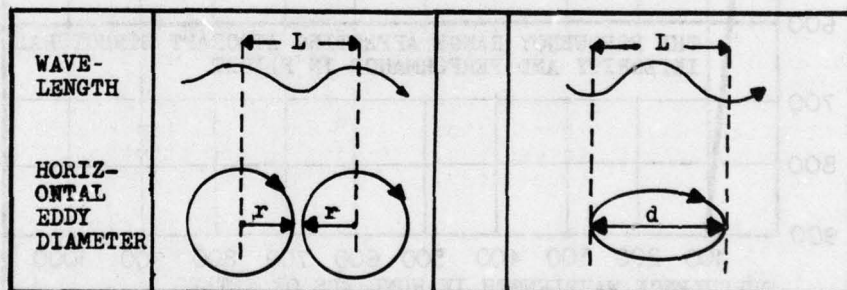


Figure 2. Examples of the Relation Between Horizontal Eddy Diameter and Wavelength to Derive a Mean Wavelength.

In this section, the range of frequencies associated with turbulence is based on a summary by Zbrozek [52], who combined the ranges affecting aircraft structural integrity (load and fatigue), performance in flight (stability and control), and two frequencies that appear to affect an unfavorable response in Man. These frequency ranges can only be general because of the wide variety of aircraft weights, designs, and speeds, as well as the complex responses of the human body, but they will serve to define a range of wavelengths sufficiently correct to give a clear picture of the sizes of turbulent eddies and waves. In Figure 3, a summary of frequencies from Zbrozek, the frequency range affecting aircraft most often is shown to be from 0.1 to 5 cycles per second, which is to say, 1 cycle in 10 seconds to 5 per second.

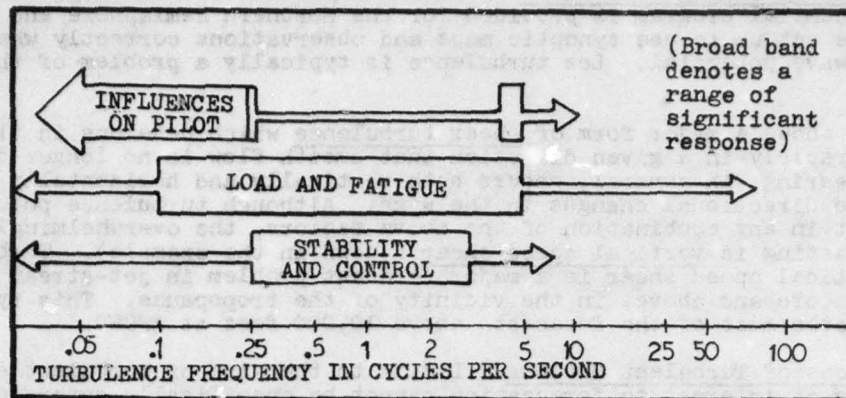


Figure 3. Frequency Ranges of Turbulence Important to Aircraft Design and Physiology.

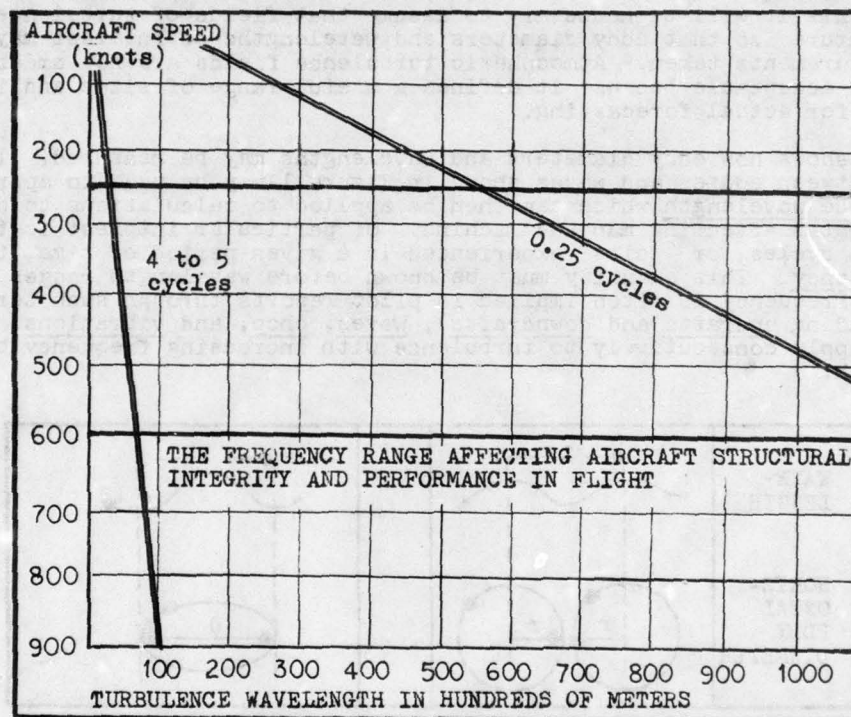


Figure 4. Dimensions of Turbulent Components Important to Aviation.

Though all frequencies of turbulence "affect" Man, two that appear to be noteworthy are at 0.25 cycles (1 per 4 seconds) and from 4 to 5 cycles per second. Zbrozek comments that the former appears to predispose people to airsickness, while the latter feels unusually uncomfortable. The cause of discomfort may be a harmonic response by human tissue to this rapid jolting. Note in the figure that the frequencies affecting Man are almost at the extremes of those affecting aircraft. There are also "influences on pilots" indicated at much lower frequencies in the figure, occurring with undulations perhaps too gradual to be called "turbulence." At this range, the general effects of rough weather begin to interfere with flying as well, so this range of influences will be omitted from further discussion.

Figure 4 shows turbulence frequency as a function of wavelength and aircraft speed. The "uncomfortable" turbulence of 4 to 5 cycles per second occurs with wavelengths under 100 meters for aircraft speeds up to 700 knots, while the "airsickness" cycle occurs with far greater wavelengths of 500 to 1300 meters for aircraft speeds of 250 to 600 knots, the usual operating range of large aircraft. In summary, turbulence wavelengths affecting Man and aircraft are on the order of tens and hundreds of meters and more, though less than 1 mile (1600 meters) for all but the fastest aircraft.

2.3. Turbulence Intensity Estimates. The correct determination of intensity is fundamentally important to turbulence forecasting because, beyond some lower limit, the phenomenon becomes hazardous to aircraft operations. The forecaster is expected to accurately state where, when, and how long turbulence will exceed minimum criteria, and by how much.

In 1956 and 1957, the NACA Subcommittee on Meteorological problems formulated definitions of turbulence intensity and established criteria for its determination. Both are summarized in Table 1.

Table 1. Turbulence Intensity Criteria.

Turbulence Effects	Turbulence Category			
	Light	Moderate	Severe*	Extreme
An Aircraft	Slight bumpiness	Moderate jolts, no loss of control	Moderate Altitude change, momentary loss of control	Tossed about, uncontrollable periods and possible damage
On People	Uncomfortable, seat belts advised	Thrown against belts, walking difficult	Violent thrusts, cannot walk about	---
On Objects	Unmoved	Move	Tossed about	---
Category	Airspeed Fluctuations		Vertical Motions	
Light	Under 15 knots		5 feet per second	
Moderate	15 to 25 knots		15 feet per second	
Severe	Over 25 knots		25 feet per second	
Extreme	---		Over 30 feet per second	

* Severe turbulence may be reported as "heavy." Extreme turbulence is considered rare except in thunderstorms.

Portions of the material above are available to pilots in Flight Information Publications (FLIP), but they tend to interpret intensity, often reporting between categories as in "light to moderate" and "moderate to severe." Pilots may not accept or otherwise follow the above intensity criteria when reporting because of their preoccupation with aircraft control.

2.4. The Distribution of Turbulence Reports. Turbulence forecasters tend to rely heavily upon pilot reports when trying to determine the potential intensity of suspect areas. When the forecast is for the Northern Hemisphere as it is at AFGWC, it becomes important to know when and where pilot reports may be expected. In this section, a general idea of the distribution of pilot reports over the hemisphere will be presented.

AFGWC forecasters have immediate access to incoming pilot reports through a series of three-hourly "CAT-AIREP" maps continually being compiled by weather observers. All usable reports are entered, along with wind and icing data. Moderate or stronger reports are verbally relayed to the forecaster. However, unless the forecaster knows the general distribution of data over the forecast area, he will have difficulty estimating the real meaning of positive (yes) or negative (none) data. Therefore, additional information on variations of data distributions with time and with certain aircraft is also necessary.

Experience has shown that the hemispheric distribution of pilot reports received at AFGWC falls into four general categories as follows:

a. Continental United States. A high density of data is typical but variations are likely, depending on the time of day and the state of the Nation's weather. A vast number of reports come from the civil airlines. These are mainly daytime and high-altitude reports. Near departure and destination points, reports are usually received by air traffic controllers. Ordinarily they cannot pass this information on. Most low-level pilot reports come from small private aircraft. Military pilot reports are usually thinly sprinkled over the country. In general, turbulence reports will be most frequent near large airports and heavily traveled airline routes. Data will be plentiful during the day and especially so wherever the weather is bad.

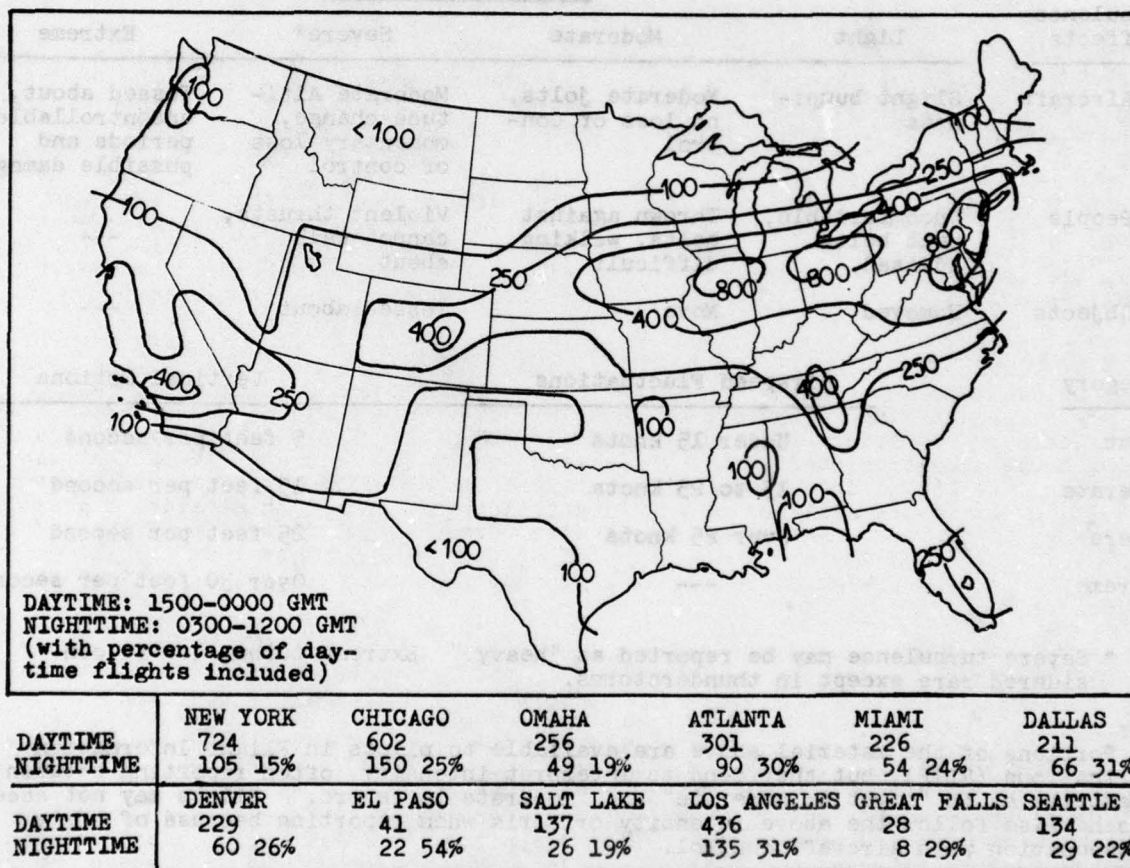


Figure 5. Frequency of Civil Airline Flights During the Day (1500-0000 GMT), taken from AFGWC Records.

Figure 5 is an estimate of the number of civil airline flights over the United States each day, the result of an informal data sampling taken at AFGWC in the late 1960's. It shows the concentration of flights across the country to major cities and stresses the difference in the number of flights between day and night. Since civil airline reports account for about three-fourths of all turbulence reports above 20,000 feet, it follows that much of the United States is going to appear relatively "turbulence free" to the unexperienced forecaster.

b. Overseas Routes with a High Density of Reports. Many turbulence reports may be expected on the major air routes across the North Atlantic Ocean from New England to Northern Europe, and again from the American Southwest to Hawaii. Many reports may be generated across the North Pacific from Japan through Alaska to the Pacific Northwest.

Almost all pilot reports occur from 25,000 to 41,000 feet and there is relatively little variation in density with weather and time of day when compared with the previous category. However, most airlines do not specifically mention turbulence unless it is moderate or greater in intensity. Their interest is in reporting winds. This fact, along with the obvious lack of terrain to further disturb the atmosphere, makes the ocean routes appear quite turbulence-free, which need not be so. Military aircraft regularly report turbulence.

c. Data-Poor Areas. Pilot reports generated in foreign countries are rare, unless they come from American military aircraft. There are no reporting networks. This includes Canada and Northern Europe at present.

There are other air routes across the oceans that irregularly generate a fair number of reports. These include routes from Hawaii westward to Guam, the Philippines, and Japan, and routes across the Central Atlantic to Southern Europe, particularly through the Azores.

d. Data Voids. Prominent voids in which pilot reports are rare include the Central North Pacific, Asia, Equatorial and Polar regions, and the Indian Ocean. Military flights across these areas do occur without notice, so forecasters must include them routinely in their search for regions of turbulence potential. It is advisable to discuss potential with upper-air analysts because synoptic maps are usually simplified or even incomplete by the lack of data in these areas.

2.5. The Probability of Turbulence Occurring in Flight. It is a fact that turbulence is most commonly associated with terrain effects and convection. When levels above 20,000 feet are considered by themselves, the frequency reports decrease sharply. Encountering turbulence at those higher levels could prove hazardous. Air Force Weather Technicians are taught in their CDC Course 25370 that only 3% of all flying hours are associated with turbulence above 20,000 feet and 75% of that was less than moderate in intensity. This unreferenced study is supported by a recent poll [8] by Lufthansa Airlines of 232 Flight Captains, each with at least 8 years experience in the air. After their estimates were averaged it was found that 6% of their time was spent in turbulence with 80% of that time in less than moderate intensity. This slightly high estimate may be due to the lack of a specific limit to altitude.

Lufthansa pilots made many more comments relevant to the subject of frequency. About 30% of all turbulence was attributed to thunderstorms and another 25% to terrain effects. This leaves 45% to fall under the general category of "clear-air turbulence." Pilots felt generally that CAT occurred unexpectedly and was often not forecast well, even though all knew of the problems involved in monitoring the forecast area for what is often an intermittent small-scale phenomenon. Most CAT encounters were due, in their estimation, to lee waves and jet streams (the former might be better grouped with terrain effects), and that periods of turbulence, in general, were of a few minutes duration. All pilots could recall at least one experience lasting an hour and two pilots recalled 8-hour ordeals. In such cases, turbulence is usually light with infrequent moderate jolting.

Lufthansa pilots mentioned areas notorious for turbulence along their routes. These areas included most major mountain ranges and extensive hilly terrain over which low-level flights are routine. Ocean routes with high frequencies included the North Atlantic tracks from the Northeast United States to Greenland and Great Britain, the North Pacific route from Japan to the Aleutians was also mentioned.

These areas are routinely visited by jet streams, implying the important relationship between jet flow and turbulence that will dominate this report.

2.6. Pilot Reports and Actual Conditions. When turbulence forecasters define an area of turbulence potential not associated with thunderstorms or terrain effects, they face difficult questions as to intensity. Will this area reach minimum forecast criteria or not? By how much will this criteria be exceeded? Similar questions arise as existing forecast areas are monitored or when indications of a new and unexpected area arise: Will parts of the current forecast require amending because of intensity? What is the correct intensity? In this section, five arguments against the representativeness of pilot reports will be presented to show where pilot reports help or mislead the forecaster. These arguments are:

a. Data Coverage. In Section 2.4 it was shown that pilot reports are scarce over most of the hemisphere. If a single report is received in an area of scarcity it constitutes an insufficient sampling. This also applies to a sprinkling of reports over a large area. However, good data coverage has its limitations as well. In the case of the Continental United States it was shown that reports tend to be concentrated along heavily flown routes, and they varied with the weather and time of day. Large aircraft tend to report at high levels and small aircraft at lower levels, affecting intensity estimates since aircraft size and intensity are inversely proportional. Therefore, if a large, deep field of turbulence straddles a flight route and extends to lower levels as well, the area of large aircraft reports will appear to define a far smaller field than what actually exists. Furthermore, during periods of bad weather, such a variety of turbulence reports may be received that the forecaster is tempted to issue a pessimistic "blanket" forecast to "cover the reports."

b. Aircraft Type and Mission. In Section 2.2 it was mentioned that aircraft size, design, degree of loading, and airspeed affect pilot reports of intensity. Forecasters can never know all the aircraft types and their individual responses to turbulence, let alone the weight and airspeed of the aircraft making the particular report of interest. Knowing an aircraft type is not likely to add much information of value to an assessment of intensity except in the broadest sense: large planes are affected a little less by turbulence.

c. Subjectivity. Though there are intensity criteria based on aircraft instrumentation (airspeed variations, rates of climb, and accelerations), pilots routinely estimate turbulence subjectively, thus bringing in an emotional factor that introduces error. For example, if turbulence wavelengths are such that frequencies are particularly unpleasant, or if sudden intense turbulence is encountered without warning, or if turbulence is presumed to be associated with a hazardous phenomenon such as a mountain wave, the report may overestimate intensity. On the other hand, if turbulence wavelengths appear too long or too short to qualify as turbulence, or if expected jolting near thunderstorms or rough terrain occurs, or if a rare intense jolt occurs in an extensive field of light turbulence, or if relatively weak turbulence is encountered where much worse was forecast, the report may be optimistic. Though this reasoning may seem hypothetical and in truth forecasters have little reason to suspect bias in reports received, subjectivity is still a real possibility.

Another danger of subjectivity is the possibility that a report may specify a cause of turbulence that is not correct, such as "waves" in thunderstorms. If certain causes are to be excluded and reports occur where thunderstorms, jets, and terrain are possible causes, their judgements may be accepted as fact.

d. Avoidance. All pilots will avoid intense turbulence if they can. They normally avoid thunderstorms, the tropopause, and turbulent clouds such as wave clouds and rotors. If turbulence is inevitable, it is routine to reduce airspeed to a specified range that reduces the hazard, or to try to leave the turbulence area by changing flight levels. With such precautions, it is easy to see how pilots can make an active turbulence field appear weaker to the forecaster.

e. The Nature of the Turbulence Field. In this report, important findings over the past 10 years or so will be presented to show that turbulence fields are composed of waves and eddies of varying wavelengths, any or all of which may vary greatly in time and space. There appear to be periodic cycles of development and dissipation occurring throughout an active field at a nonuniform rate and some portions may be intermittently active apart from the cycles. Atmospheric turbulence fields are inherently disorderly and any aircraft unknowingly penetrating such fields

does so at random. Almost any extreme of intensity may affect the aircraft in an active field and the plane's individual dimensions and characteristics lose relevancy.

It remains to show where pilot reports are of definite value. Since it is illogical to forecast turbulence potential from existing reports, the true value of the pilot report must be as an indicator of present conditions. Forecasters continually monitor the forecast area, watching current forecast areas and looking for unforeseen new ones. Reports differing from the forecast within an area suggest further investigation. Those agreeing with a forecast serve to verify it. Therefore, pilot reports, plus sound analysis procedures, experience, and good judgement are used to arrive at forecast decisions and the problem of representativeness downgrades pilot reports to the level of the other factors. The aim is to forecast from a cause and to monitor that forecast with reports. It is faulty technique to deviate substantially from this procedure.

FUNDAMENTAL CONCEPTS FOR JET ANALYSIS

3.1. Introduction. Before a thorough study of jet streams is possible, certain concepts must be introduced and discussed. For example, the choice of minimum criteria for jet flow has never been agreed upon, so some sort of working definition will be necessary in this report. Jet-stream depictions and terminology, as well as certain analytical quantities, should be presented initially before detailing jet flow in terms that assume familiarity with quantities. Included are various forms of shear, components of fluid motion such as divergence and vorticity, the concepts of geostrophic and gradient balance, two important forms of stability, the various energy forms, and comments on the use of isentropic analyses.

3.2. The Definition of a Jet Stream. Jet streams are a concentration of wind within the atmosphere strong enough to meet certain subjective criteria. Meteorologists should recognize any flow which has:

- a. a length in thousands of kilometers,
- b. a width in hundreds of kilometers,
- c. a thickness of 1 km or more,
- d. a velocity of at least 50 kt,
- e. vertical speed shears of at least 15 kt per kilometer (about 5 kt per thousand feet), and
- f. horizontal speed shears of at least 5 kt per degree latitude on the side of least shear.

Throughout the year there will be a few concentrations of flow throughout the hemisphere which meet the above criteria. Since at 45° latitude, the earth's circumference is over 28,000 km, any jet stream thousands of kilometers long will span much of the globe, perhaps even becoming nearly continuous. The entire jet stream is actually a series of flow maxima and minima segmented by ridges and troughs of various sizes that distort the flow. Some are quasi-stationary long waves on the order of thousands of kilometers in wavelength, while others are cyclone scale or short waves hundreds of kilometers long that move in the westerlies, often associated with surface frontal systems. Each wave has a jet maximum or streak accompanying it, usually mainly on the ridge portion of the wave. Because short waves move through long waves, the size, shape, and intensity of any particular streak in the westerlies may vary greatly in a short period of time. Jet streaks are of greater operational importance than the jet stream as a whole, because each streak presents its own set of forecast problems to the analyst, including turbulence fields requiring individual attention.

3.3. Depicting a Jet Stream. The jet stream is conventionally depicted on a constant-pressure surface and includes a flow maximum and bounds where minimum speed criteria are met. Panel A of Figure 6 portrays the jet streak as a maximum wind line bounded by isotachs, the outermost of which may be assumed to meet minimum speed criteria, for example, 50 kt. The maximum wind line is the representation on a constant-pressure surface of the central jet core or axis, a three-dimensional feature that can only be approximated because it does not remain on a single pressure surface or anywhere near it. Thus, the maximum wind line and jet axis do not coincide on an analysis, though the maximum deviation between the two is on the order of 2° of latitude, a small quantity in the macroscale. If the proper constant-pressure surface is chosen for a jet analysis, the difference between the two quantities will be minimal.

Constant-pressure surface maps depict the jet stream in the horizontal but give little indication of vertical distributions of jet quantities. The vertical cross-

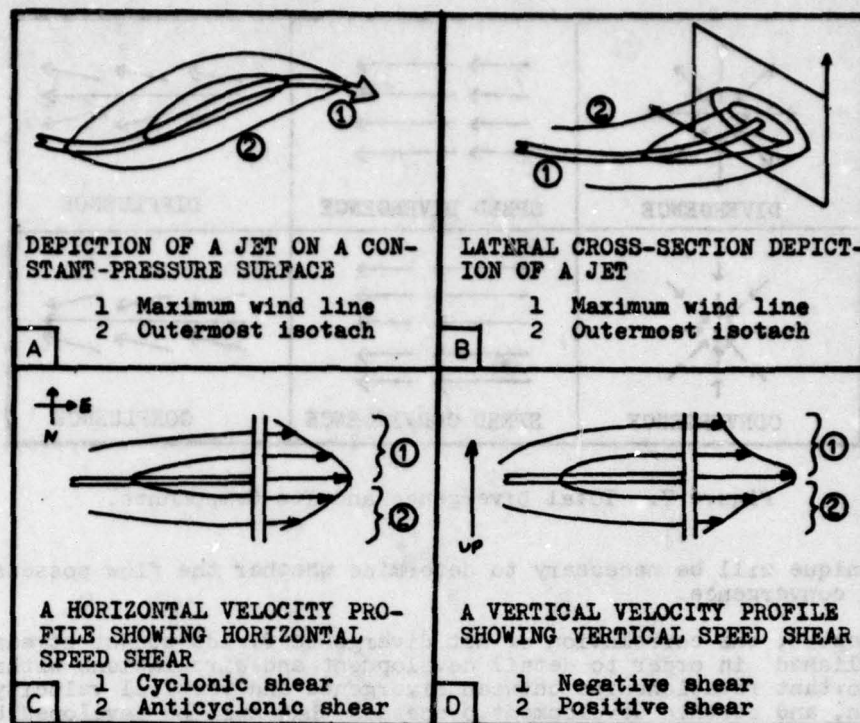


Figure 6. Jet-Stream Depictions and Velocity Profiles.

section analysis can show jet-stream structure as a central core with approximately concentric rings of isotachs about it, as in panel B of Figure 6. Cross sections are a powerful analysis tool not ordinarily available for operational use. Forecasters are forced to visualize cross sections when they seek the distribution of certain jet features only portrayable in this manner. Once standard schemes are familiar, one can use plotted soundings, raw data, or even satellite pictures to recognize them. In this report, these jet features will be introduced, portrayed in cross sections, and standardized so that the forecaster can recognize them as part of his analysis routine.

Panels C and D show how horizontal and vertical speed shearing are arrayed about the maximum wind line. On the "south" side, anticyclonic shear will be found over a larger area than cyclonic shear on the "north" side because of dynamic limitations to shearing. Because this occurs in both ridges and troughs, isotach analyses tend to give the jet streak a "banana shape." Vertical speed shear is particularly important because of its direct association with turbulence. Moderate or stronger jets have pronounced vertical speed shear and high turbulence potential both above and below the core.

Shearing also comprises directional changes in the vertical and horizontal. Vertical directional shear has a complex association with turbulence and occurs internally within the jet or externally through interactions of the jet with other jets or synoptic features. Such shear is involved in processes of intensification of much interest to turbulence forecasting.

3.4. Divergence. Divergence is a component of motion that applies to the acceleration and spreading of flow with time in space. More precisely, total or net divergence has two components, an acceleration called (speed) divergence or convergence and nonparallel flow known as diffluence or confluence. These may coexist in any combination, or one may be absent altogether. Figure 7 depicts these components separately, but in nature it may be difficult to determine the sign of the net divergence. For example, a decelerating flow (convergent) might also be diffluent,

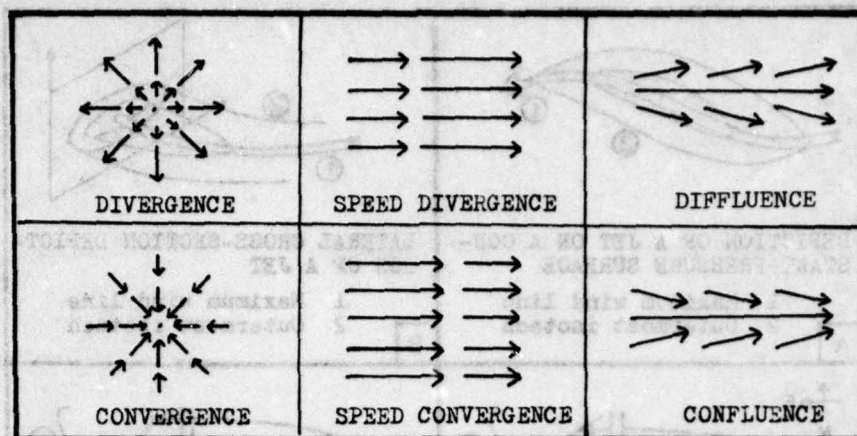


Figure 7. Total Divergence and Its Components.

and some technique will be necessary to determine whether the flow possesses a net divergence or convergence.

In this report, the correlation of net divergence fields to jet-stream structure must be established in order to detail development and circulations within the jet. There are important relationships between divergence and vertical velocity, temperature advection, and certain development processes that must be developed before the relationship of turbulence to jet flow becomes clear. Unfortunately, maps of divergence fields in nature are not ordinarily available to the forecaster, so this report will have to present standard divergence patterns in jet flow. This may be done through graphical techniques (Graham [14]) to be presented in Chapter 6.

3.5. Vorticity. Vorticity is that component of fluid motion having to do with rotation. Though vorticity exists in all spatial planes, only the vertical component is important in many meteorological applications. The fundamentally important Stokes Theorem states that the circulation about the perimeter of a given horizontal area of the atmosphere equals the product of that area and its vertical vorticity. Circulation may be related to vorticity through the mathematical expression stating that an air parcel's vorticity when in such a circulation equals a value twice that of its circular motion (angular velocity).

$$\left(\frac{\text{The change in absolute vorticity}}{\text{with time}} \right) \sim (\text{Convergence}) (\text{Absolute Vorticity})$$

where absolute vorticity is the "vorticity of the atmosphere," including the effect of the earth's rotation.

The above expression has been applied to pressure surface by Sutcliffe [49] in his work with development, the change of pressure with time also known as intensification. Vorticity maps are commonly used to show centers of intensity aloft. Centers of positive (cyclonic) vorticity are associated with convergence, while negative (anticyclonic) vorticity is related to divergence in these maps. However, these relationships need not hold in the lower troposphere. Furthermore, vorticity and divergence centers aloft will not quite coincide. Vorticity maps may be prepared from graphical techniques similar to those mentioned with divergence in the previous section.

3.6. Gradient Flow. Sweeping simplifications of the atmospheric equations of motion are necessary if they are to be applied to operational forecasting. In such cases, it is popular to assume an incompressible, steady state (unchanging), frictionless flow aloft in which air parcels may be expected to move parallel to contours on constant-pressure surfaces. Such flow will have static temperature and density

fields, and developmental processes will not occur, but this model of the flow will effectively demonstrate the major components to motion.

Figure 8 shows how air parcels in this modeled flow behave under the effects of the various components that combine to create gradient balance, the state in which winds parallel contours. In panel A of the figure, it is shown how an air parcel placed within a pressure gradient will be accelerated towards lower pressure, where density is less, and is also deflected to the right in the Northern Hemisphere by the rotating earth. Eventually the parcel will move in balance between the pressure gradient force and the Coriolis acceleration, paralleling contours so long as they are straight and parallel. This is geostrophic balance, a "straight-line" gradient balance.

When contours are curved, the air parcel cannot parallel them unless it is accelerated towards the center of curvature of every bend in the flow. Panel B shows that the addition of a centripetal acceleration acting toward centers of curvature supplies the necessary adjustment to permit gradient balance in any flow, so long as contours remain parallel.

It is now evident that the air parcel moves in gradient balance under the influence of the pressure gradient force and the Coriolis and centripetal accelerations. The latter two are not forces because they affect only the direction of the parcel's movement. The Coriolis and centripetal accelerations may be called apparent forces, because they appear to supply the necessary accelerations to deflect the air parcel. In fact, the parcel moves at a rate proportional to the degree to which it was accelerated by the pressure gradient force. Thus, the speed of the flow is proportional to the pressure gradient.

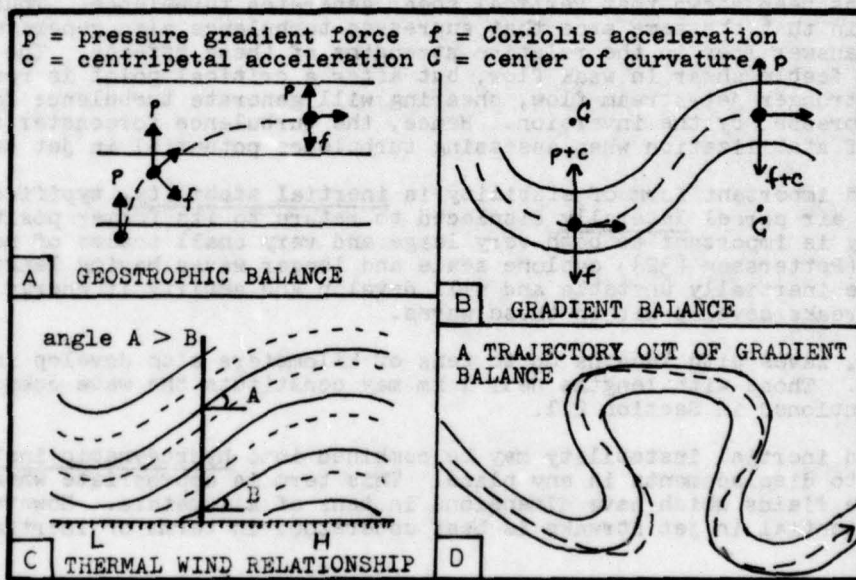


Figure 8. Gradient Balance and Its Applications.

Panel C in Figure 8 demonstrates the importance of the pressure gradient force through its relationship to temperature in the Equation of State (directly proportional if density is constant). Consider a cold-core low and a warm-core high adjacent to each other. Meteorologists know that these will intensify with height, so that pressure and temperature gradients increase progressively in that direction and that the flow must also strengthen as well. In middle latitudes over much of the world, the horizontal temperature gradient may be concentrated into a narrow band above and nearly over major polar frontal chains. Jet-stream flow is also observed. The thermal wind relationship states that vertical wind-speed shearing above a given level is proportional to the strength of the horizontal temperature

gradient at that level. It not only explains the existence of jet streams above polar frontal chains but may also be used to explain their development. This will be shown in Chapter 6.

In nature it is common to see instances when upper-air contours are not parallel such as in sharp ridges and troughs, and also where the flow is diffluent or confluent. In such regions the flow is ageostrophic, the steady-state modeling of the flow is invalidated by development processes, and observed winds deviate from the orientation of the contours. Developmental processes are important to turbulence forecasting because they indicate changes in jet-stream strength and movement, and certainly change the potential for turbulence in various portions of the flow.

3.7. Stability. This property of motion assumes that an air parcel is in some form of balance so that if displaced it returns to its former position. Stability is important to this report in two forms, depending on whether the displacements are vertical or horizontal.

Vertical displacement is characteristic of hydrostatic or static stability. Forecasters know that as buoyancy, where an air parcel having a given density "floats" on denser air below and will not ascend into less dense air above unless forced upward. If the parcel is heated from below it will become less dense and rise, but it is typical in nature that warm-air layers aloft called inversions overlie many lower level turbulent areas in which air is being heated and is rising. Inversions may be strongly stable, inhibiting turbulent motions.

It will be shown later in this report that there are two regions in jet-stream flow where pronounced inversions may develop, one below the jet core and the other over it at the tropopause. In both areas pronounced vertical speed shear is prominent and it has been shown that vertical shear generates turbulence. Thus, there is a paradox in that the same area that suppresses turbulence also generates it. However, the answer lies in the relative strengths of these effects. The inversion overrides the feeble shear in weak flow, but after a critical point is reached in moderate or stronger jet-stream flow, shearing will generate turbulence faster than it can be suppressed by the inversion. Hence, the turbulence forecaster seeks out major areas of stabilization when assessing turbulence potential in jet streams.

The second important form of stability is inertial stability, typified by the ability of an air parcel laterally displaced to return to its former position. Inertial stability is important to both very large and very small scales of motion. It can be shown (Petterssen [32]) cyclone scale and longer waves having lengths of 3000 to 8000 km are inertially unstable and will develop and amplify if energy is available. Jet streaks develop within these waves.

Similarly, waves with lengths up to tens of kilometers also develop in inertially unstable flow. Those with lengths near 1 km may constitute the wave component of turbulence mentioned in Section 2.1.

Static and inertial instability may be combined into hydrodynamic instability which refers to displacements in any plane. This term is appropriate when considering turbulence fields which have dimensions in tens of kilometers. However, overall turbulence potential in jet streaks is best understood in terms of inertial instability.

3.8. Energy. By definition, energy is the capacity to do work and overcome resistance. Energy appears in various forms, and interrelationships between these forms called conversions or transformations are important in many areas of meteorology, including jet streams and turbulence fields. In this section several important energy forms will be presented and linked together in the atmospheric energy equation through which energy conversions of later interest may be discussed.

a. Internal energy, a measure of the degree of molecular activity of matter that is dependent on temperature alone and is approximated by the term sensible heat, the "heat one feels." Sensible heat is found in adiabatic processes which involve no heat contributions outside the system.

b. Kinetic energy, "energy of motion," is the primary interest in jet-stream analysis because the speed of the flow is proportional to the amount of kinetic

energy it possesses, and furthermore, this energy form is drawn from the flow for the generation and maintenance of turbulence fields.

c. Potential energy is "energy of position" in a gravitational field, proportional in intensity to the distance above the ground. A measure of potential energy is the work done to move an air parcel vertically. It can be shown that potential and internal energy forms are related closely in the atmosphere. For example, if an air column is heated, it can only expand vertically since it is hemmed in by adjacent air columns. Heating a parcel of air increases the molecular activity and, therefore, it increases the internal energy of the parcel. Because warm air is less dense than cooler air, and because a warm parcel of air has a higher center of mass, heating the parcel also increases its potential energy. This internal and potential energy is transformed to kinetic energy in jet streams and atmospheric turbulence.

d. Latent heat is a form of energy released or absorbed as water in the air undergoes a phase change (solid-liquid-gas). This energy form is not associated with adiabatic processes and is thus separated from sensible heat.

The next two energy forms involve work, itself an energy form arising from the motion of a system against a force. Work exists only within this process, two forms of which are:

e. The energy transformation which occurs when work is done to force air parcels across pressure surfaces in ageostrophic flow.

f. The energy transformation which occurs when work is done by friction and turbulence to retard flow, incurring a loss of kinetic energy of that flow.

g. The atmospheric energy equation, which interrelates energy forms is:

$$\begin{aligned} \left(\frac{\text{The heat capacity of an air parcel}}{\text{per unit of mass}} \right) &= \left(\frac{\text{Heat absorbed or released by the parcel}}{\text{corresponding temperature change}} \right) \\ &= \left(\frac{\text{Change in}}{\text{time of}} \left[\begin{array}{l} \text{Potential} \\ \text{energy} \end{array} + \begin{array}{l} \text{Kinetic} \\ \text{energy} \end{array} + \begin{array}{l} \text{Sensible} \\ \text{heat} \end{array} \right. \right. \\ &\quad \left. \left. - \begin{array}{l} \text{Latent} \\ \text{heat} \end{array} - \text{Friction} \right] \right) \end{aligned}$$

The heat capacity of an air parcel of unit mass is defined as specific heat. The atmospheric energy equation may be simplified by assuming an adiabatic, frictionless, steady-state atmosphere, thus eliminating latent heat, friction, and the time changes of all energy forms and reducing the equation to:

$$\left(\begin{array}{l} \text{Potential} \\ \text{energy} \end{array} + \begin{array}{l} \text{Kinetic} \\ \text{energy} \end{array} + \begin{array}{l} \text{Sensible} \\ \text{heat} \end{array} \right) = 0$$

3.9. Isentropic Analyses. Most weather maps are displays of parameters such as pressure, heights, temperature, and wind fields on constant heights and constant-pressure surfaces. In many instances, however, it is more correct to analyze on isentropic surfaces, which are surfaces of constant entropy. The concept of entropy is somewhat difficult to visualize, but it may be thought of as a state in which a measure of the energy of a system which is being lost irretrievably during a process. If entropy is increasing, the system has less and less energy with which to carry out a process.

The important part of this discussion is the use of isentropic analyses. The most commonly seen parameter in such analyses is potential temperature, the temperature a parcel of dry air would have if displaced adiabatically to 1000 mb. Isentropic analyses represents jet flow better because air parcels follow isentropic surfaces as they move in trajectories. The deviation of the flow from constant-pressure surfaces may be seen in satellite pictures, where jet cirrus shields clearly

baroclinity in cross-sections.

THE ROLE OF JET STREAMS IN THE GENERAL CIRCULATION

4.1. Introduction. When the global upper-air network was established over the Northern Hemisphere immediately after World War II, it became possible to model the tropospheric circulation in detail. One major goal was to determine the mixing processes by which equatorial heat and solar cold were transported throughout the hemisphere to maintain the observed global heat balance. It happened that not only did circulation schemes include jet streams but that ways in which jet streams formed were also implied.

In this section, particular attention will be paid to the nature of jet streams and the ways in which they interact with other portions of the hemispheric circulation. Basic analysis tools will include a meridional circulation model and temperature cross-section analyses. Of particular interest will be methods of identifying the individual jet streams and distinguishing between polar and subtropical jets.

4.2. The Hemispheric Meridional Circulation. Meridional circulation models are a north-south cross section of the atmosphere along some meridian. Perhaps the most familiar model is that introduced in the early 1940's by Palmén [28]. It was designed to apply to a winter circulation, when all features are strong and show up to their best advantage. In this chapter, the Palmén model will be shown in a slightly revised form to incorporate certain features recently brought to light and it will be coupled with temperature cross sections averaged for a winter month at a particular meridian to provide additional detail.

The logical starting point in the description of the meridional hemispheric circulation is the primary area of heat input into the atmosphere, the earth's surface at the equator near the intertropical convergence zone, shown as "I" in Figure 9. Air ascending from here approaches the tropical tropopause level (T1) with its heat content greatly reduced, as can be seen in the temperature cross section in Figure 10. Note also in the figure that a substantial horizontal temperature gradient has been

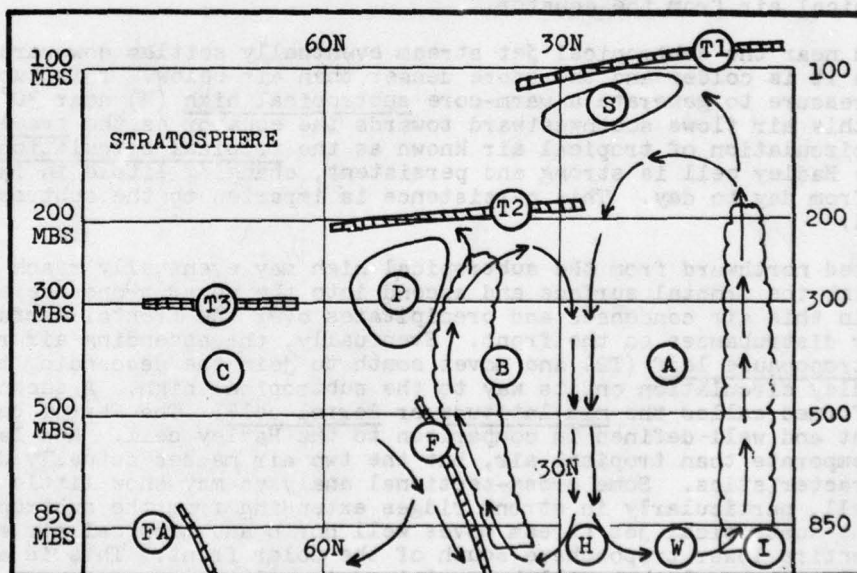


Figure 9. A Northern Hemisphere Meridional Circulation Model for Winter (adapted after Palmén [28], with symbols explained in the text).

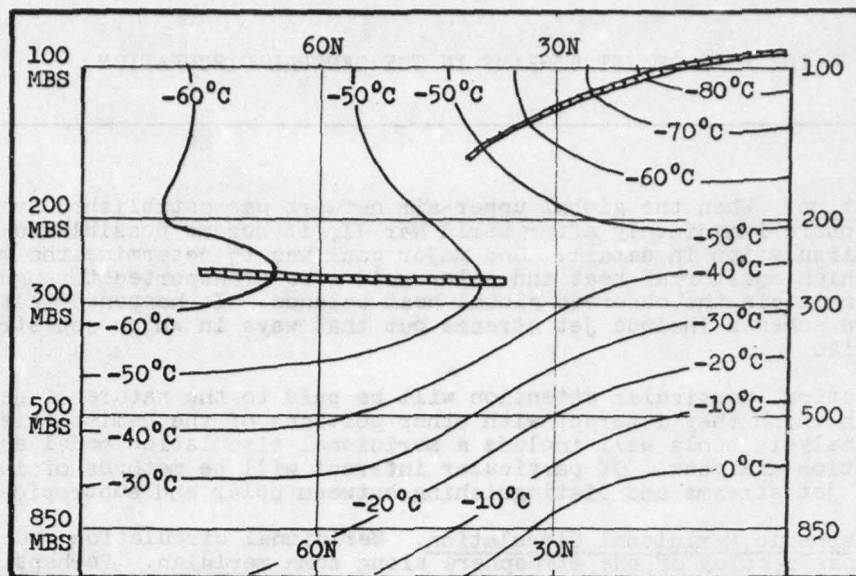


Figure 10. Mean January Meridional Temperature Field for 147.5°E (from United States Air Force, 3rd Weather Wing records).

formed to the north that necessarily includes a pressure gradient as well. Thus, a pressure gradient force will draw this air northward and the Coriolis acceleration eventually steers it to the right (eastward) as it accelerates, forming the sub-tropical jet stream (S). In Figure 10 the horizontal temperature gradient aloft ends near 45° latitude, apparently restricting this jet stream to high levels of the troposphere in the subtropics. It is likely that a fundamental cause of the sub-tropical jet is that temperature gradient, which in turn depends on the rate of ascending tropical air from the equator.

Air in and near the subtropical jet stream eventually settles downward because of gravity, since it is colder and therefore denser than air below. This subsiding air heats by compressure to generate a warm-core subtropical high (H) near 30° latitude. A portion of this air flows southwestward towards the equator as the trade winds (W), completing a circulation of tropical air known as the tropical circulation or Hadley cell (A). The Hadley cell is strong and persistent, changing little in intensity and position from day to day. This persistence is imparted to the subtropical jet stream as well.

Air directed northward from the subtropical high may eventually reach a polar front (F), climb the frontal surface and ascend into the upper troposphere. Much of the moisture in this air condenses and precipitates over the frontal surface, particularly near disturbances on the front. Eventually, the ascending air reaches the mid-latitude tropopause leaf (T2) and moves south to join the descending tropical air of the Hadley circulation on its way to the subtropical high. A second circulation is thus formed called the mid-latitude or Ferrel cell. The Ferrel cell is much less persistent and well-defined in comparison to the Hadley cell. Mid-latitude air may be more temperate than tropical air, but the two air masses actually differ little in characteristics. Some cross-sectional analyses may show little indication of a Ferrel cell, particularly in strong ridges extending from the subtropics. In such cases, the subtropical jet stream moves well north and tropical air appears to dominate the entire lower troposphere south of the polar front. This is a deviation from the circulation model that will be explained in a later section.

North of the polar front and below the polar tropopause leaf (T3) is an uncertain circulation of polar air (C), a backwater of assorted highs and lows that vary greatly in intensity and location in short periods of time. In winter a low-level arctic

front (AF) may appear in polar regions, but it does not appear to be related closely to other features in the circulation model, especially the major jet streams. One likely component of any polar air circulation is descending air behind the polar front.

The polar front is perhaps the most important part of the entire meridional circulation (excepting the heat source) because of its separation of polar and tropical air in the lower half of the troposphere, becoming a barrier to heat redistributions over the hemisphere. Because vastly contrasting air masses lie on either side, there is a pronounced horizontal temperature gradient across the front. Through the thermal wind relationship discussed in Section 3.6, it follows that there must be a vertical increase in flow above the front that may become substantial if the thermal gradient is great enough. There is, in fact, a strong band of winds above the polar front called the polar jet stream (P) that is the most important manifestation of the westerlies. Figure 10 shows a broad horizontal temperature gradient in the middle and lower troposphere from 20° to 55° latitude that is an averaged display of the polar front. This great broadness is caused by the extreme degree of meandering which is characteristic of the polar front and it is significant that, despite such meandering, the gradient is so obvious in a mean cross section.

The link between a surface polar front and the polar jet stream above is not quite as simple as has been implied. Surface polar frontal chains are never continuous around the hemisphere. On the other hand, it is possible to trace the polar jet-stream maximum wind line over almost the entire hemisphere at 300 mb, as is done every 12 hours at AFGWC. Furthermore, the polar jet stream may be well developed in both ridging and troughing, while surface fronts are usually weakly defined or absent in many ridges and some troughs. While polar frontal chains must have a polar jet stream aloft, the converse is not true, especially in ridging.

The pronounced variability of the polar front is partly due to its hindering of meridional heat transfer. In time, the increasingly differing contrasts across the front generate a powerful polar jet stream that possesses a vast reservoir of kinetic energy available for the amplification of perturbations in the westerlies. These disturbances may be seen both in the jet stream and also on the surface fronts as developing waves. These perturbations will redistribute polar cold and equatorial heat in the middle latitudes. As the waves become mature and occlude, great and extensive penetrations of polar air are drawn south behind the system and much tropical air moves north in ridging ahead. This macroscale process continually occurs over the hemisphere, but there is a periodic nature inherent to the redistributions that is called the index cycle, in which the effectiveness of the polar frontal barrier varies with the buildup of contrasting air masses and the inevitable breakdown as mixing finally occurs on a large scale. In a high index the westerlies are zonal with broad polar jet streaks of great length and long polar frontal chains. In a low-index pattern, the westerlies meander greatly in meridional flow, having pronounced north-south components of motion. Also notable are cut-off highs and lows with obstacles to westerly flow called blocking patterns. Polar fronts on the surface tend towards deep occlusions accompanied aloft by short but intense polar jet streams. Turbulence potential is known to be much greater in low-index periods. The entire index cycle is variable in length, though it tends towards a length of 4 weeks on the average.

In summer, the atmosphere is far less disturbed as both jet streams weaken and move north. Irregular and intermittently significant jet movements are not of high turbulence potential, so this is the quiet season for the forecaster. The summer meridional temperature cross section of Figure 11 shows a very weak mid-tropospheric gradient and a significant tropopause gradient that is, nevertheless, half of its winter counterpart. A summer meridional circulation model is of little interest because of the lack of a well-defined polar and middle-latitude pattern.

4.3. Criteria to Identify the Major Jet Streams. When forecasting turbulence, one must know which jet stream is involved. Criteria established here may not be universally accepted as definitive. Most forecasters identify jet streams subjectively even though there are always exceptions to the rule. If basic rules are made that apply to commonly-used analyses, the forecaster may test them in time by his own experience and requirements. In this section, criteria will be presented and depicted in both horizontal and vertical analyses. The Palmén circulation model [29] supplies the foundation for this section through its interrelationship of circulation

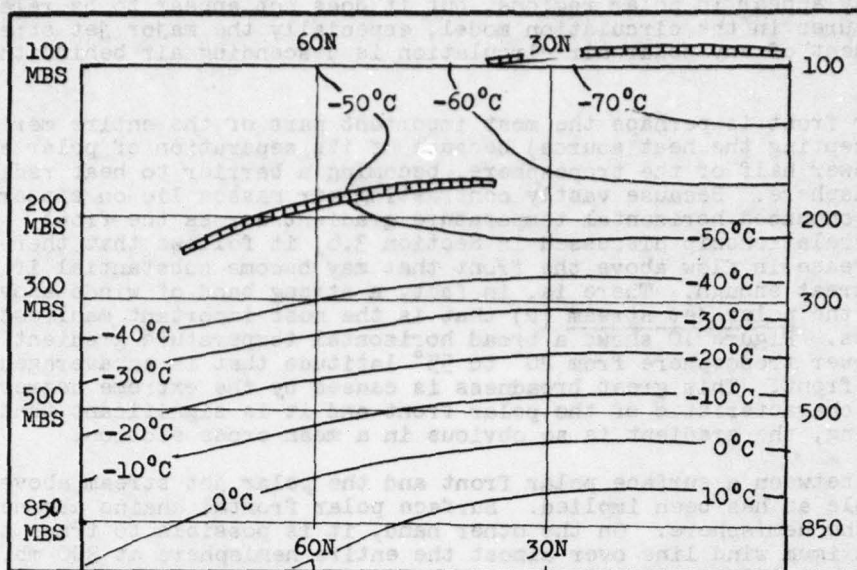


Figure 11. Mean July Meridional Temperature Field for 147.5°E (same source Figure 10).

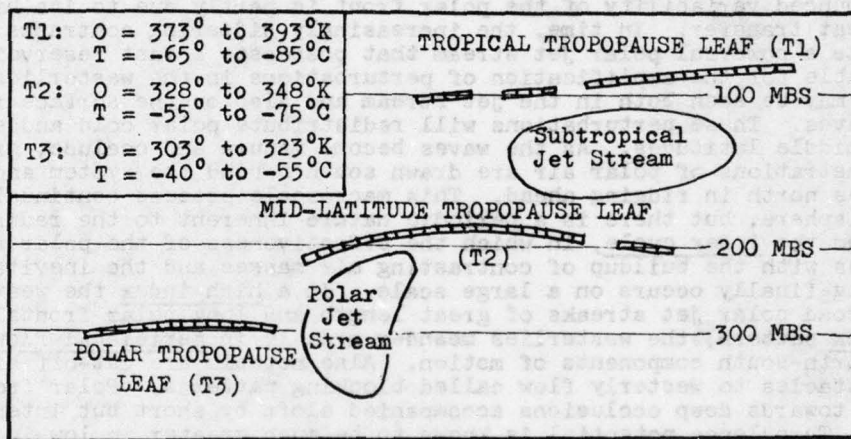


Figure 12. The Normal Relationships of Jet Streams to Tropopause Leafs, Including Leaf Temperature Ranges. Potential temperatures from Air Force CDC 25370 Weather Technician Course. Potential temperature-temperature ranges do not exactly coincide.

cells, jet streams, and tropopause leaves. Figure 12 shows a particularly useful link between tropopause and jet core along with a range of potential temperatures that defines each individual leaf. These potential-temperature ranges have been modified to accent easily remembered statistics. The following relationships between tropopause leaves and jet cores hold:

a. The polar jet stream lies near 300 mb under the northern edge of the mid-latitude tropopause leaf. It is south of, and at nearly the same elevation as, the polar leaf. The mid-latitude leaf itself lies very near 200 mb and that level is very useful in polar jet-stream identification. Above a moderate or stronger jet core (certainly meeting jet criteria as in Section 3.2), 200-mb temperatures fall

below -55°C , often below -60°C . This strong relationship is dependent upon the influences of the subtropical jet stream, to be discussed later in the section.

Analysts familiar with 300-mb hemispheric analyses are aware of a tendency toward a double polar jet stream that shows up particularly well in split flow around cut-off pressure systems. Despite a certain amount of confusion that such flow adds to turbulence forecasts, the temperature relationships hold well above each portion of the flow unless the subtropical jet stream interferes.

b. The subtropical jet stream lies near 250 mb under the northern edge of the tropical tropopause leaf and usually over the southern edge of the mid-latitude leaf. The tropical leaf is near 100 mb, usually well above most analysis efforts, so the affect on the mid-latitude leaf is of greater interest. When a jet stream appears to be subtropical at 200 mb (the mid-latitude leaf level), temperatures range in irregular patterns above -55°C , often near -50°C . This rule holds even when a jet stream appears to have had both polar and subtropical origins.

Figures 13 through 16 demonstrate clear examples of polar and subtropical jets both horizontally and vertically. In Figure 13, strong polar jet flow at 200 mb is accompanied by a temperature field ranging from above -50°C in the trough to below -60°C in the ridge in the Ohio Valley. The trough temperatures are routine, but -60°C temperatures in the ridge positively identify the mid-latitude leaf, so that the flow must be polar. The cross section, Figure 14, indicates that the height of all features are slightly higher than standard. High levels are typical of ridging, while lower heights of features occur in troughing. Note that the mid-latitude tropopause leaf is generally within the -60°C isotherm. The tendency of this leaf to curl down around the north side of the jet flow is another indication of intensity; Hoskins [17] hypothesized that this "bending of the tropopause" occurs with a lateral counterclockwise circulation around the jet.

Figure 15 is a 200-mb analysis of the subtropical jet stream over Japan. Note the weak temperature gradient and overall warm temperatures which are almost entirely above -55°C . The cross section of Figure 16 shows concentrated flow near 40,000 feet under a very high tropopause leaf, above 50,000 feet; this can only be tropical.

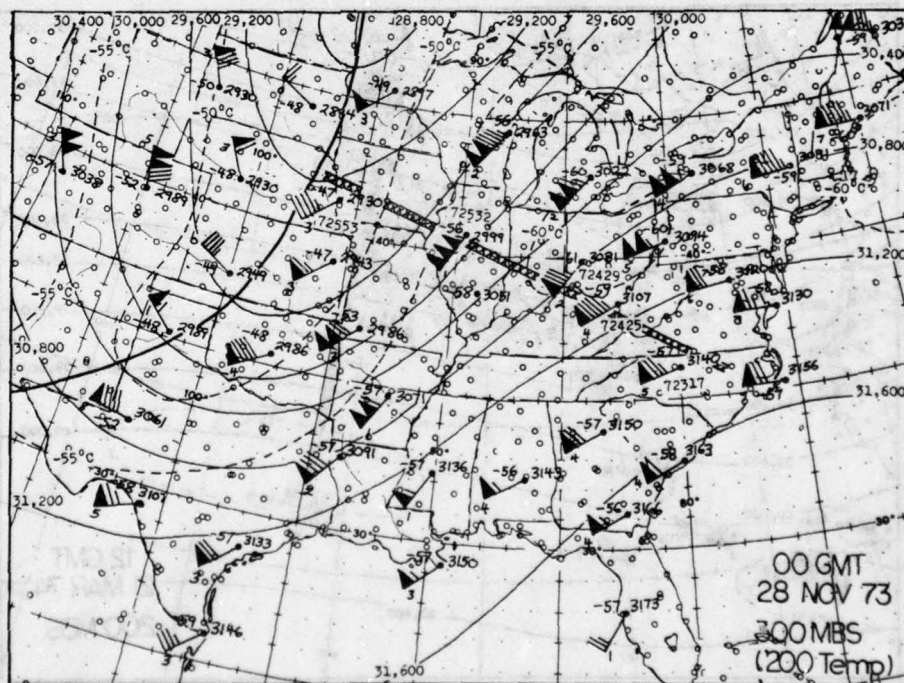


Figure 13. Polar Jet Stream.

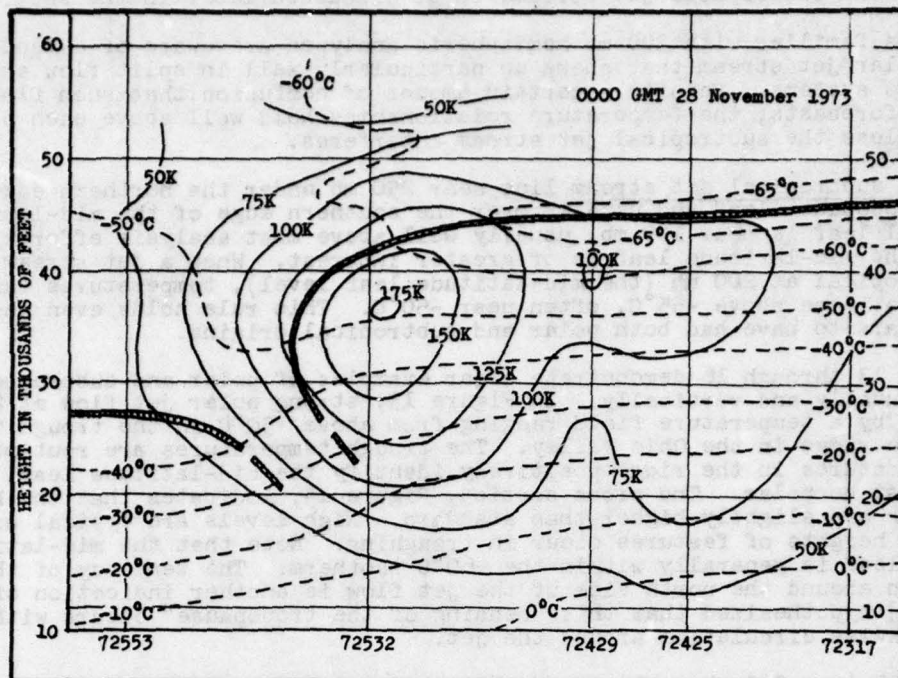


Figure 14. Cross Section of Polar Jet Stream, 0000 GMT, 28 Nov 73.

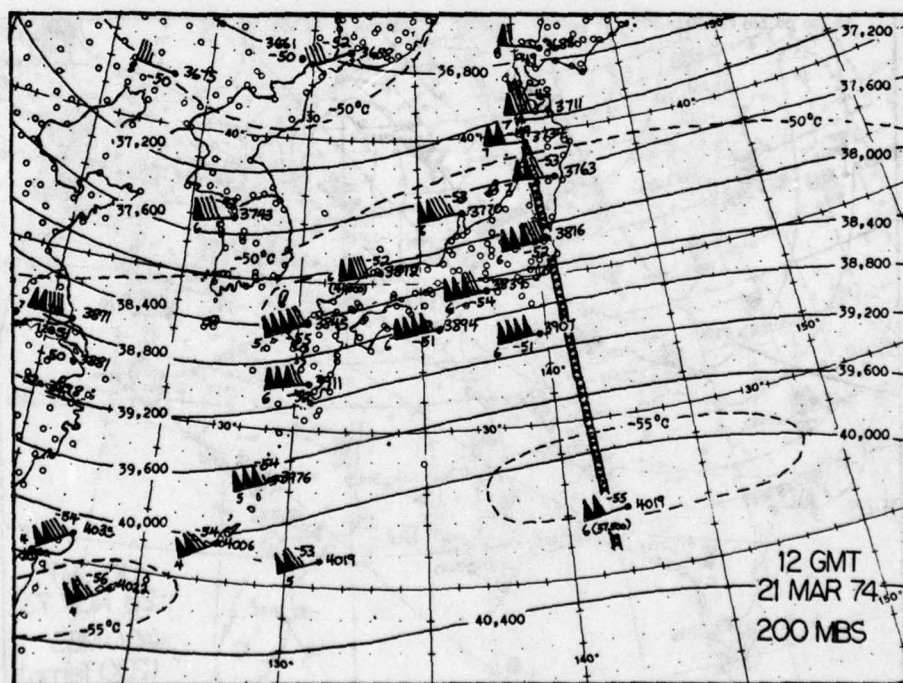


Figure 15. Subtropical Jet Stream.

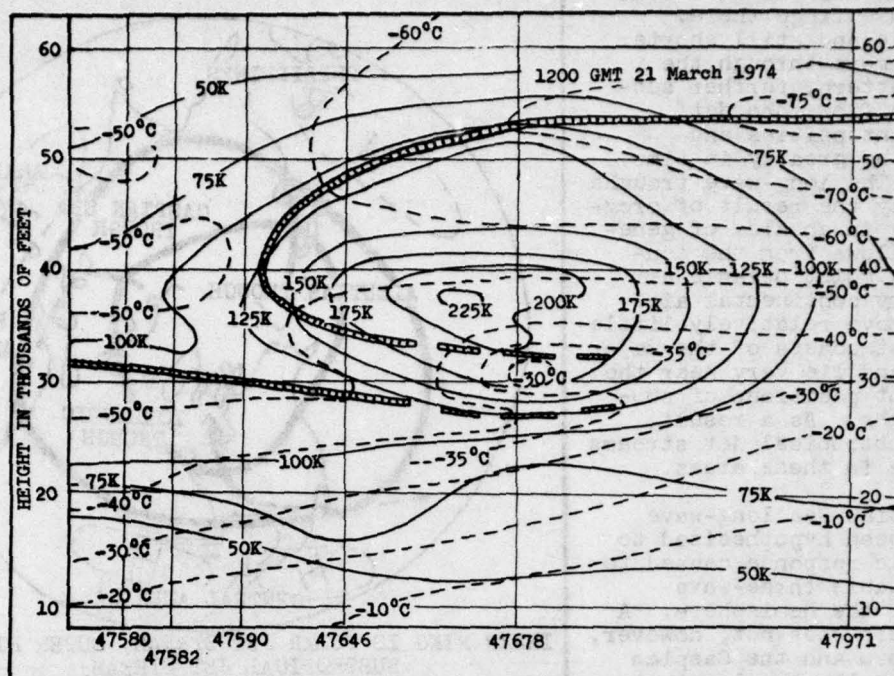


Figure 16. Cross Section of Subtropical Jet Stream, 1200 GMT, 21 Mar 74.

There are no standard cross-sections of the subtropical jet stream. Many varieties may exist in different synoptic patterns as shown in the next section. In this case, the 200-mb temperature field and the lack of a well-defined jet core except under the northern edge of the tropical tropopause identifies this jet core as subtropical.

4.4. Interacting Polar and Subtropical Jet Streams. Because of the close association of the polar jet stream to the polar front and the subtropical jet stream to the Hadley circulation, it is possible to determine averaged tracks for these jets around the Northern Hemisphere. Most of the year in the tropics, there are large areas dominated by the subtropical highs of the Hadley circulation. Climatic maps of cloud cover [21] show these areas to be relatively cloud-free, a fact following from these semipermanent and extremely dry pressure systems. The subtropical jet stream is well-developed in association with these highs and the Hadley cell in general, so that mean tracks of this jet stream are possible to draw. The polar jet stream varies tremendously, but the semipermanent long-wave troughs of the east coasts of Asia and North America, plus troughing in the Caspian Sea area do limit polar jet-stream flow and help in describing what are admittedly crude tracks.

Figure 17 is a generalized scheme of preferred polar and subtropical jet-stream tracks (taken from Riehl [38]) with the addition of typical positions of subtropical highs and long-wave troughs. The subtropical jet stream has been shown by Krishnamurti [20] to be best-developed in three broad low-latitude areas from North Africa to Arabia, the general region of the Philippines, and from Central America to the Caribbean. Strong subtropical jet flow occurs most frequently near the Philippines during the winter. Mohri [26] has hypothesized that the Himalaya Mountains aid the development of strong flow in this area which may help explain the maximum occurrence here. North Africa has the second highest frequency of occurrence of strong subtropical jet streams, and Central America has the third highest frequency.

The polar jet stream is generally best-developed in the broad ridges between the major long-wave troughs over the middle North Pacific and Atlantic Oceans. However, flow across Russia between the Caspian Sea and Aleutian Troughs is usually unremark-

able because of terrain influences and the lack of a substantial long-wave ridge there. Cyclone scale and still shorter scale waves move through the long-wave pattern, further subdividing the flow into jet streaks of intensities and forms changing greatly in time and space. The long-wave troughs are basically the result of orography, lying in an area of genesis that follows from the contrasts warm, moist oceanic air and cold, dry continental air. Thus, they move relatively little from the east coasts of the major continents and lie very near the semipermanent positions of subtropical highs. As a result, polar and subtropical jet streams may converge in these areas.

The Caspian Sea long-wave trough has been hypothesized to be a harmonic response caused to achieve a stable three-wave pattern over the hemisphere. A stable pattern does not, however, appear to form and the Caspian Trough is usually the least significant of the long waves. Polar and subtropical jet streams tend to remain apart and are further separated by the high mountain ranges characteristic of this area. Thus, regions of likely jet-stream interactions are the east coasts of Asia and North America.

The manner in which the two jet streams coincide varies, depending upon the relative strengths of the long-wave trough and the Hadley circulation. Figure 18 shows two variants of this merging, both assuming moderate or strong jet streams. Panel A shows the more common pattern of a long wave penetrating well south and then trailing southwestward so that the subtropical jet stream moves northeastward ahead of it and meets the polar jet stream as the latter also moves in that direction. Such a configuration may often be seen with the Caspian Sea trough, in which the trailing trough extends southwest across the Mediterranean into the Atlantic off Northwest

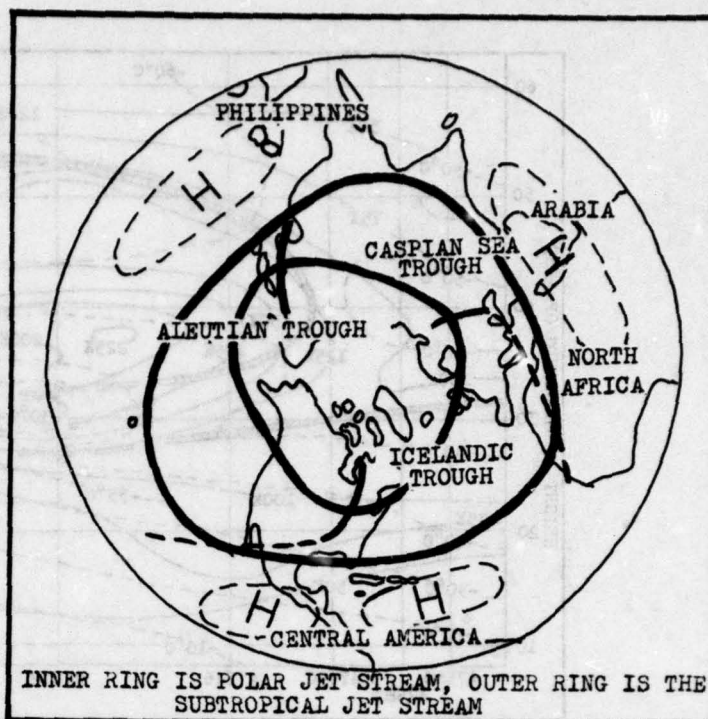


Figure 17. Average Winter Tracks of the Polar and Subtropical Jet Streams.

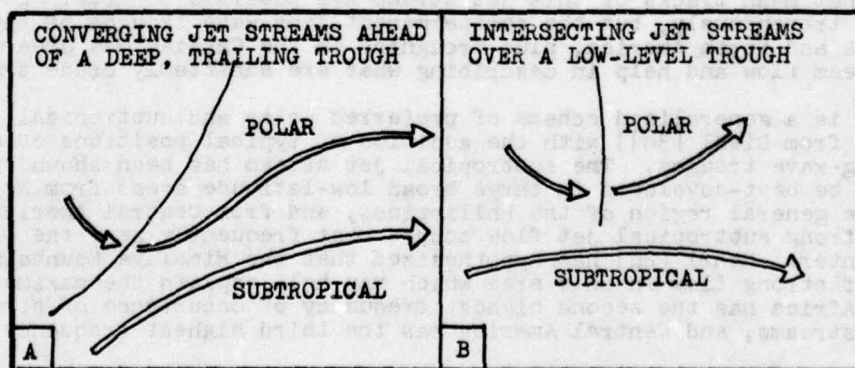


Figure 18. Basic Polar-Subtropical Jet-Stream Intersections.

Africa. On occasion, another trough extends from the Icelandic Trough across the United States into the Pacific Ocean west of Mexico. Trailing troughs are apparently not so common or extensive in the case of the Aleutian Trough, possibly because of Himalayan effects.

The pattern of panel A presents difficult challenges to the analyst because the flow into the ridge east of the trough may be very broad and vague. The subtropical jet stream need not be present for an equivalent configuration to be observed. Two polar jet branches may exist instead. A method of resolving the difference between these two situations will be shown by example later in the section.

Panel B in Figure 18 shows a short long-wave trough extending due south into a well-developed Hadley circulation marked by a strong subtropical jet stream. This uncommon pattern is most often seen in winter near Japan with the Aleutian Trough. Since the two jet streams are completely out of phase with each other, the polar jet moves briefly under the subtropical jet and then out to the northeast alone. A variation of this pattern occurs occasionally in winter when a deep cut-off low moves into low latitudes and lies partially under a subtropical jet streak. Such lows may be seen on occasion near the Azores in the Atlantic and near Hawaii in the Pacific Ocean. They usually move little and dissipate gradually, so that the polar jet branch within the cut-off is only briefly important.

The series of drawings, Figures 19 through 32, show four cases depicting patterns mentioned previously in this section. They are discussed in the next sections.

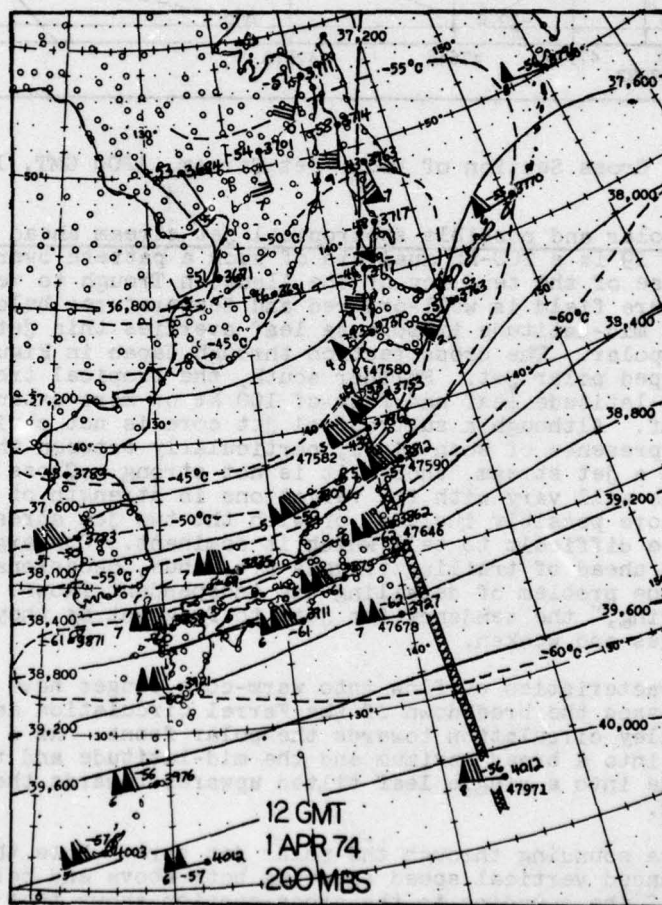


Figure 19. Polar Jet Stream Ahead of a "Trailing Trough."

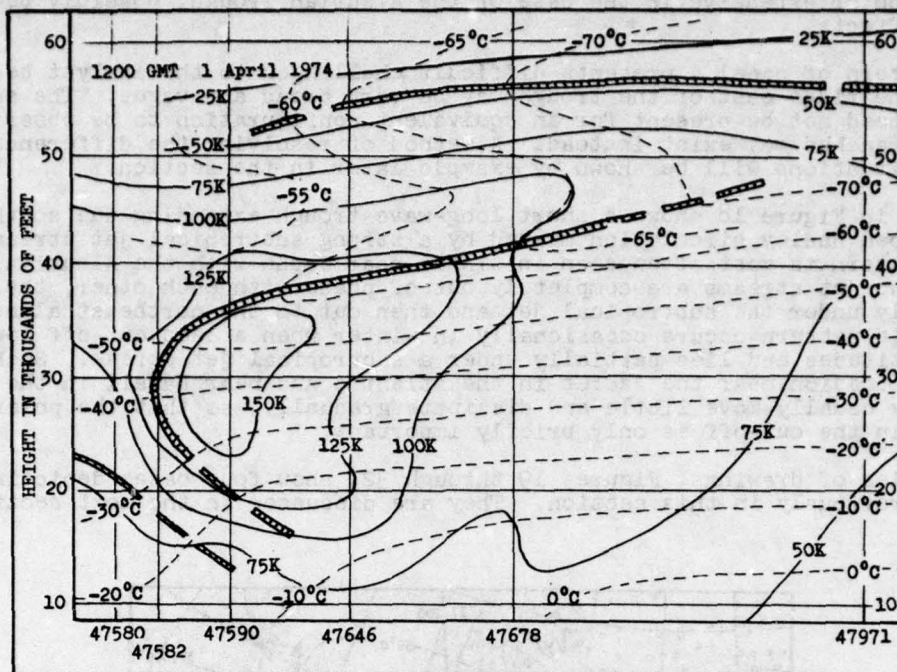


Figure 20. Cross Section of Polar Jet Stream, 1200 GMT, 1 Apr 74.

a. Converging polar and possible subtropical jet stream ahead of trailing long-wave trough: Figure 19 is a 200-mb analysis of such a pattern over Japan, an unusual occurrence because of the tendency of the Aleutian Trough to remain north-south. Because the temperature field is well-ordered and temperatures below -60°C are seen over a large area, a mid-latitude tropopause leaf overlies this jet stream and the latter is therefore polar. The cross section through Japan in Figure 20 is that of a normal well-developed polar jet. Further south, the tropical tropopause leaf overlies much of the mid-latitude leaf and flow of 100 kt or more extends southward along the mid-latitude leaf. Although a subtropical jet core is not obvious in this region of sparse data, the presence of such winds, particularly between the two tropopause leaves, suggests such a jet stream, though it is not strong. Cross sections of equivalent situations will vary with the variations in strength of the subtropical jet stream, with a core possibly included or with the two jet streams so close together that it may be difficult to tell which is dominant. Converging polar and subtropical jet streams ahead of trailing troughs are, thus, occasionally difficult to analyse because of the problem of detailing the independent flows. A further complication is "fingering," the tendency for jets to fragment as they progress into broad long-wave ridges and weaken.

The general characteristics of flow into warm-core ridges have been detailed by Defant [7], who stresses the breakdown of the Ferrel circulation and the northward extension of the Hadley circulation towards the polar front. As a rule, jet-stream flow tends to blend into a broad maximum and the mid-latitude and tropical tropopause leaves may merge into a single leaf tilted upwards towards the south if the overall flow is weak.

Figure 21 shows a sounding through the polar jet core. Note that the speed profile includes pronounced vertical speed shearing both above and below the flow maximum. A comparison of the sounding to the cross-section shows that the zone of strong positive speed shear and a zone of stability in the temperature lapse rate coincides with that portion of the tropopause folded under the jet core. This jet front is

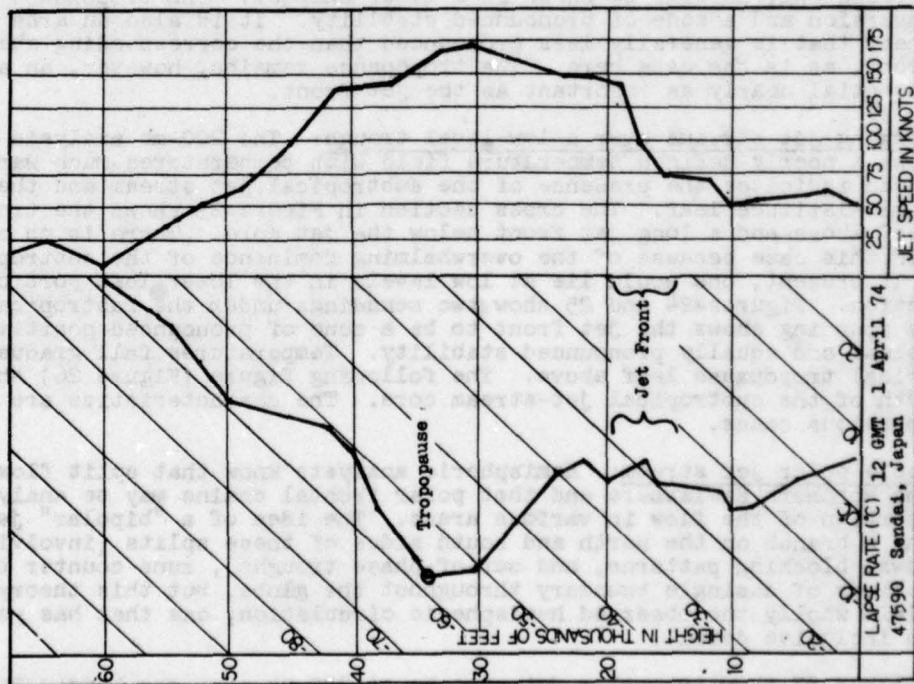


Figure 21. Lapse Rate and Speed Profile for Sendai, Japan (47590), the Station Under the Polar Jet Core.

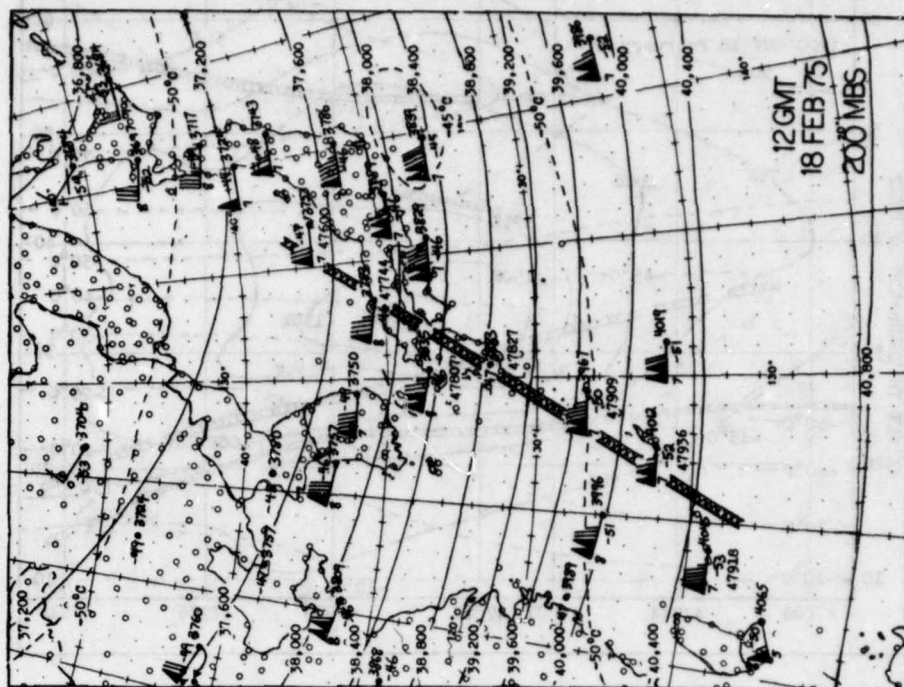


Figure 22. Subtropical Jet Stream Overlying a "Short" Long-Wave Trough.

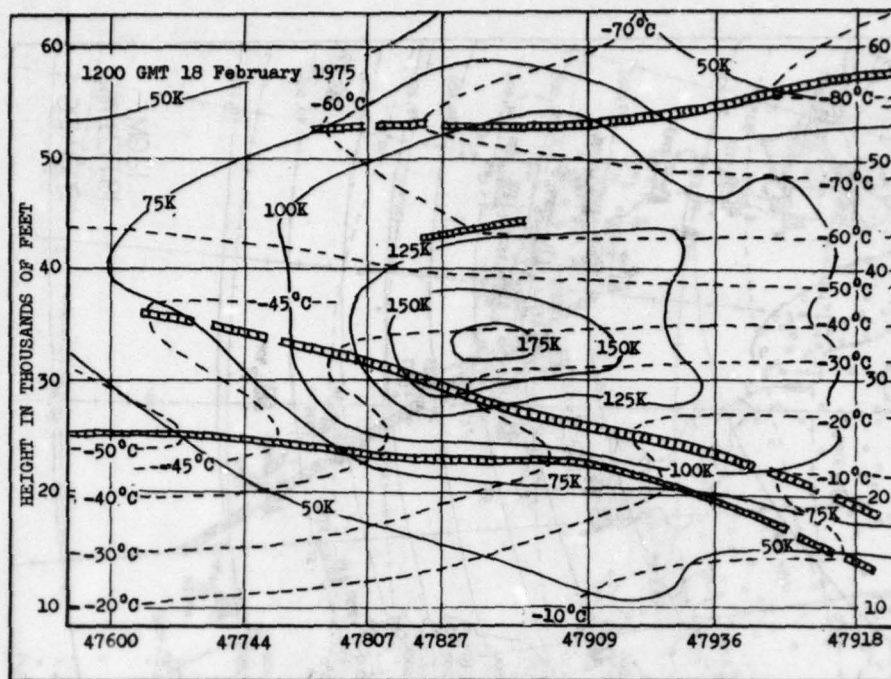


Figure 23. Cross Section of Subtropical Jet Stream, 1200 GMT, 18 Feb 75.

present with all moderate or stronger jet streams and is particularly important to turbulence forecasting, as will be shown in a later chapter. The tropopause is, of course, an inversion and a zone of pronounced stability. It is also an area of negative speed shear that is generally less pronounced than the corresponding shear zone at the jet front, as is the case here. The tropopause remains, however, an area of turbulence potential nearly as important as the jet front.

b. Converging jet streams over a low-level trough: The 200-mb analysis in Figure 22 shows a poorly-defined temperature field with temperatures much warmer than -55°C which indicates the presence of the subtropical jet stream and the absence of any mid-latitude leaf. The cross section in Figure 23 shows the tropical tropopause leaf above and a long jet front below the jet core. There is no obvious polar front in this case because of the overwhelming dominance of the subtropical jet stream. If present, one would lie at low levels in the lower left portion of the cross section. Figures 24 and 25 show two soundings under the subtropical jet. The Kagoshima sounding shows the jet front to be a zone of pronounced positive vertical speed shear and equally pronounced stability. Temperatures fall gradually to the cold tropical tropopause leaf above. The following figure (Figure 26) shows the jet front south of the subtropical jet-stream core. The characteristics are the same as for previous cases.

c. A double polar jet stream: Hemispheric analysts know that split flow is typical of the Northern Hemisphere and that polar frontal chains may be analyzed with either portion of the flow in various areas. The idea of a "bipolar" jet stream, having a branch on the north and south sides of these splits (involving cut-off highs, lows, blocking patterns, and out-of-phase troughs), runs counter to the polar-front theory of a single boundary throughout the globe, but this theory is not meant to explain wholly the observed hemispheric circulation, one that has yet to be defined in inclusive detail.

Figures 26 and 27 show two polar jet streaks at 300 mb over the United States. The isotach analysis shows clearly two maxima and the 200-mb temperature field in

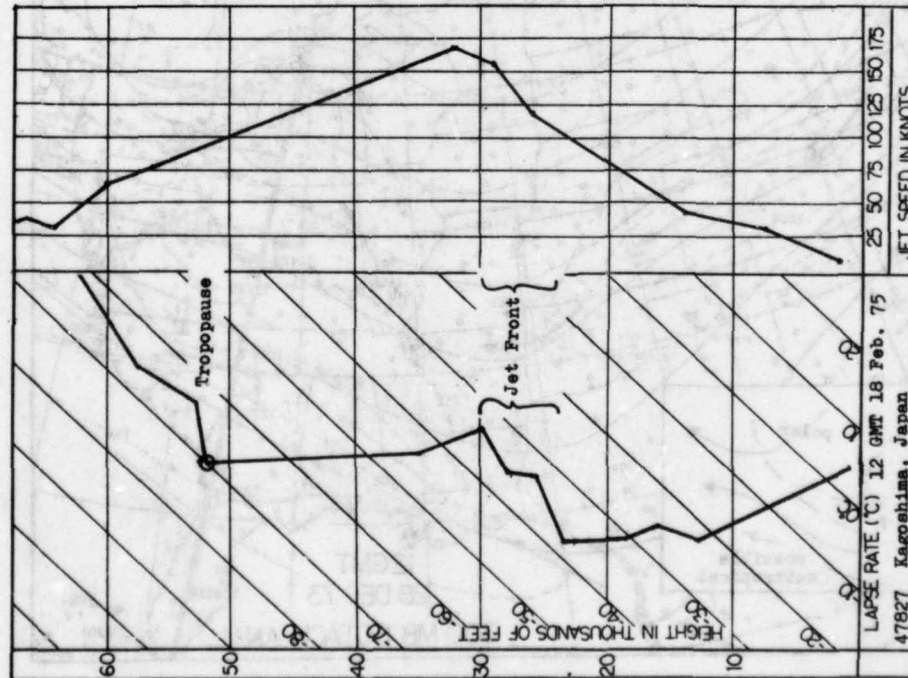


Figure 24. Lapse Rate and Speed Profile for Kagoshima, Japan (47827), Under the Subtropical Jet-Stream Core and Jet Front.

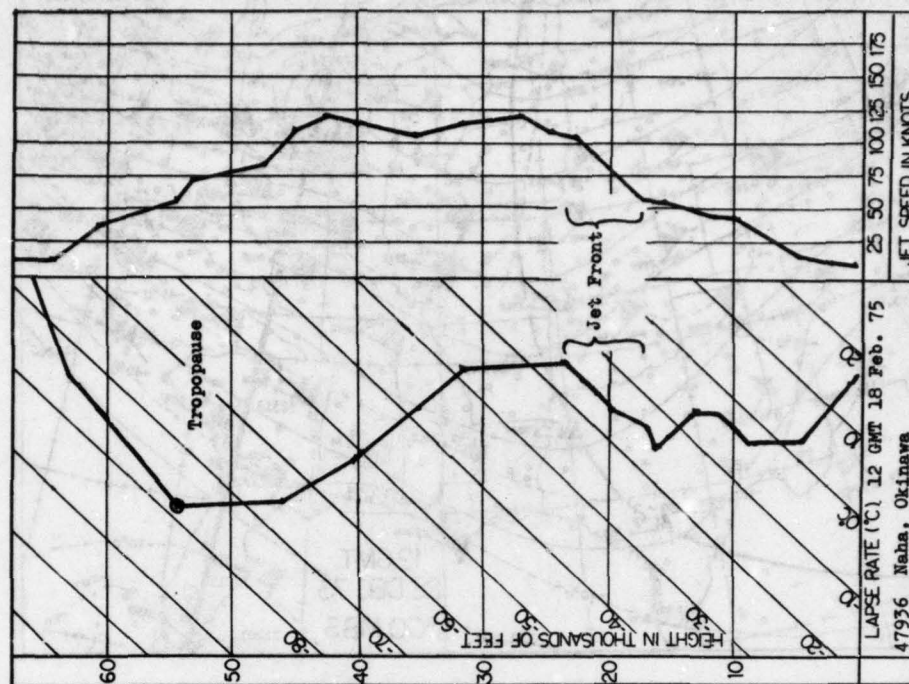


Figure 25. Lapse Rate and Speed Profile for Naha, Okinawa (47936), Showing Low-Level Inversion.

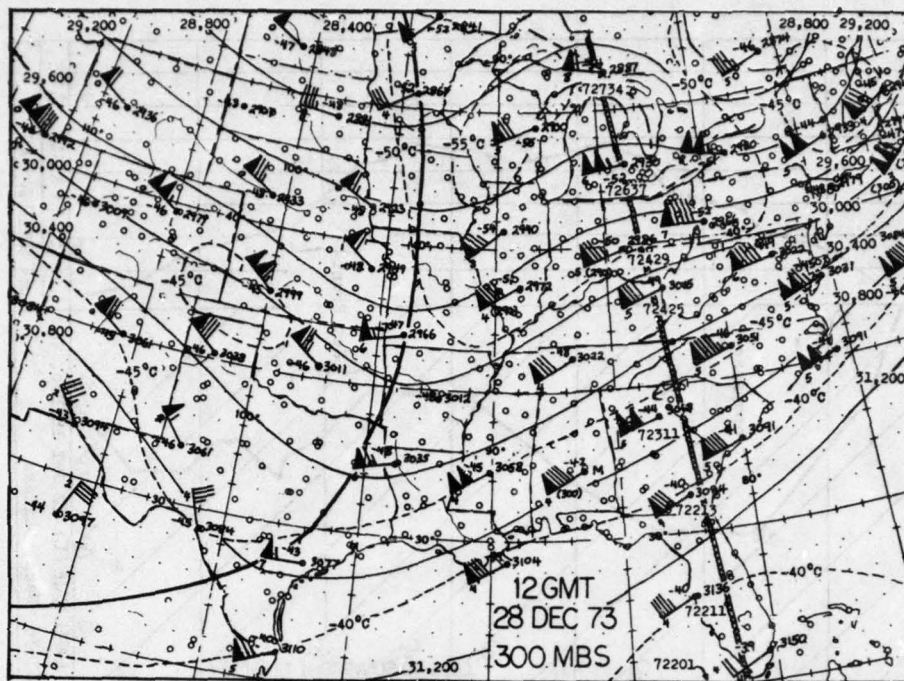


Figure 26. Double Polar Jet Stream (300 mb).

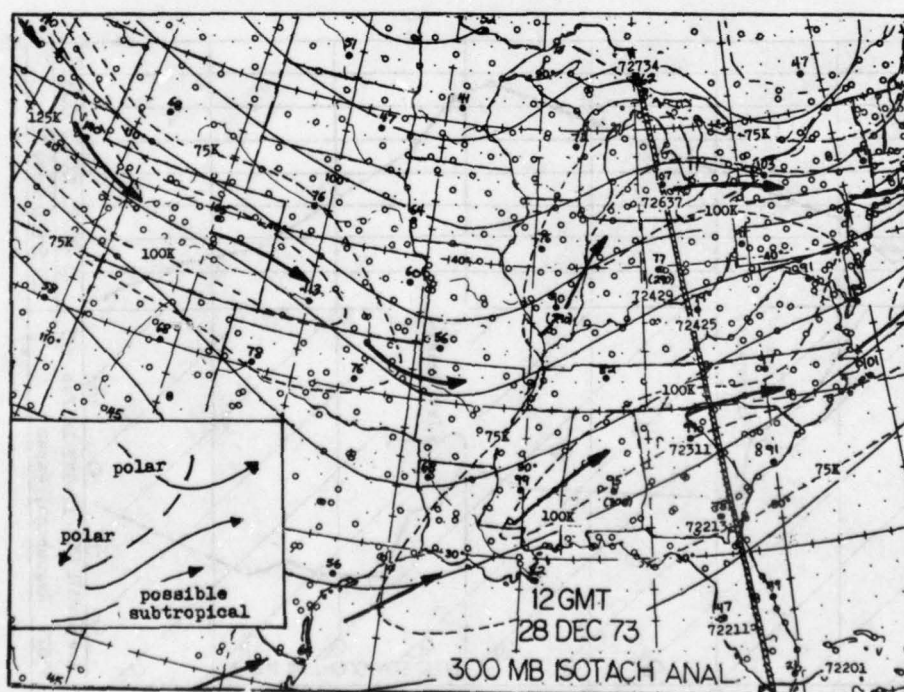


Figure 27. Isotach Analysis of Double Polar Jet Stream.

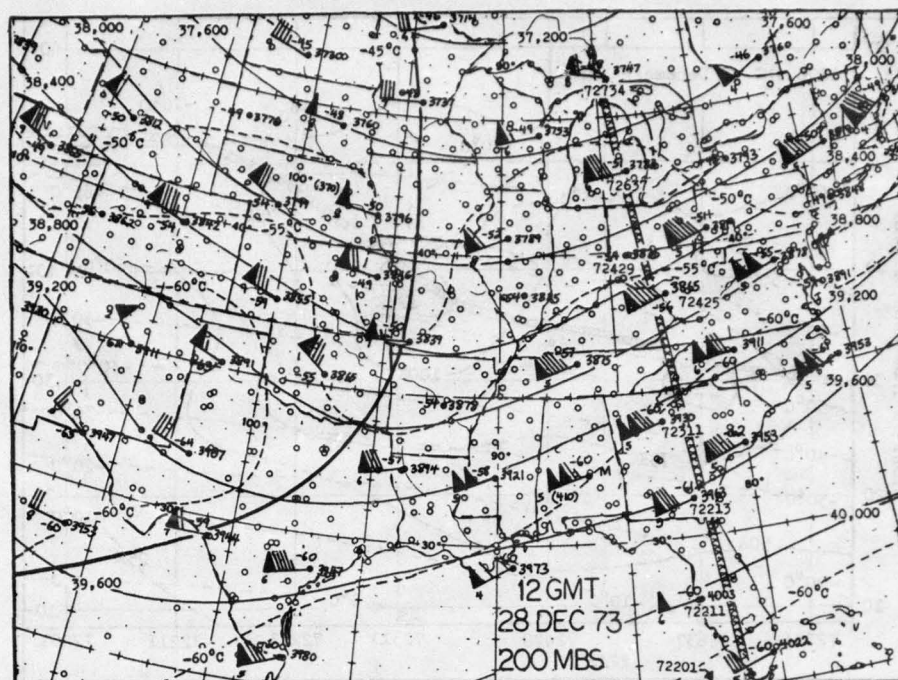


Figure 28. Double Polar Jet Stream (200 mb).

Figure 28 shows the well-ordered field with temperatures below -60°C , even at lower latitudes. The mid-latitude tropopause leaf prevails throughout the analysis area and the jet streaks are polar. The cross section in Figure 29 shows that the tropopause leaves are connected in this instance, indicating relatively weak jet flow. The tropical leaf definitely does not overlie the south jet core. A schematic of this pattern is shown in the inset in Figure 27. It resembles the trailing trough-type pattern except that the subtropical jet is inactive and a polar branch has replaced it. In such cases, some sort of cut-off system such as a low off western Mexico is likely to have split the polar flow. The subtropical jet stream simply has not intensified. This particular pattern can be distinguished only through the 200-mb temperature pattern on standard analyses, a further demonstration of the value of the criteria offered in Section 4.3.

d. Multiple tropopause: This case is an example of various infrequent synoptic patterns that may arise when broad, weak ridging dominates the analysis area. The 200-mb analysis of Figure 30 shows a chaotic temperature field that nevertheless has at least one area at low latitudes where temperatures are -60°C or less. Since the jet flow is well to the north, the jet stream here may be polar. The following cross section (Figure 31) indicates that there is no dominant tropopause leaf near the jet core. The mid-latitude leaf is better developed at 40,000 feet to the south of the jet, which is most unusual. Some semblance of a tropical leaf may overlie much of the area above 50,000 feet. The sounding at Monett, Missouri (Figure 32) is quite complex. In general, if some sort of forecast problem such as turbulence were to arise, all of the resources of the forecaster would be taxed. Fortunately, the criteria indicating a polar jet stream seem to prevail (note the 200-mb temperature field), a severe test that the criteria have again surpassed.

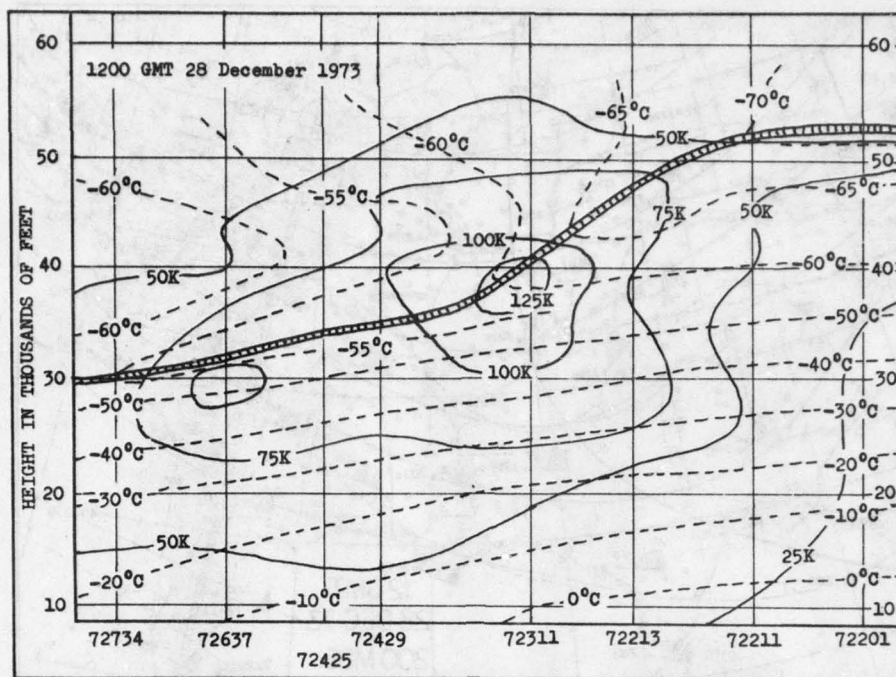


Figure 29. Cross Section of Double Polar Jet Stream.

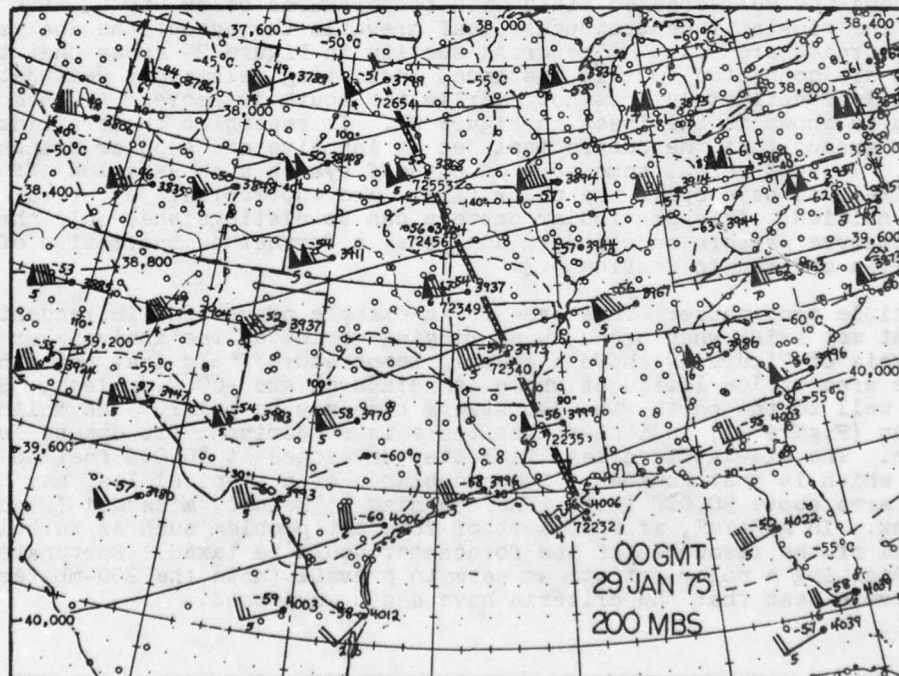


Figure 30. Polar Jet Stream with Multiple Tropopause.

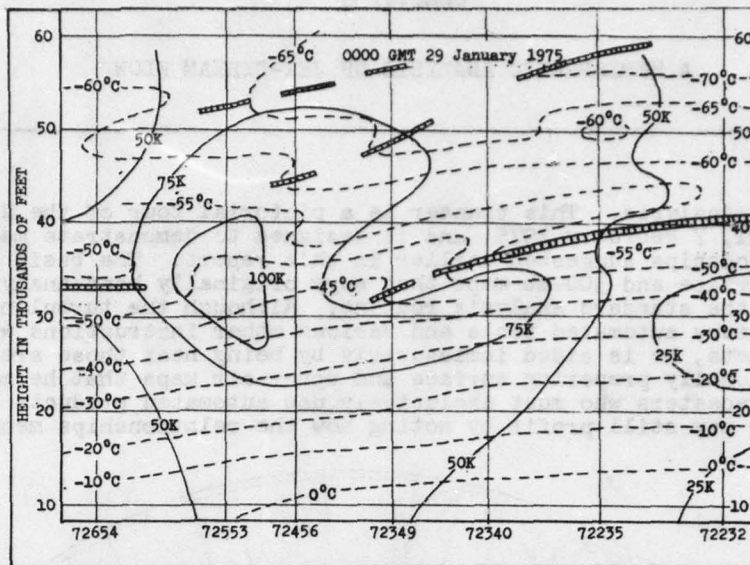


Figure 31. Cross Section of Polar Jet Stream with Multiple Tropopause.

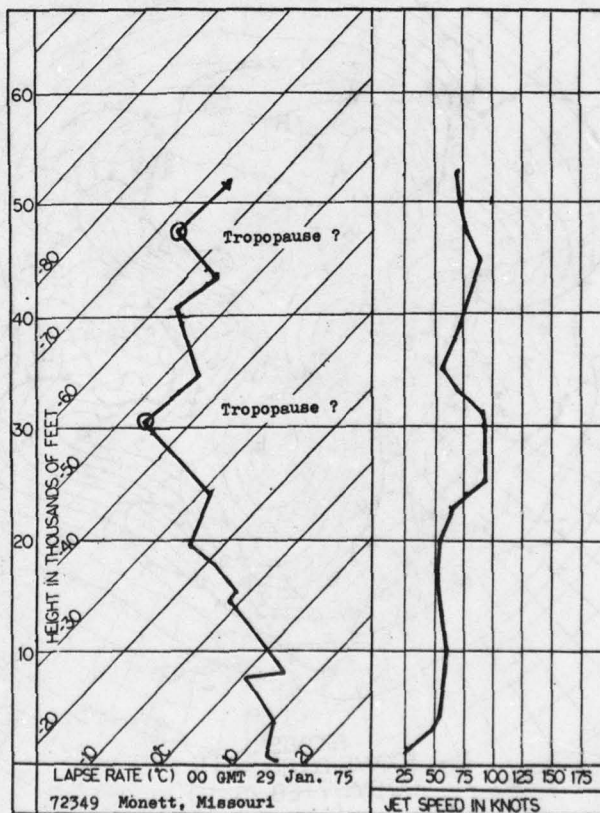


Figure 32. Lapse Rate and Speed Profile for Monett, Missouri (72349), Under the Multiple Tropopause.

Chapter 5

A HEMISPHERIC ANALYSIS OF JET-STREAM FLOW

5.1. Hemispheric Analysis. This chapter is a pictorial tour of the Northern Hemisphere for 0000 GMT, 7 February 1975, and is designed to demonstrate many of the techniques and relationships suggested earlier in this report. The basic analyses used here are AFGWC surface and 300-mb maps that were originally hand-analyzed and produced as part of the standard analysis routine. Although the turbulence forecaster is provided with many automated tools and various other instructions with which to produce his products, he is aided immeasurably by being near those areas where analysts are personally preparing surface and upper-air maps that he may reference and discuss. Forecasters who must exclusively use automated products over a limited area of the globe may still profit by noting how the relationships mentioned through-

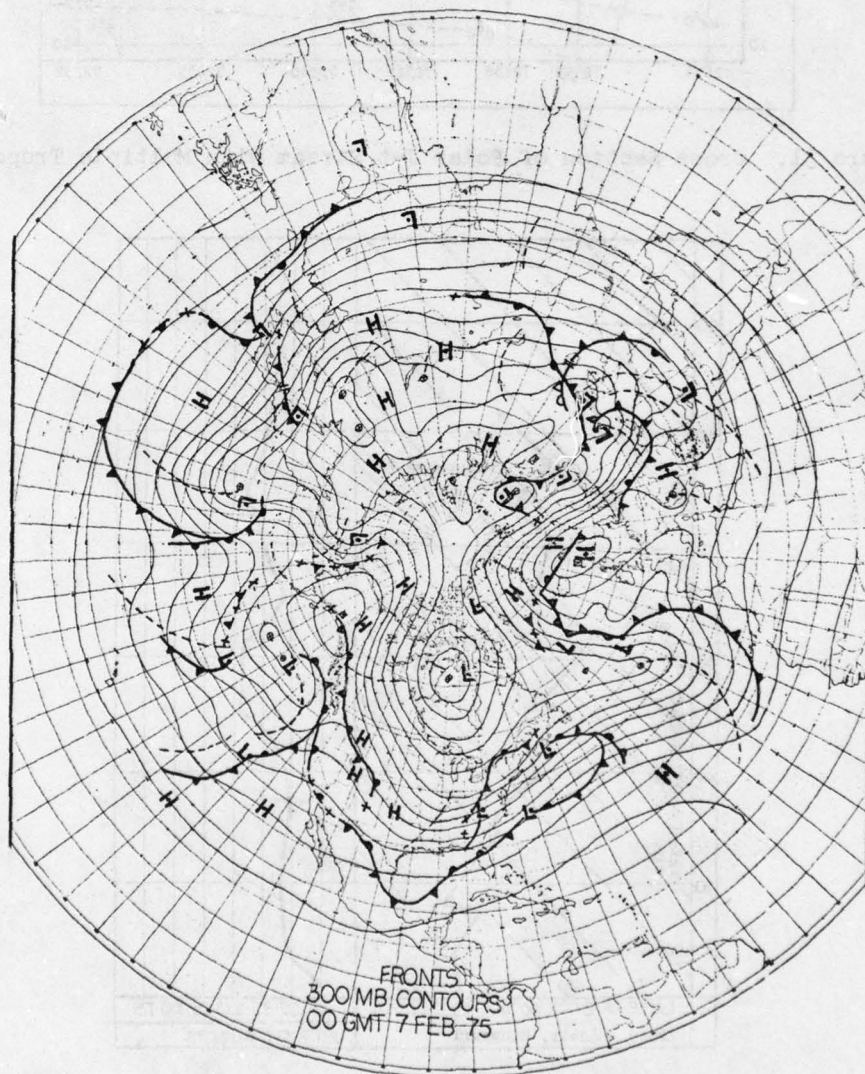
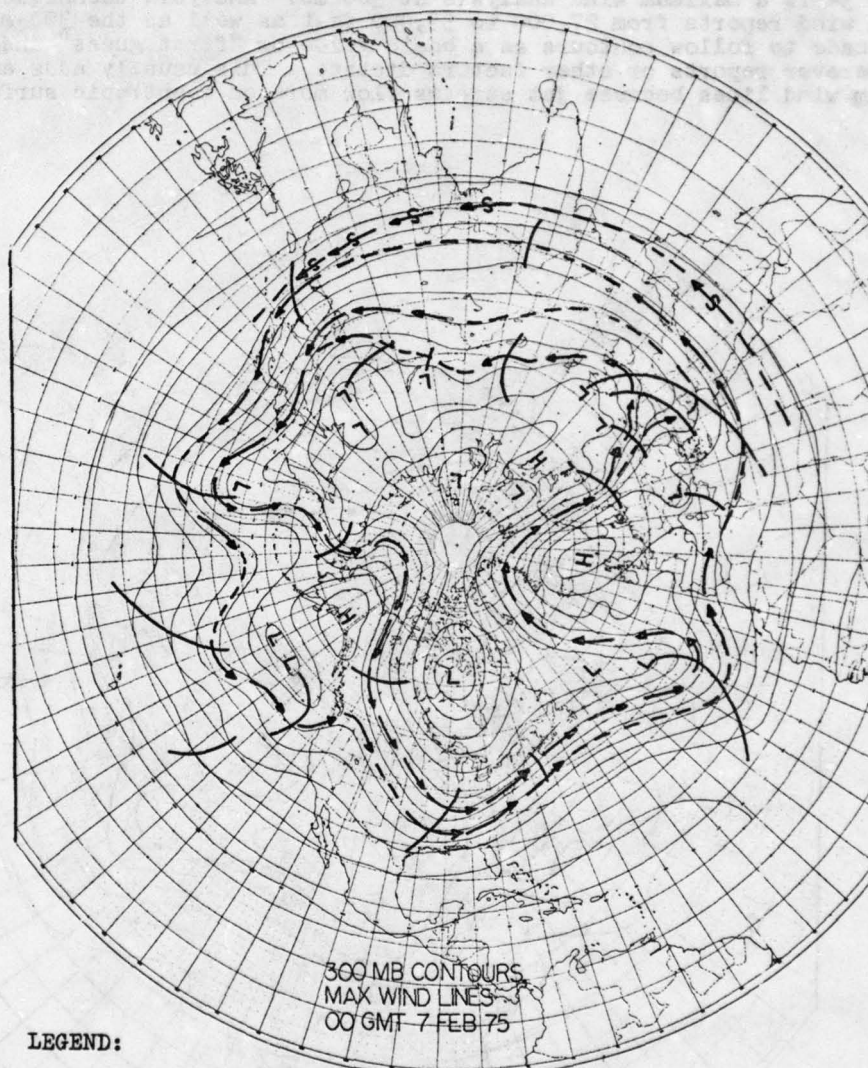


Figure 33. Surface and 300-mb Analysis Composite.

out this report actually look when applied to the test of a real situation, one that has been selected at random for this paper.

Figures 33 through 37 demonstrate analyses and composites important to this section. Figure 33 shows the surface and 300-mb pattern, marked by a wide variety of noteworthy features. North America is dominated by a deep Hudson Bay Low which passes for the Icelandic Trough in this instance. A medium-sized blocking high lies over Alaska in a position typical of this occasional winter feature. A moderate amount of flow is passing over the top of the high and several surface lows are moving into the United States under it, so this high is not a formidable obstacle to westerly flow. A strong, broad ridge with good jet flow lies over the Western Atlan-



LEGEND:

- Maximum Wind Line (polar jet stream) —————→
- Subtropical jet-stream maximum wind line ————S———→
- Weak or marginal wind maximum, meant to suggest continuity of a flow over the globe - - - - -

Figure 34. Maximum Wind Analysis.

tic, but the flow then turns almost entirely north around a very large European blocking high. Surface systems in their usual form are unable to survive the passage over this high so Eastern Europe is continually under the influence of polar out-breaks associated with the remnants of these systems. The Caspian Sea Trough is about normal in appearance and as usual it trails into the Mediterranean. The Asian circulation is frequently marked in winter by a band of winds north of the Himalays, but the flow in this case is unremarkable. The Aleutian Trough is not particularly deep on this day. The Pacific Ocean is under a series of occluding systems. Because of the lack of upper-air data, surface analyses and satellite pictures are normally used to model the upper-air analysis, resulting in a moderate degree of smoothing. This presents a particular problem to turbulence forecasters.

Figure 34 is a maximum wind analysis at 300 mb. Analysis techniques include the use of all wind reports from 27,000 to 33,000 feet as well as the 300-mb data. Efforts are made to follow contours as a basic guide or "first guess" and then to deviate wherever reports or other factors dictate. This usually adds amplitude to the maximum wind lines because jet streams flow more on isentropic surfaces than on

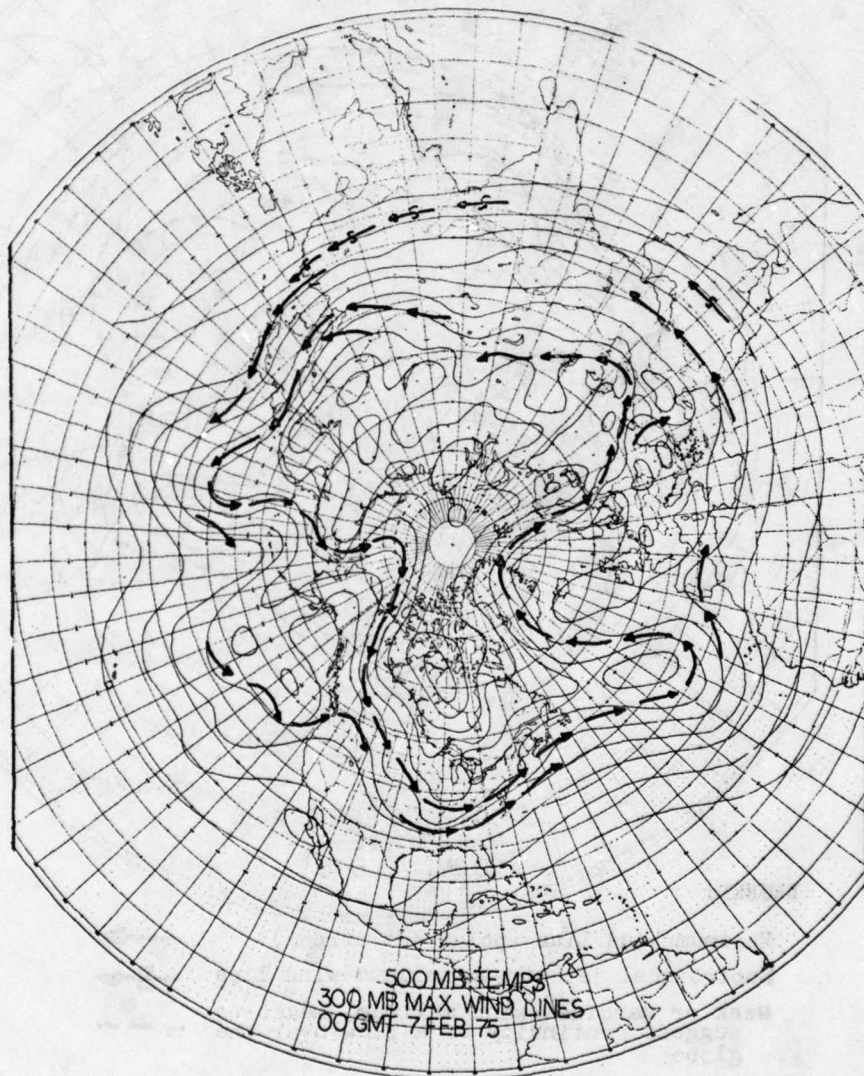


Figure 35. An Example of the Thermal Wind Relationship.

constant-pressure surfaces (as mentioned in Section 3.9). The deviation of the maximum wind line from the jet core at 300 mb is trivial throughout almost the entire hemisphere with this map scale.

The maximum wind analysis shows almost two continuous polar jet streams with some indication of subtropical flow (see the legend with Figure 34). It is not necessarily implied that the polar jet stream is a double flow. It does, however, split readily around significant cut-off systems such as the blocking highs in this pattern. Downstream of the split, the jet branches may or may not rejoin as they draw near. More times than not it is impossible to detect more than one maximum wind line in strong, broad flow (such as in the Western Atlantic), so a double line in that area is inappropriate. On the other hand, the weak pattern over Asia invites the analysis of many maximum wind lines.

The thermal wind relationship states that wind flow must increase above a horizontal temperature gradient and it was further mentioned in Section 4.2 that the polar front is marked by a thermal ribbon about much of the hemisphere. The 500-mb

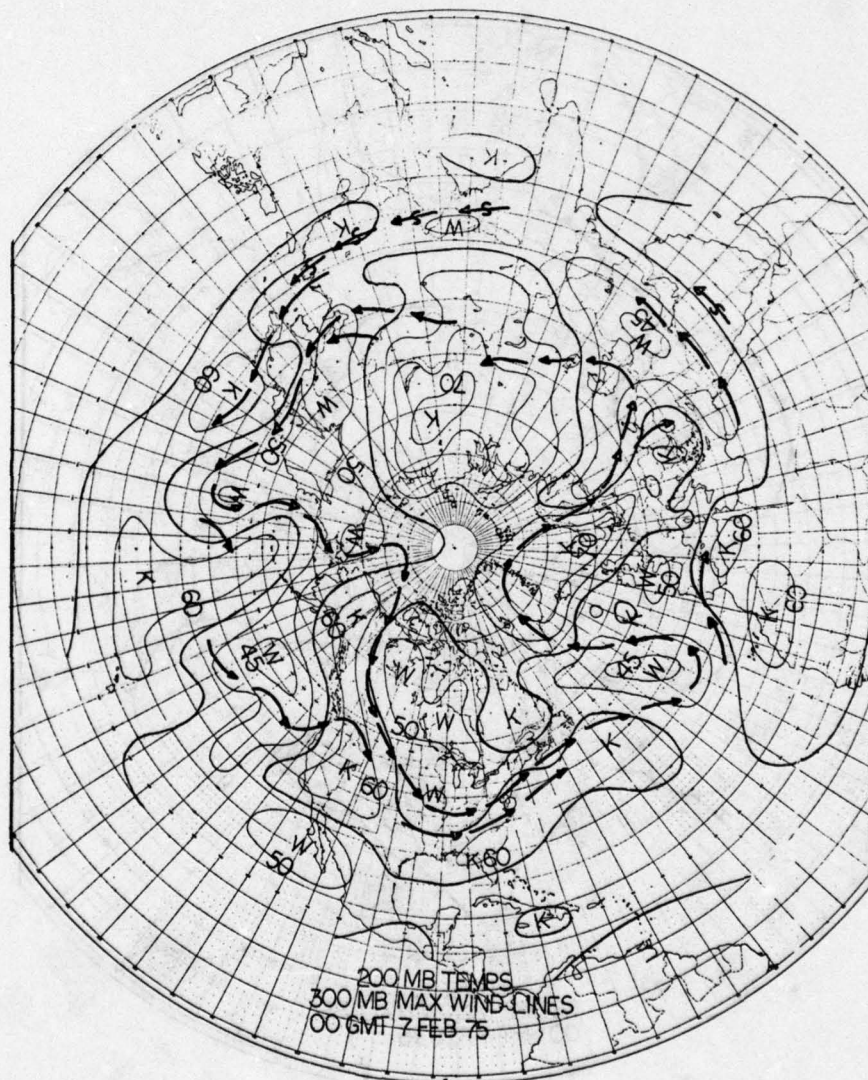


Figure 36. Identifying Jet Streams from the 200-mb Temperature Field.

temperature analysis in Figure 35 shows little evidence of an unmistakable hemispheric thermal ribbon because of the 5°C increments and the problems of assessing gradients over the data voids of the oceans, but concentrations of the gradient are apparent in the Mississippi Valley to the east of the blocking highs in Alaska and Europe and near North Korea. Note that the maximum wind lines do tend to demonstrate the thermal wind relationship. Part of the problem in performing maximum wind analyses may be in the concept of jet-stream flow. If it is thought of as an entity which tends to sustain and preserve itself, it might be logical to assume that the jet stream is a continuous band of flow that must be detectable by some means everywhere. If, however, the jet stream is thought of as a response to the intensity of the polar front, as indicated by the horizontal temperature gradient, it becomes easier to expect accelerated flow wherever perturbations are developing. Split flow may be the result of accelerations occurring on either side of a feature as much as by a physical dividing of the flow. Rejoining jet flow may not be so much a mending of the split as a general flow accelerated by a wide-reaching influence downstream from the split. In summary, maximum wind analyses become much easier to perform when the true nature of the jet stream is firm in the mind.

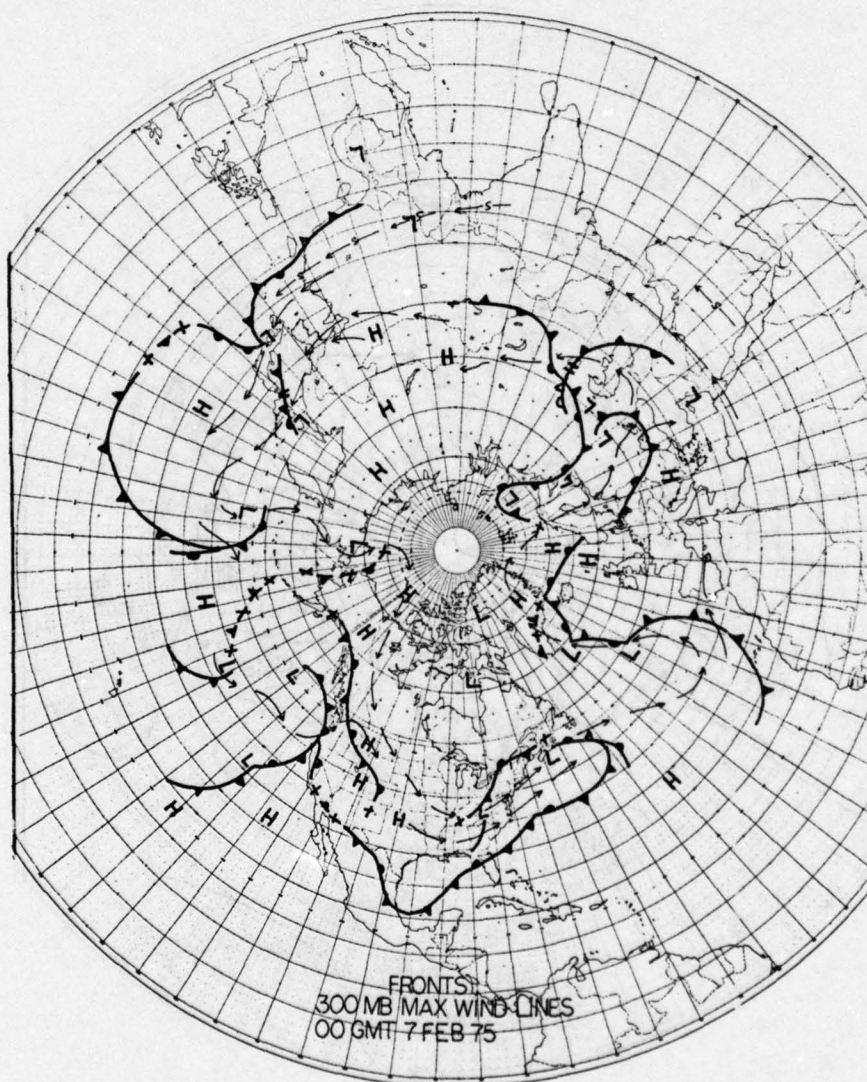


Figure 37. Relating Fronts and Maximum Wind Lines.

Figure 36 is a 200-mb temperature analysis upon which the maximum wind lines are superimposed. From the criteria of Section 4.3, it appears that this level helps to identify the tropopause leaf over a jet streak and thus the streak itself. Temperatures below -55°C identify the mid-latitude tropopause leaf and thus a polar jet streak.

Over North America, a cold pool of air from the southwest to Alaska identifies the mid-latitude leaf. Both jet streaks in this area should be polar. Cold air over Florida south of the streaks reinforces this. In Europe, the maximum wind lines split, but both progress over temperatures below -60°C . Central Asia is an anomaly because very cold temperatures here are in response to the polar night vortex, a purely Arctic phenomenon seen only in winter. Both maximum wind lines pass through more cold air in the Central Pacific, so it appears that the polar jet stream is split throughout much of the hemisphere in this basically meridional pattern. A closer look at this conclusion will be made in the following section.

Figure 37 relates maximum wind lines to surface fronts. One well-known rule of satellite interpretation is that jet streaks cross the triple or occlusion points of polar frontal systems. Streaks usually cross over just north of moderate open waves, but may be several degrees north of a weak low-amplitude wave. It has been possible here to connect just about every tripple point and moderate low with maximum wind lines. Note that over Japan, both maximum wind lines link different polar frontal systems. One powerful argument for a "bipolar jet stream" is the daily occurrence of double and (usually) unrelated frontal chains over much of the hemisphere in winter, e.g., in the Pacific where surface systems are passing to both sides of the high.

The Western Atlantic occlusion is an interesting case often seen in mid-ocean under strong, broad jet-stream flow. The front lies under the ridge and a maximum wind line rides over the entire system. Satellite pictures may sometimes hide such occlusions with a jet cirrus shield. This occlusion does not extend to high levels and is difficult to link to jet-stream flow unless it is noted that the triple point is obviously progressing quickly eastward, apparently under the southern maximum wind line. It is still connected across the United States to another system so linked. In general, the same maximum wind line connects all parts of a polar frontal chain, the exception being a trailing cold front such as off western Mexico. If a cut-off low develops near Hawaii and a wave generates, it will in all likelihood be influenced by a different flow.

The fronts in Europe link up fairly well, although the cold front over the Black Sea seems to lie on both sides of jet flow. Either the flow is indistinct here or the front should be partly occluded. The Siberian High precludes any Asian discussion.

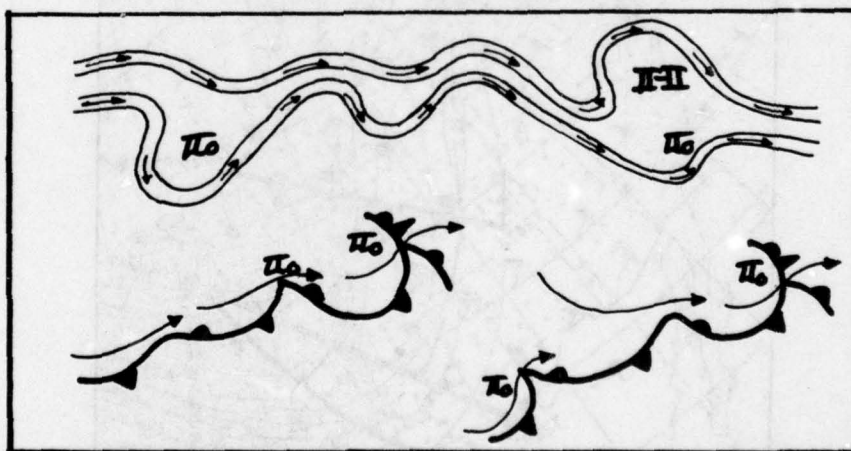


Figure 38. Relating Maximum Wind Lines to Split Flow and Frontal Systems.

Figure 38 shows how maximum wind lines might lie on either side of splits in the westerly flow and also over polar frontal chains. The maximum wind lines need not be obvious throughout split flow nor over all polar frontal chains, but a certain con-

tinuity exists that helps the analyst locate these lines in data voids and to connect the jet stream about the hemisphere.

5.2. A Closer Look at Portions of the Hemisphere. Figure 39 shows an instance of parallel maximum wind lines upstream from the trough over the Midwest. As the two following cross-sections (Figures 40 and 41) show, there are indeed two jet cores, both of which are polar. Neither is strong. There is but one tropopause above and one sign of weakness is when the leafs are fused together. Note that the strength of the jet cores varies in that the north core is gradually being absorbed by the higher, stronger south core.

Figure 42 shows the Eastern United States east of the trailing trough in the Midwest. The following cross section (Figure 43) shows a much more developed flow complete with jet front and winds over 150 kt. Only a single maximum wind line can be appropriate at 300 mb east of the trough. There is a hint of subtropical flow in the small maximum over Waycross, Georgia (72213) in the cross section despite the clear dominance of polar jet flow. Note that even here a nearly equal flow lies just below the tropopause. The basic polar jet-stream configuration is a variation of that in panel A of Figure 18. This pattern often presents an analysis problem and is the subject of controversy.

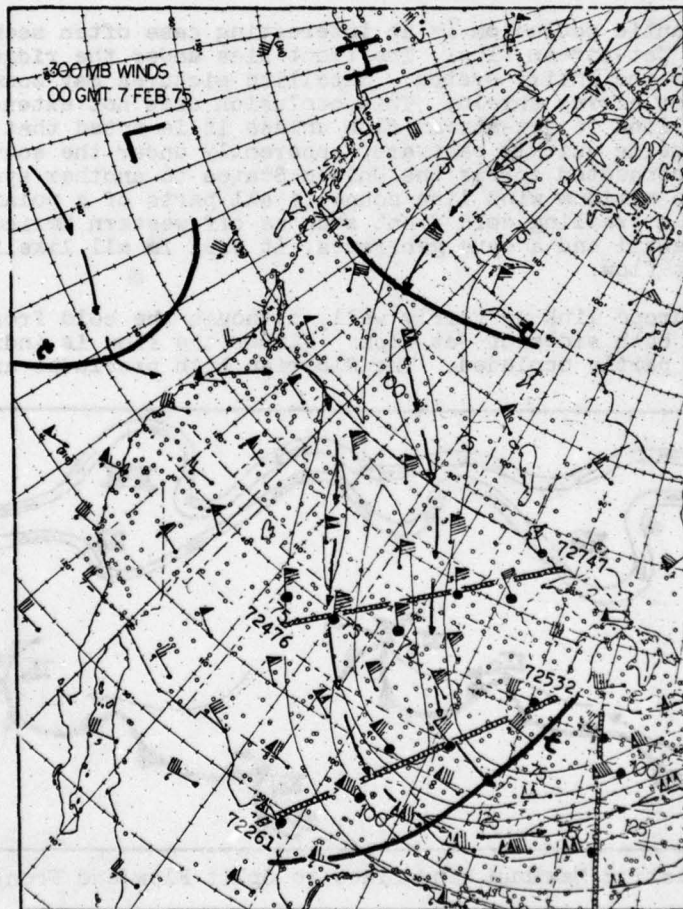


Figure 39. 300-mb Wind Analysis, Western United States.

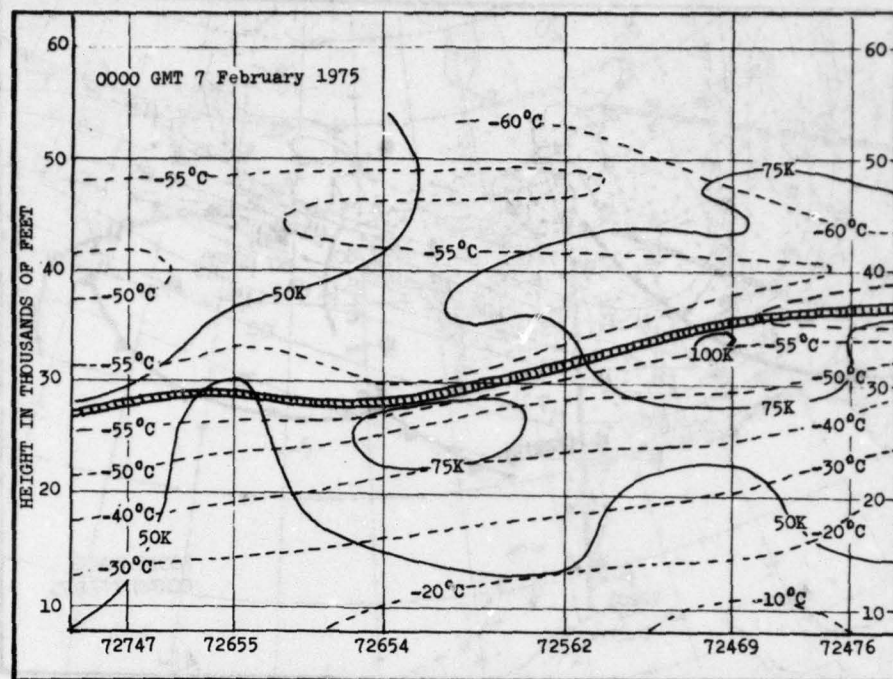


Figure 40. Cross Section Through International Falls, Minnesota (72747) to Grand Junction, Colorado (72476).

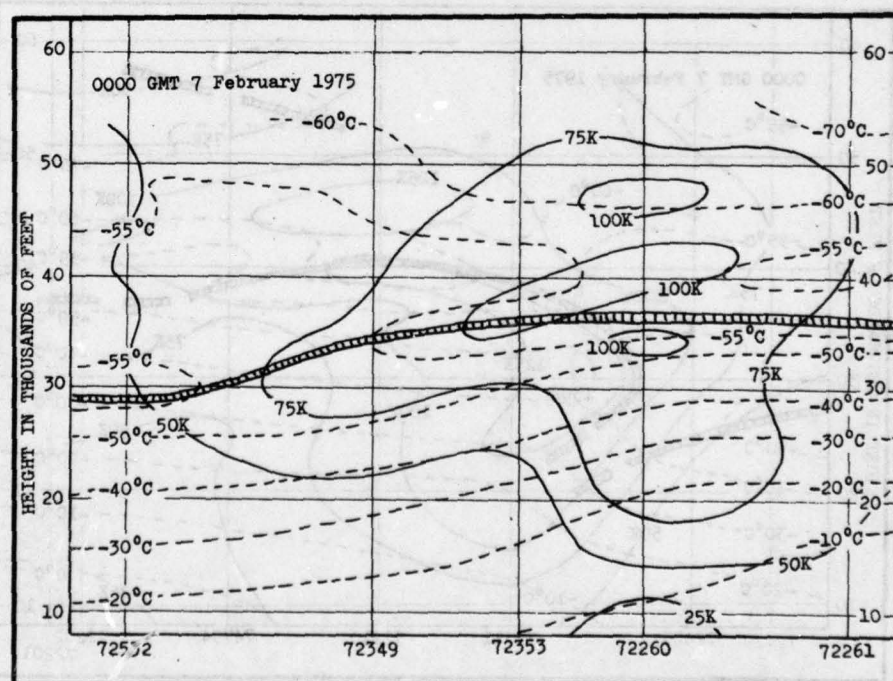


Figure 41. Cross Section Through Peoria, Illinois (72532) to Del Rio, Texas (72261).

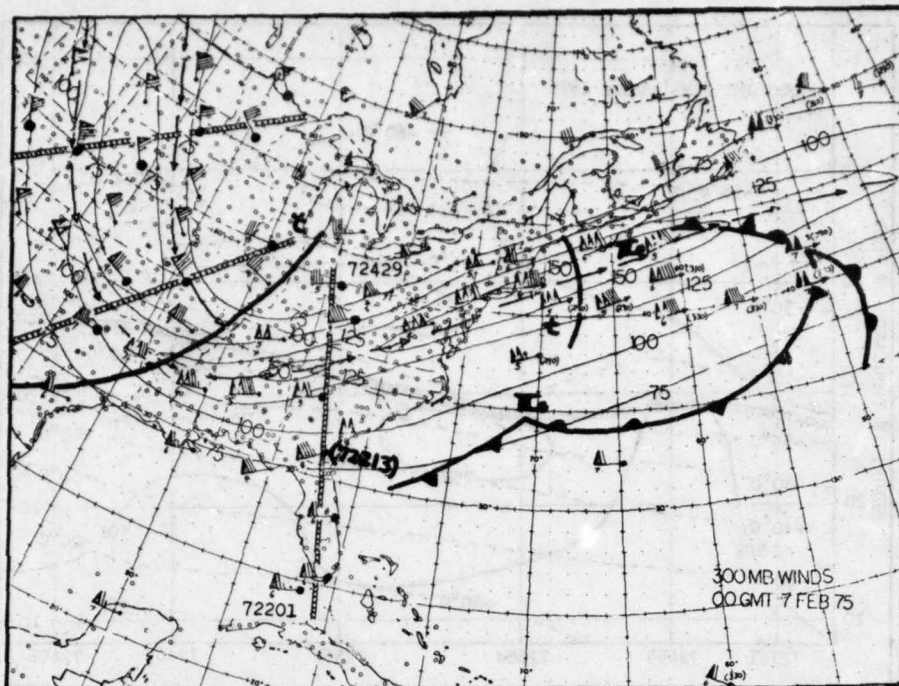


Figure 42. 300-mb Wind Analysis, Eastern United States.

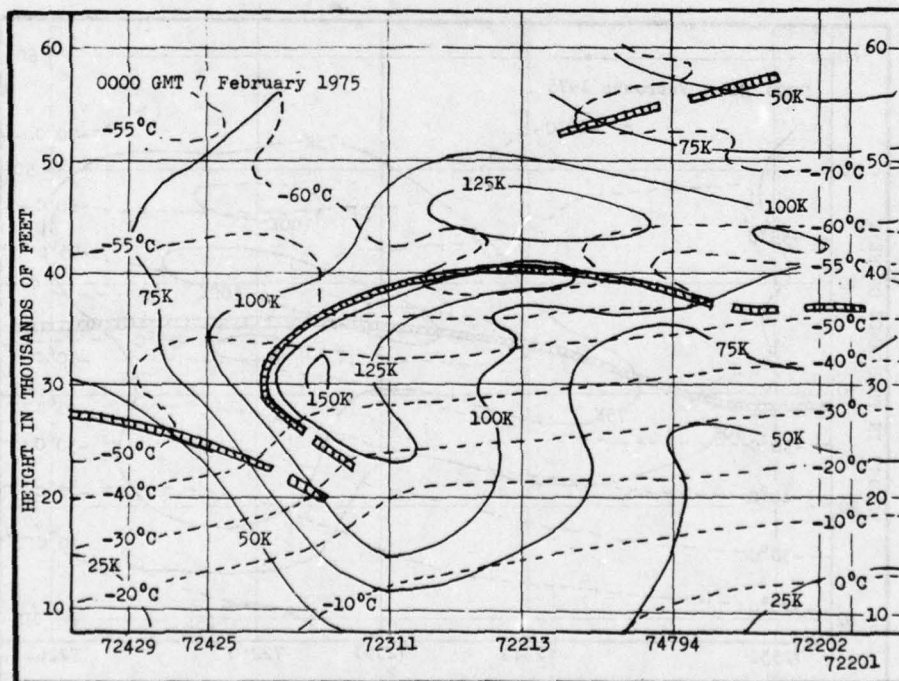


Figure 43. Cross Section Through Dayton, Ohio (72429) to Key West, Florida (72201).

Figure 44 shows some of the nature of the strong flow into Eastern Europe downstream of the great North Atlantic blocking high. Small, fast-moving turbulence fields may be detected in minor waves progressing through such flow and the forecaster may be hard-pressed to forecast future intensity and positions of such features, when they are detected at all. In the United States, one valuable tool is the National Meteorological Center (NMC) vorticity analysis and forecast, always available to forecasters at AFGWC.

Figures 45 and 46 are two cross sections in this northwesterly flow. Two important points are apparent. First, the jet core descends significantly in northerly flow, in this case 10,000 feet with 7° of latitude. Secondly, despite the complex maximum wind analysis, the cross sections show relatively smooth jet cores. The variation in sensing devices between countries may have much to do with the difficulty of determining the real maximum wind lines. Analysts sometimes are tempted to detail every little maximum in such cases. The fact is that wind analyses at constant-pressure surfaces are not always helpful. Only a cross section would suffice in such a case.

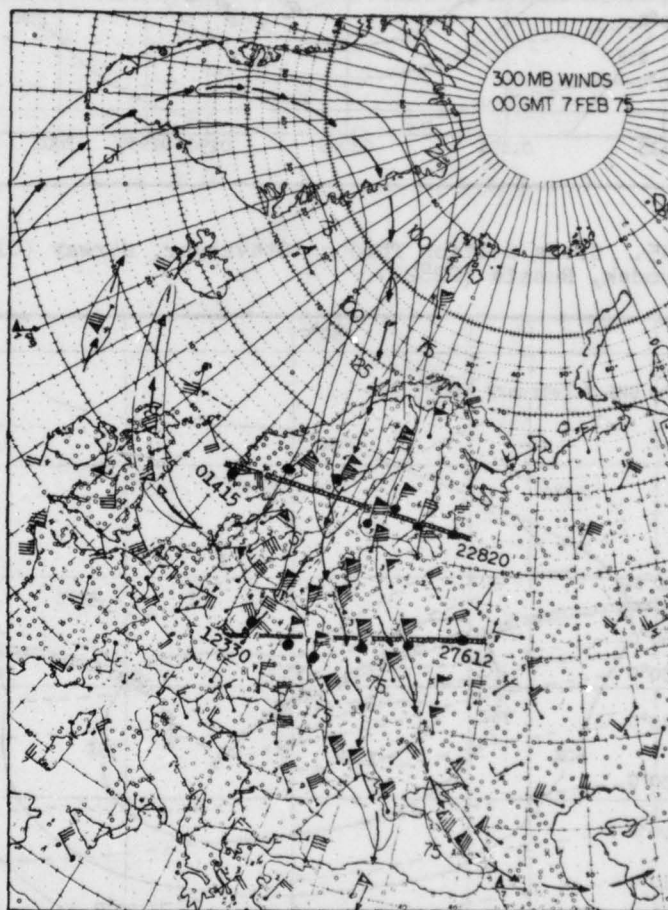


Figure 44. 300-mb Wind Analysis, North Atlantic-Europe.

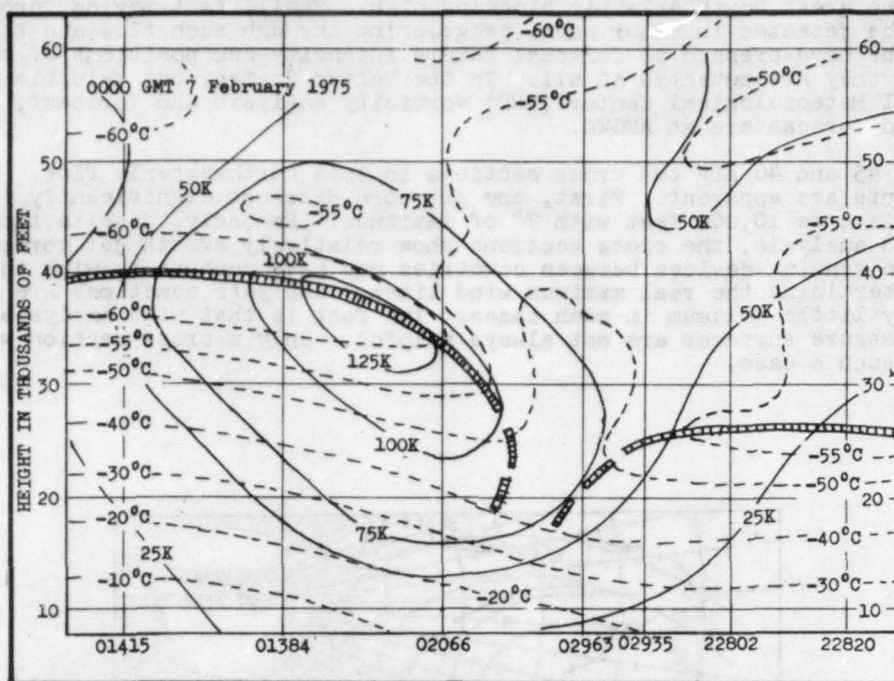


Figure 45. Cross Section Through Stavanger, Norway (01415) to Petrozavodsk, Russia (22820).

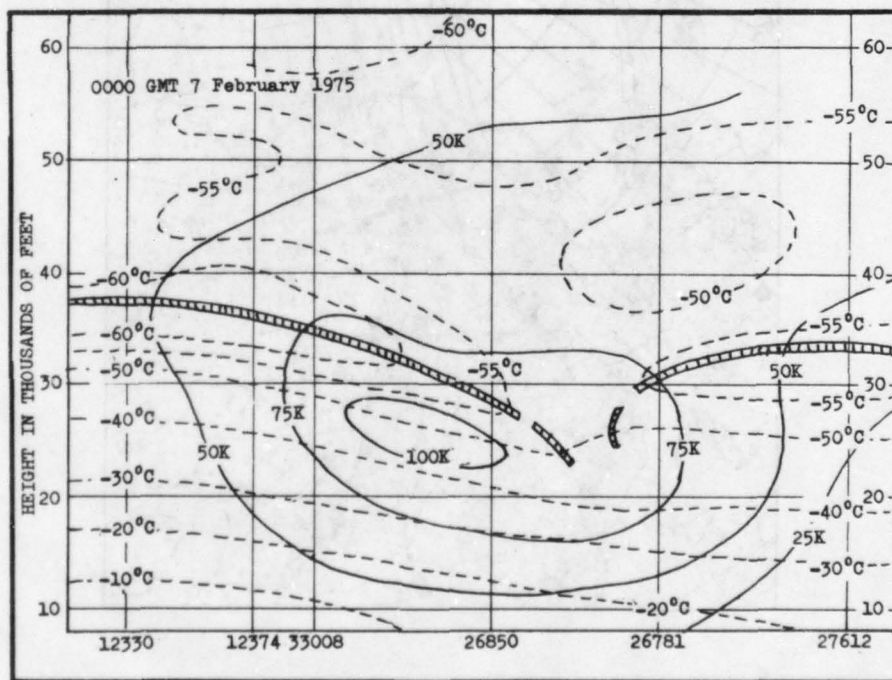


Figure 46. Cross Section Through Poznan, Poland (12330) to Moscow, Russia (27612).

Figure 47 shows another complicated pattern over China with three cross sections designed to locate the main jet cores. The complex flow over Asia, further obscured by a poor data field in some areas, usually regroups into a well-defined jet maximum in the Aleutian Trough, but analysts may have difficulty in linking this flow with that upstream in Europe. As usual, the cross sections show a simpler pattern. The westernmost sectional (Figure 48) shows a single significant core, but two show up in the next cross section (Figure 49). The last (Figure 50), over Japan, shows that the new northernmost core is now dominant, a further indication of split flow. As was the case in the Eastern United States, there is some indication of weak subtropical jet flow, though a jet core is not obvious. This jet stream is not an important part of the hemispheric circulation on this date.

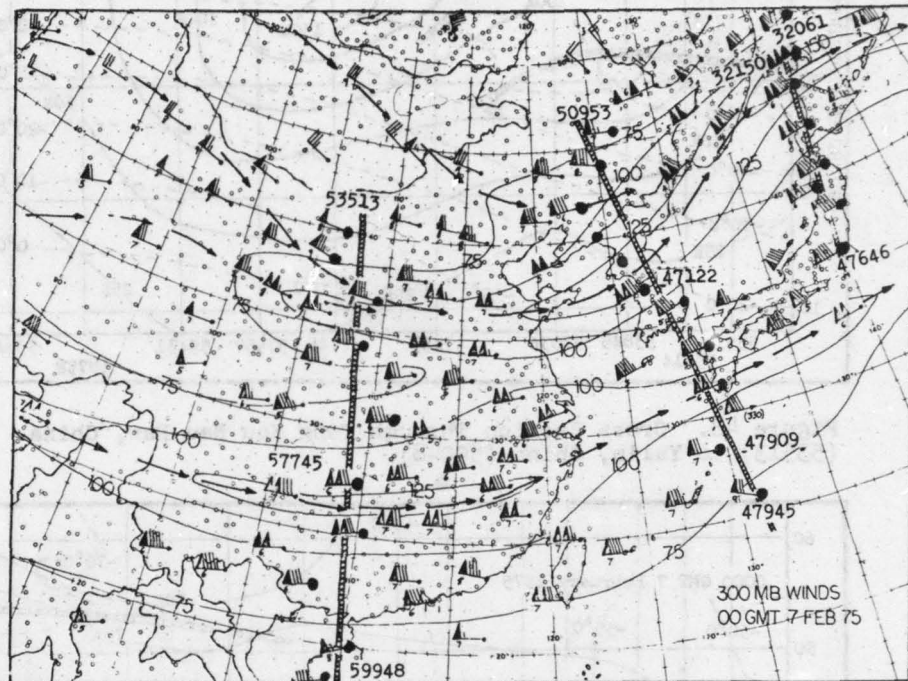


Figure 47. 300-mb Wind Analysis, Western Pacific-Japan.

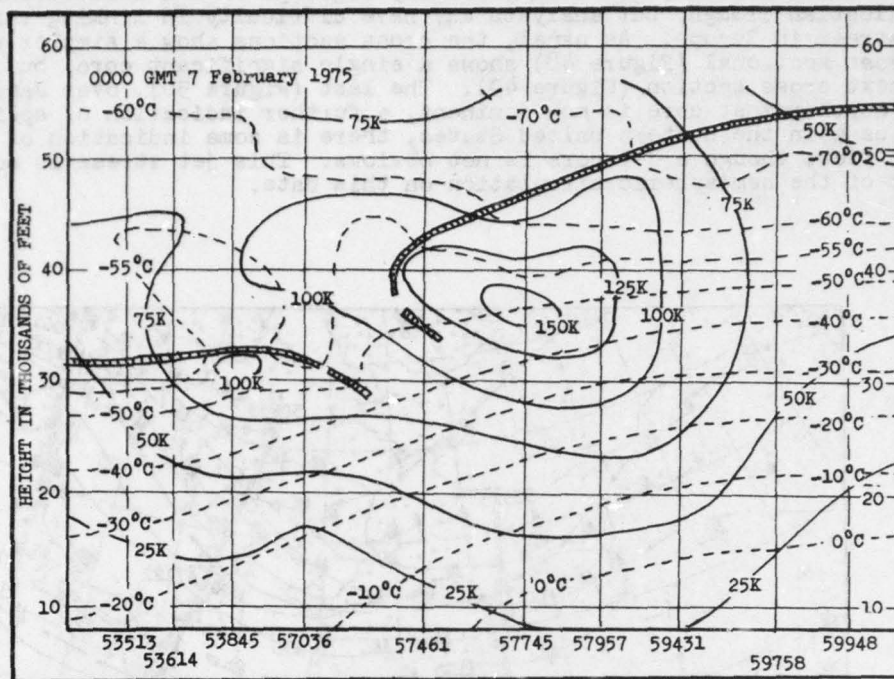


Figure 48. Cross Section Through Teng Kou Nau Pao, China (53513) to Yulin, China (59948).

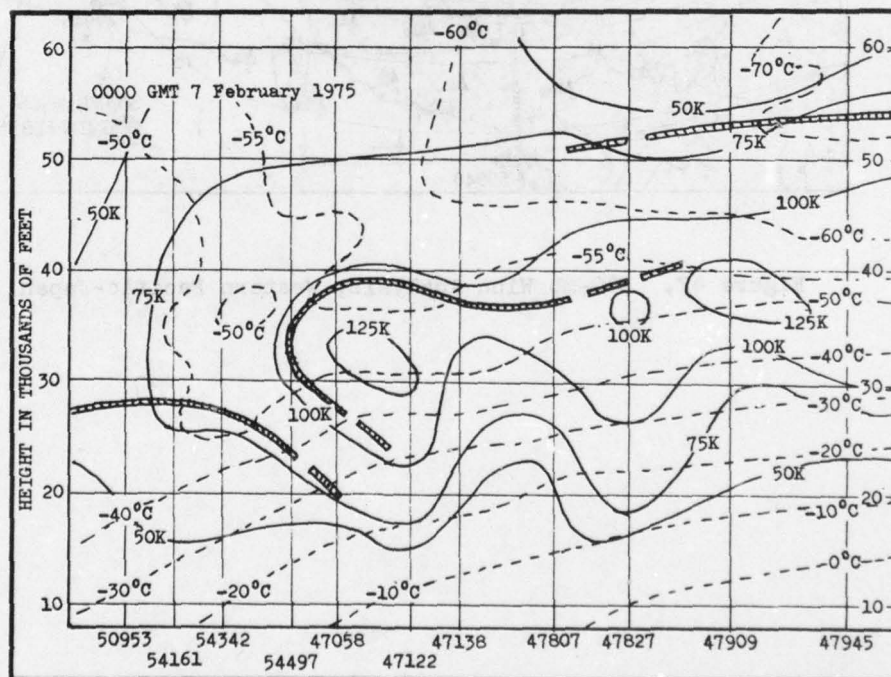


Figure 49. Cross Section Through Harbin, China (50953) to Minamidaitojima, Japan (47945).

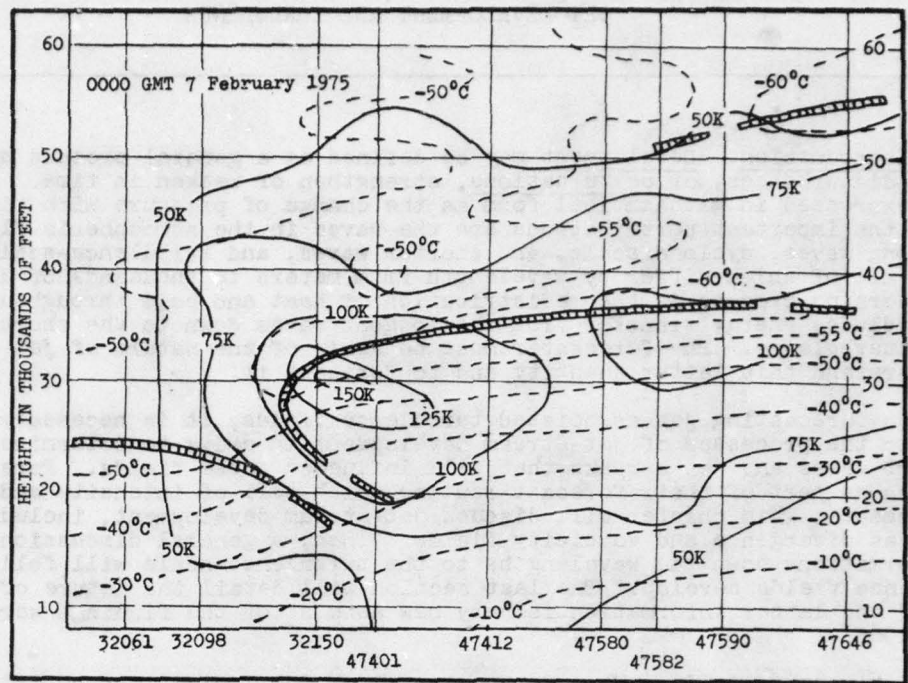


Figure 50. Cross Section Through Aleksandrovsk, Sakhalin (32061) to Tateno, Japan (47646).

JET DEVELOPMENT AND TURBULENCE

6.1. Introduction. Development may be defined as a general process by which atmospheric disturbances, or perturbations, strengthen or weaken in time. It is sometimes expressed in mathematical form as the change of pressure with time. In this report the important perturbations are the waves in the atmospheric flow that constitute long waves, cyclone scale, and shorter waves, and turbulence-scale gravity waves, all of which differ by wavelength from meters to thousands of kilometers. The governing process is the redistribution of heat and cold throughout the hemisphere that includes energy transfer from the longest waves down to the shortest, culminating in turbulence. The forecaster must be aware of the nature of jet flow in order to understand this latter quantity and to forecast it.

When forecasting jet-associated turbulence fields, it is necessary to go backwards to the processes of jet-stream development in order to determine the intensity of short waves and jet streaks that will influence these fields. Forecasters use analyses as part of their forecast routine which tell of intensity and hint of future development. This chapter will discuss jet-stream development, including such indicators as divergence and vorticity fields. Then, a general discussion of energy transformations down the wavelengths to the turbulence scale will follow to show how turbulence fields develop. The last section will detail the nature of these fields. Much of the latter information is very new as most of the findings were arrived at after 1965.

6.2. Divergence Fields. When forecasters look for indications of intensity in upper-air features they reference forecast tools based in part on divergence and vorticity. Divergence is the least familiar of the two quantities since vorticity maps are more commonly used. However, divergence is particularly important to any understanding of development because of its direct relation to vertical motions. Vertical motion completes the three-dimensional circulation of pressure systems which forecasters see as horizontal depictions. Vertical motions indicate instability and influence condensation and precipitation as well.

The relationship of divergence to vertical velocity may be approximated as:

$$\text{Divergence} \sim - \left(\frac{\text{change in vertical velocity}}{\text{with changing pressure}} \right) \sim - \left(\frac{\Delta w}{\Delta p} \right)$$

where: $w > 0$ for ascending air

$w < 0$ for descending air

$\Delta w > 0$ for accelerating upward and decelerating downward

$\Delta p < 0$ for ascending air

$\Delta p > 0$ for descending air

From this relationship, a three-dimensional scheme of divergence fields about highs and lows may be constructed by noting the way the expression changes throughout the circulation. Panel A of Figure 51 shows a circulation in which the divergence fields at both low and high levels in the tropopause may be detailed through the relationship. The scheme, however, implies that pressure centers are also centers of divergence. This is not so. Panel B shows the combined vertical and eastward flow across such a cross section (an adaptation from Haltner and Martin [15]), that shows that the vertical-motion fields change in direction through ridge and

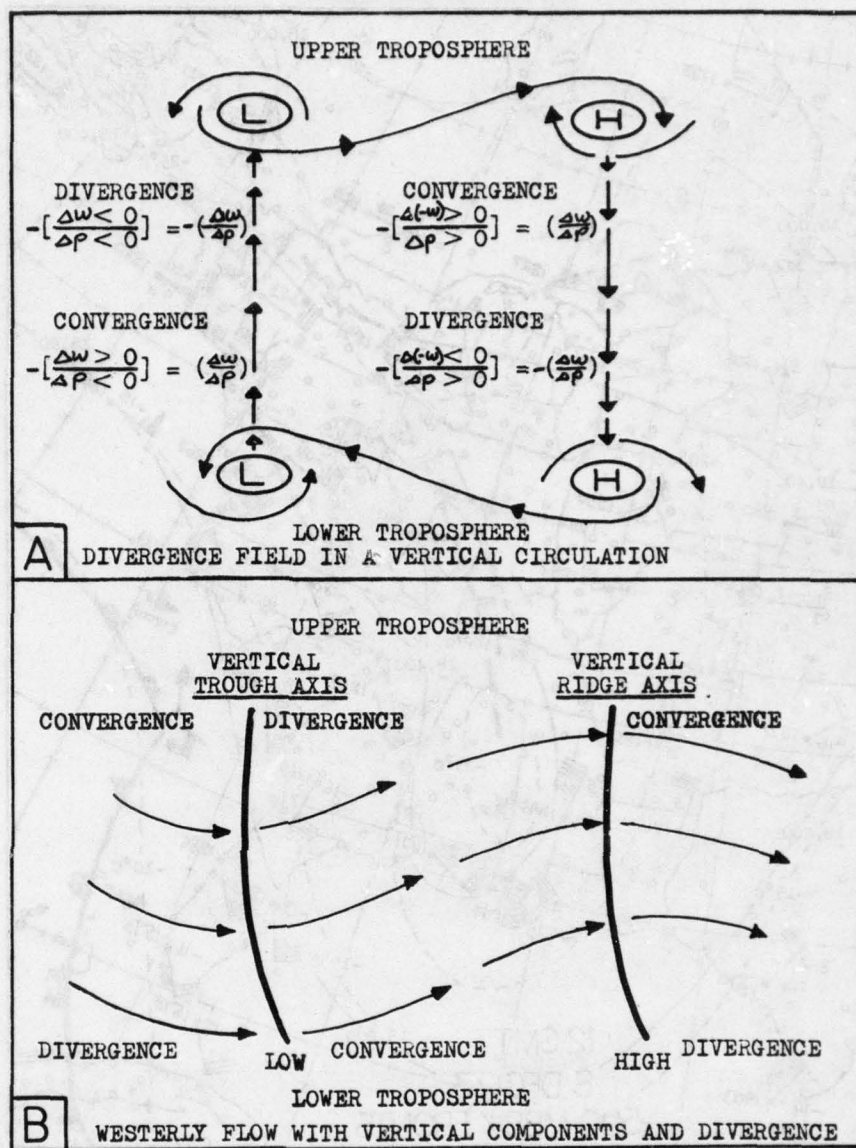


Figure 51. Schemes for Divergence and Vertical Velocity Circulations (panel B is after Haltner and Martin [15]).

trough lines so that convergence and divergence centers are offset from the pressure centers. Isolines of zero divergence should approximate ridge and trough lines in horizontal depictions.

Figures 53 and 54 show an actual calculation of low- and high-level divergence fields for an Atlantic Coast storm shown in a surface 500-mb composite in Figure 52. The upper-level low is part of a trough extending from the Deep South to the Great Lakes and a moderate surface storm is moving northward towards Cape Hatteras. There is a great center of convergence in the Southeast at 700 mb. The major low is in Alabama and is almost surrounded by divergence except for that portion of the Southeast east of it. Through the divergence vertical velocity relationship, it follows that ascending air lies east of this low and around the north and west portions of the surface storm where air is being uplifted over the warm front. Descending air

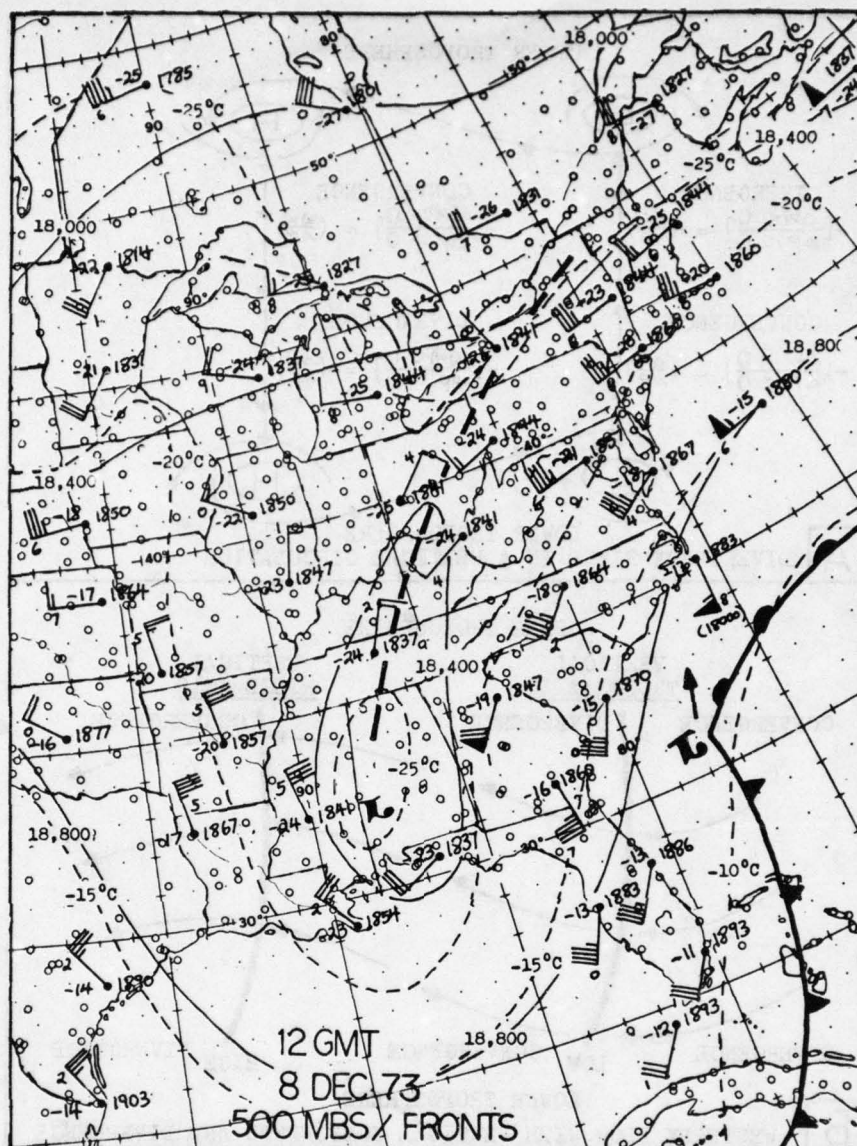


Figure 52. Upper-Level Analysis of Synoptic Pattern Used in Divergence and Vorticity Calculations in Sections 6.3 and 6.4 with Surface Fronts Included.

may be found north and west of the upper-level low in Alabama as part of general ridging.

At 300 mb the pattern is reversed. There is convergence behind the trough in the jet flow while an extensive area of divergence follows the jet flow from the trough northeastward. Both the 700- and 300-mb divergence fields agree with the panel B scheme in Figure 51.

The divergence fields here have been calculated by a graphical kinematic method by Graham [14]. As has been mentioned in Haltner and Martin [15], this method cannot be precise because it assumes an extremely detailed data field that cannot be acquired except possibly by computer. Nevertheless, sufficient accuracy to show general fields and to verify the schemes can be obtained through careful analysis. It is



Figure 53. Lower Tropospheric Divergence Field.

noteworthy that divergence centers tend to lie along the jet-stream maximum wind line at 300 mb, implying that the jet stream is a center of development at this level. A scheme of the divergence pattern along an entire jet streak is presented in Figure 55, along with meridional circulation cross sections at the jet entrance and exit. The jet-stream entrance region is north of the Ferrel circulation and is marked by a counterclockwise circulation of its own. At the jet exit the Ferrel circulation is extremely weak or even absent. This area tends to be the scene of a northward extension of the Hadley circulation in a warm-core ridge so that subsidence into a surface high of possible subtropical origin occurs near the jet. However, the jet circulation is unchanged. Note that a subtropical jet may lie very nearly at the tropopause.

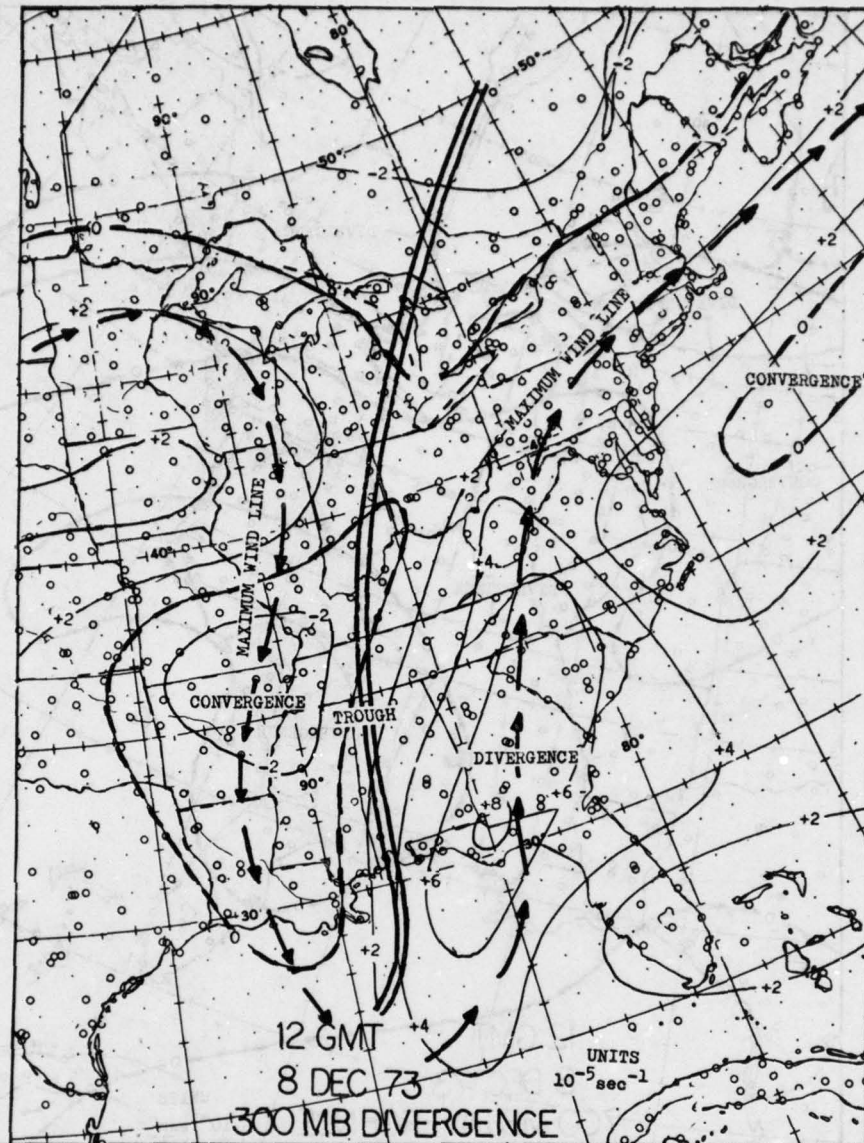


Figure 54. Upper Tropospheric Divergence Field.

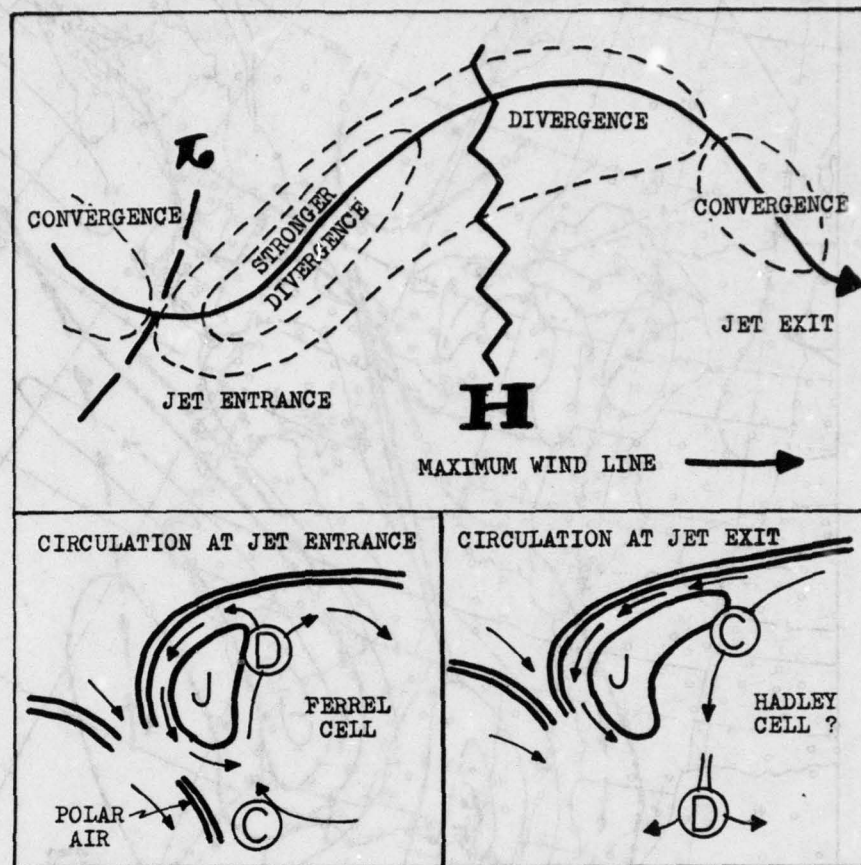


Figure 55. Jet-Stream Divergence Pattern and Possible Meridional Circulation at the Jet Entrance and Exit. Note: J is the jet core, D is divergence, and C is convergence.

6.3. Vorticity Fields. In Section 3.5 it was shown that convergence and absolute vorticity are directly related so that low-pressure areas and troughs are positive vorticity centers while highs and ridges are negative centers. Figure 56 is a 500-mb vorticity analysis graphically accomplished by the Graham Method (outlined in the discussion of divergence). The upper-level low and general area of the trough to the north is in a field of positive or cyclonic vorticity, while negative vorticity dominates areas of ridging. Forecasters are familiar with vorticity analyses and forecasts enough to use them when detailing the location and intensity of both long- and short-wave ridges and troughs.

The association of vorticity with processes of intensification is demonstrated through the vorticity equation, which contains four important contributions to intensification processes:

$$\begin{aligned} \frac{\text{The change of vorticity}}{\text{in time}} = & - \text{horizontal divergence} & (1) \\ & - \text{latitudinal displacement} & (2) \\ & + \text{horizontal gradient of vertical velocity} & (3) \\ & + \text{pressure-volume solenoids} & (4) \end{aligned}$$



Figure 56. Middle Tropospheric Vorticity Field.

The first right-hand term follows from the relationship of vorticity to convergence ("negative" divergence) given earlier in the section. This term might also be called "vorticity import" because the divergence fields also draws in vorticity from outside the immediate circulation.

Latitudinal displacement refers to the changes in vorticity that occur in meridional movement as the system moves north or south and is affected by a changing Coriolis acceleration. Southward-moving (digging) lows intensify but weaken if they move north (pulling out). Highs weaken if they move south but intensify (build) if they move north. It is assumed, of course, that all other contributions remain the same.

The third term is a "small-scale" contribution best seen in frontal zones or very short waves where vertical-motion fields vary greatly in time and space. Variations

in vertical velocity can be shown to increase the vertical component or vorticity at the expense of the less important horizontal components. It was mentioned in Section 3.5 that "vorticity" in meteorology is actually this vertical component.

The generation of vorticity by pressure-volume solenoids is a familiarly-known process to many forecasters. They are the intersection surfaces of pressure and density that indicate development in a given region and the number of these vortices details the degree of baroclinity, or development potential.

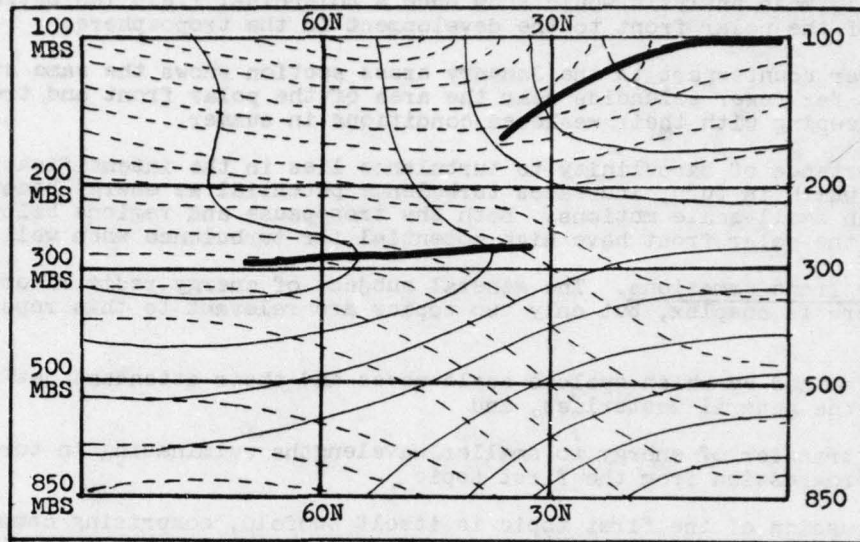


Figure 57. Mean January Meridional Temperature Field for 147.5°E with Corresponding Potential Temperature Field.

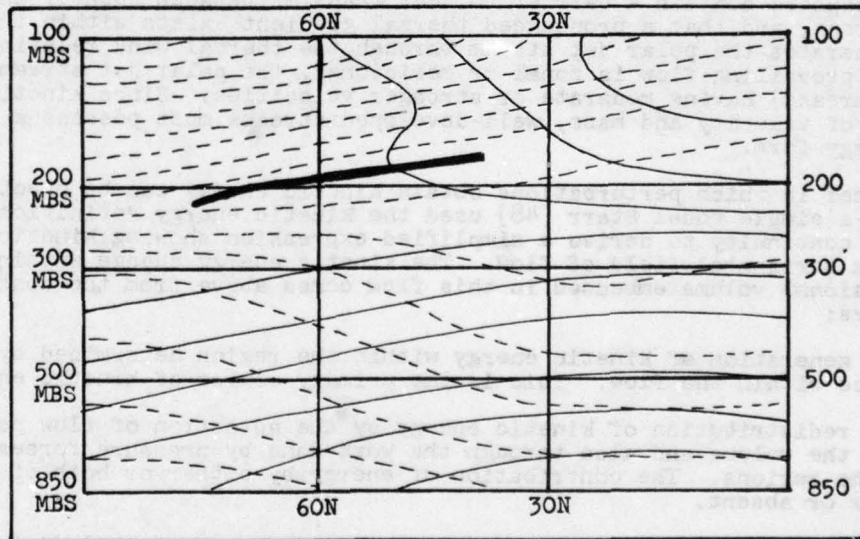


Figure 58. Mean July Meridional Temperature Field for 147.5°E with Corresponding Potential Temperature Field.

It can be shown mathematically that pressure-density solenoids are equivalent to temperature-potential temperature solenoids, that is, that intersecting surfaces of temperature and potential temperature are also solenoids. Figures 57 and 58 show

solenoidal cross sections using temperature. Their advantage is that once the temperature field is known the potential-temperature field can be computed manually with relative ease and with no loss of accuracy. The January cross section shows potential temperature "packing" above the tropopause leafs indicating that the stratosphere is an area of pronounced stability. This is a well-known fact. Intersecting surfaces occur mainly south of 60°N near these leafs, which means that the tropopause is an area of development potential, a baroclinic region. Intersecting surfaces also occur throughout the troposphere from about 60°N to 20°N , the general latitude range of polar fronts in this part of the world (Japan) in January. The fact that even a monthly mean analysis would show such a solenoidal field indicates the extreme importance of the polar front to the development in the troposphere.

The summer counterpart to the January cross section shows the same stratospheric packing, but far fewer solenoids near the area of the polar front and tropopause. This is in keeping with their weakened conditions in summer.

The importance of baroclinity to turbulence lies in the intensification of the jet stream, which in turn, increases turbulence potential as energy becomes available for such small-scale motions. Both the tropopause and regions below the jet stream near the polar front have high potential for turbulence when well developed.

6.4. Energy Transformations. The general subject of energy redistributions over the hemisphere is complex, but only two topics are relevant to this report. They are:

- a. The method by which cyclone-scale waves and their attendant jet streaks gain energy from the general westerlies, and
- b. The transfer of energy to smaller wavelengths culminating in turbulent dispersion, a progression from the first topic.

The discussion of the first topic is itself twofold, comprising comments on the nature of energy transferral and the introduction of methods for determining that energy transfer is occurring, so that conclusions can be arrived at.

In Chapter 4, it was mentioned that meridional circulations in the lower and middle troposphere contain a barrier to heat transfer between equator and pole called the polar front, and that a pronounced thermal gradient exists within this zone that directly generates the polar jet stream through the thermal wind relationship. Whether the prevailing flow is zonal or meridional, the polar jet stream will contain segments (streaks) having moderate or stronger velocities. Since kinetic energy is the product of velocity and mass, well-developed streaks must possess a vast quantity of this energy form.

The manner in which perturbations obtain kinetic energy can be hypothesized, for example, in a simple model Starr [48] used the kinetic energy definition and the equation of continuity to derive a simplified expression showing kinetic energy changes in a horizontal field of flow. The kinetic energy change within a fixed three-dimensional volume embedded in this flow comes above from the contributions of three factors:

- a. The generation of kinetic energy within the region determined by the extent of divergence within the flow. This is the primary source of kinetic energy.
- b. The redistribution of kinetic energy by the advection of flow possessing energy into the volume and also through the work done by pressure forces at the bounds of the regions. The contribution of energy by either or both of these sources may be minor or absent.
- c. The loss of kinetic energy by dissipative forces that include friction and turbulence.

The first factor directly relates divergence and kinetic energy generation. From Figure 55, it is clear that divergence prevails throughout much of a jet streak, particularly at the jet entrance in the southeast quadrant of a trough. The flow here is clearly going to be accelerating, positive proof of a kinetic energy gain. At this point, the fixed volume of the Starr model will be placed near the jet entrance, a kinetic energy source.

The primary ways in which kinetic energy is obtained in the divergence field can be shown from the simplified total energy equation presented in Section 3.8. Solving for kinetic energy gives:

$$(\text{Kinetic})_{\text{energy}} = - (\text{Potential}_{\text{energy}} + \text{Sensible}_{\text{heat}})$$

In the area of the jet entrance, ascending air ahead of the trough gains potential energy by virtue of its increasing height and internal energy (which includes sensible heat) from low-level warm-air advection and condensation. Since at jet level the air must cease to rise and warm, the loss of potential and internal energy must be converted to kinetic energy, at least in part. This conversion is responsible for most of the effect of the first and most important factor.

The second factor, energy redistribution by advection and pressure forces, will be a contributor in the jet entrance because jet flow is passing into the area from upstream and it contains kinetic energy by virtue of its velocity. The effect of the pressure forces has been presented as an energy form in Section 3.8.e. The work done to force flow through the volume in a pressure gradient is a positive contribution to kinetic energy proportional to that gradient. Jet entrances, being so near the trough, may be in a very pronounced horizontal pressure gradient. Furthermore, cyclonic curvature increases the gradient still more because if gradient balance is assumed (see Figure 8b), the addition of the centripetal acceleration forces air parcels to move inward still more in order to maintain balance. In summary, the second factor may prove to be a major contributor to kinetic energy in moderate or stronger troughs.

The third factor is a kinetic energy loss due to the energy form in Section 3.8.f, demonstrated by the small-scale effects of friction and turbulence. Friction in the upper atmosphere is trivial, and its influence on macroscale motions and turbulence tends to be too intermittent and localized to be very effective. Therefore, the magnitude of this factor is hardly comparable to the other two. However, the presence of turbulence in this discussion is critical because it is more likely to occur in this very productive portion of the jet stream. Turbulence in jet flow occurs because excessive kinetic energy within the area of the jet entrance can only be dissipated and advected out and this is the most likely area of excessive energy. This is, in fact, the area of greatest turbulence potential.

In the area of the jet exit, Figure 55 showed a convergence field. Therefore, the first and most important factor is reversed to be an energy sink aided by the third factor. The anticyclonically-curved flow over much of the area counters the energy generated by the pressure gradient and even the energy advected into the area must be insufficient to overcome the energy loss because the flow always weakens in the jet exit. Despite the kinetic energy loss in the area of the jet exit, turbulence potential remains significant because turbulence is one manifestation of this loss and excessive amounts of kinetic energy must be lost when the flow of strong jet streaks quickly decelerates.

So far, this discussion has centered on the polar jet stream. Slight modifications of some of the factors will enable the subtropical jet stream to be included. In the first factor, the substituting of ascending equatorial air with its moisture for ascending air up the polar frontal surface achieves the equivalent results. The second factor is probably weakened by the intermittent nature of the subtropical jet stream (reducing the likelihood of substantial kinetic energy advection) and the tendency for a much more gradual pressure gradient (which reduces the pressure differential across the area that generates energy). The dissipative forces remain secondary in importance, though it should be noted that turbulence is associated with substantial kinetic energy accumulations here as much as in any other flow.

6.5. The Initiation and Maintenance of Turbulence. It has been shown at this point that turbulence is a kinetic-energy dissipator that acts against jet development on a modest scale. Turbulent motions mix and diffuse atmospheric particles mainly through the actions of the eddy component, comprising roughly spherical roils of vastly differing sizes. By definition, these rotating bodies must possess vorticity and it takes kinetic energy to maintain their individual circulations. As diffusion occurs, the smaller eddies are drawn into the circulations of waves and the largest eddies are extended in one dimension into intensely rotating tubes that possess even more

vorticity and acquire even more kinetic energy. There is, therefore, a transfer of energy from larger to smaller waves and eddies that is part of the general energy transfer from long waves to short waves to turbulence-scale waves to molecular dispersion. This transfer is known as the energy cascade. It permits jet development as perturbations feed upon westerly flow and it permits turbulence to develop at the expense of relatively smooth (often jet stream) flow if a trigger is present.

Initiation processes of turbulence-scale perturbations are few in number and are sometimes very simple to understand. For example, the flow of air across rough terrain or over hills and mountains necessarily generates eddies that may maintain themselves if kinetic energy is available. This requires a substantial flow with moderate velocity. Forecasters are usually not concerned with terrain-induced turbulence because it is found only near the ground and is familiar to all. Lee turbulence, however, which involves flow over mountains or hills is a more sophisticated quantity not merely explained away by rough terrain. Numerical simulations of flow over ranges for computer analysis have shown that certain quantities ought to be present for interesting results. These include mountain profiles in the direction of flow which are as tall and narrow as possible, increasing wind speed and decreasing stability in the vertical. In general, the flow over the range differs from air at low levels that it overlies in the lee of the ranges in such a way that a stable zone or inversion develops at mountain-top levels upon which waves may generate when energy is available.

At this point, jet-stream characteristics will be brought in because air layers with differing velocities and temperatures are brought together in the jet front below the jet core, and at the tropopause above the core. Ample energy may also be available for waves and turbulence to develop in these areas as well. But what is it that uses air-layer contrasts and shear and stability to initiate turbulence? The answer lies mainly in the shearing.

When smooth flow is subjected to vertical speed shearing, molecules will be able to progress without displacement from their trajectories up to a certain critical point which depends on density and other parameters. Beyond this critical point eddies develop that may feed upon the energy of the flow to amplify into significant turbulence. The forces that the flow has been subjected to that cause it to become turbulent are called Reynolds stresses. These stresses depend on the degree of shearing, not the way in which shear occurs (increasing or decreasing with height). This means that jet fronts, tropopauses, and inversions in the lee of ranges are source regions for turbulence if the flow is moderate and vertical speed shearing is sufficiently large.

The role of inversions or stable layers may appear confusing because decreasing stability with height was said to be favorable for lee turbulence and because decreasing static stability encourages convective turbulence which can only intensify a pre-existing field. However, in this case the stable layer over a less stable one results in a narrow zone or interface upon which wave motions may develop when Reynolds stresses initiate turbulent motions. Everyone has seen waves form on such interfaces. In the case of water, for example, the interface is the zone between water and air. Therefore, even though stability counters turbulence development, it is an important part of the turbulence field. In moderate or strong jet flow, there is more than enough kinetic energy in the flow to overcome all obstacles to turbulence formation if a trigger and process of maintenance are present.

In hydrodynamics, there is a relationship between vertical speed shear and stability called the Richardson Number that has been frequently applied to turbulence. Numerous technical reports have successfully correlated certain values of this number to observed turbulence demonstrating the power of these quantities when acting together. One such report by Defant [7] has found that appropriate values of the Richardson number are present at the jet front and tropopause, proving that these features are major areas of potential that always must be investigated as part of any proper forecast routine. Forecasters at AFGWC use the relationship between stability and shear through a turbulence-potential nomogram called the "Millergram" after the originator of the technique (Burnett [4]). When used on acetate over plotted soundings, the potential for turbulence of a specific intensity as a function of stability, or excessive static instability, and vertical-speed shear is readily obtained. An example of the nomogram is shown in Figure 59.

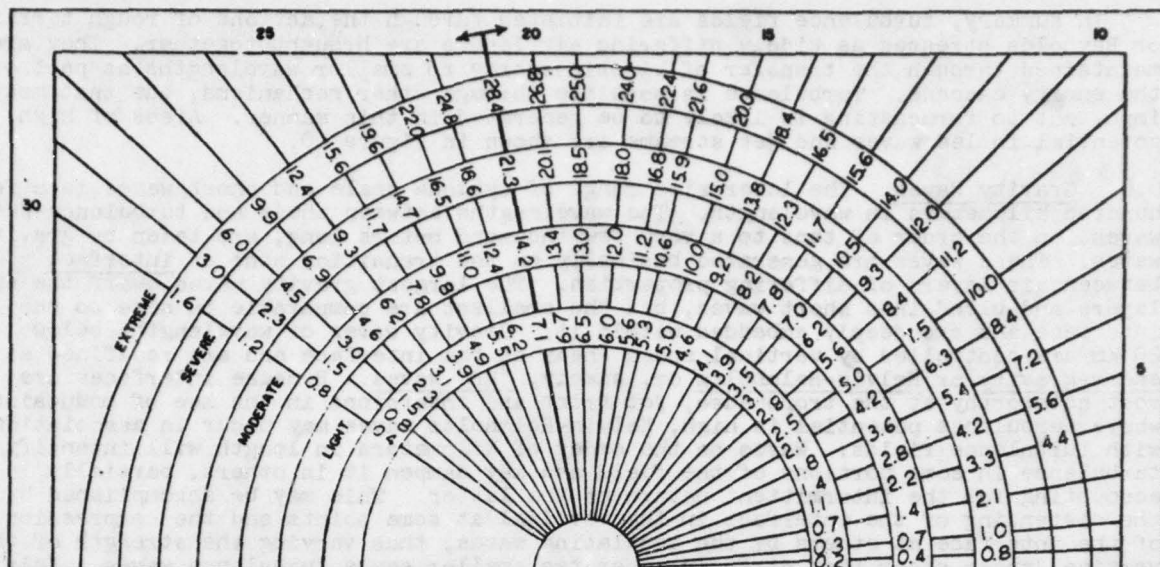


Figure 59. Turbulence Potential Nomogram. Critical speed shears in kt/1000 ft. This "Millergram" is used at AFGWC. (After Burnett [4].)

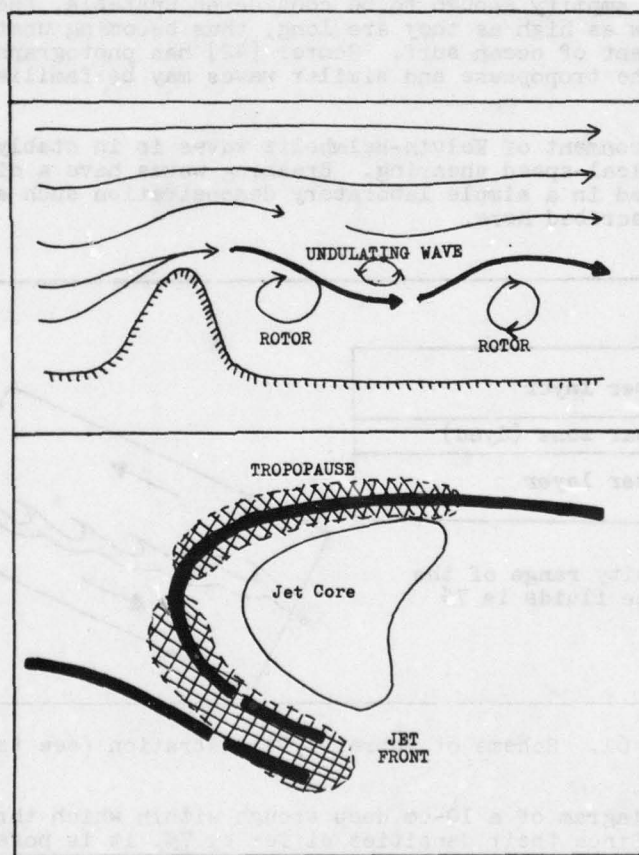


Figure 60. Areas of High Turbulence Potential in Lee Waves and Jet Streams.

In summary, turbulence fields are initiated through the actions of rough terrain or Reynolds stresses as widely differing air layers are brought together. They are maintained through the transfer of kinetic energy to smaller wavelengths as part of the energy cascade. Turbulence is possible through other mechanisms, but that most important to forecasting is likely to be generated in this manner. Areas of high potential in lee waves and jet streams are shown in Figure 60.

6.6. Gravity Waves. The lower size range of cyclone scale and short waves is a few hundred kilometers in wavelength. The wavelengths between these and turbulence-scale waves, on the order of tens to a very few thousand meters long, are taken by gravity waves. These waves are generated basically on the transition zone of interface between air layers of differing properties. The largest gravity waves dwarf the air layers and blend into short waves, but the smallest are comparable in size to the interface and are deeply embedded within it. Gravity waves of wavelengths below 20 km are controlled by vertical speed shear at the interface and are redefined as shear-gravity or Kelvin-Helmholtz or, simply, "KH" waves. Because interfaces are most noteworthy at the tropopause, jet front and inversions in the lee of mountains where turbulence potential is high, Kelvin-Helmholtz waves may occur in association with turbulence fields. Waves on the order of kilometers in length will intensify turbulence in some portions of the field and may dampen it in others, partially accounting for the intermittent nature of the latter. This may be accomplished by the distending of the interface in the vertical at some points and the compression of the interface at others by the undulating waves, thus varying the strength of the vertical speed shear that directly generates smaller scale turbulence waves. Kelvin-Helmholtz waves on the order of tens or hundreds of meters are within the scope of turbulence scale waves and actually comprise the wave component of this phenomenon. While the larger wave forms have lengths much greater than the depth of the interface and thus cannot amplify enough to be considered unstable, the turbulence scale waves can easily grow as high as they are long, thus becoming unstable and "breaking" in a manner reminiscent of ocean surf. Scorer [42] has photographed breaking Kelvin-Helmholtz waves at the tropopause and similar waves may be familiar to more experienced pilots.

The classic environment of Kelvin-Helmholtz waves is in stably-stratified flow with pronounced vertical-speed shearing. Breaking waves have a distinctive profile that can be duplicated in a simple laboratory demonstration such as one by Scorer [42] that will be described here.

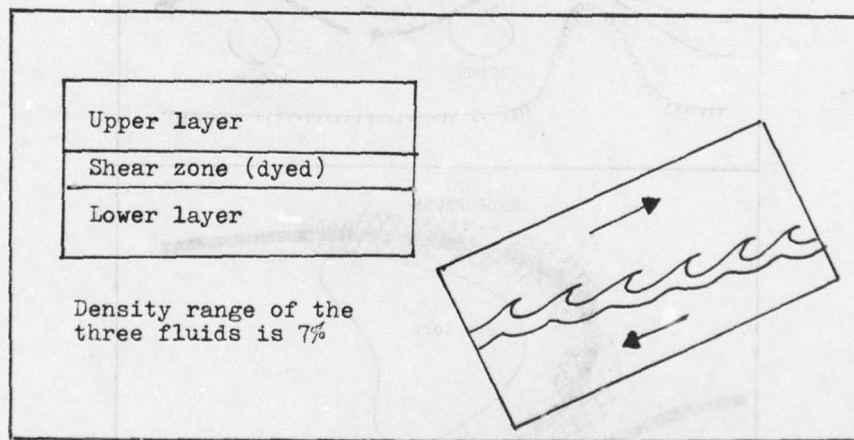


Figure 61. Scheme of Scorer's Demonstration (see text).

Figure 61 is a diagram of a 10-cm deep trough within which three fluids have been poured separately. Since their densities differ by 7%, it is possible to have them stratified as long as their placement is done carefully. The middle fluid, meant to depict the shear zone, is dyed black to accentuate the waves developed. Because the degree of shearing generates the waves, a simple tilting of the trough is enough to send the light fluid to the top end and the lower dense fluid to the lowered end.

The oppositely-moving fluids effectively double the contrasting speeds, as shown in the figure, and establish a shear zone capable of developing waves through Reynolds stresses that form the classic pattern of breaking waves, also in the figure.

It has already been mentioned that waves resembling these in the figure have been photographed at the tropopause. One sighting from the ground at Denver, Colorado in 1953 has been documented by Colson [6]. He obtained a striking picture very much like that of the model. Kelvin-Helmholtz waves occurring in contrasting air layers may be seen far more often on radar as echo returns can show density and moisture gradients not visible to the eye. In general, it is necessary that the waves be nearby and well-defined because distant waves cannot show up well on the RHI scopes of conventional radar sets. Radars are further hampered by fixed wavelengths which, in turn, limit the detection of waves of many lengths that would otherwise be detected. Thus, only part of the true turbulence field can be detailed with one conventional set. Nevertheless, after the mid-1960's, many articles appeared in meteorological journals that detected and described Kelvin-Helmholtz waves and further associated them with turbulence. Some of the findings are surveyed briefly in the next paragraphs.

Atlas [1] and Gossard [13] took advantage of a high sensitivity-resolution radar and a very favorable synoptic condition to study Kelvin-Helmholtz waves in detail. Their location was under the low-lying marine inversion at San Diego, California where moist, cool marine air is replaced by warm, dry subsiding air near 3000 feet. Though wind speeds are light, small slow-moving waves still form on the interface of the layers that conform to classic shear-gravity waves. Such small waves are aided by the mechanism of different density gradients in sustaining waves, one subordinate to and nearly overwhelmed by vertical speed shear when the latter is significant. Both small and larger Kelvin-Helmholtz waves were seen to occur together, indicating that the wave components alone of a turbulence field are a complex phenomenon. Breaking waves were studied extensively in both reports.

Browning [3] undertook the more difficult task of using radar to analyze billow clouds in jet flow. His and Ludlam's work [23] are particularly important to turbulence forecasting because of the association of waves in which wave or billow clouds lie with jet streams. Reed and Hardy [36] detailed Kelvin-Helmholtz waves in strong jet flow in association with an aircraft penetration to verify turbulence near the jet front and were successful in correlating all features. Civil pilot reports also linked the tropopause with turbulence in wave motions. This short survey has shown that certain meteorological features work together to produce jet-associated turbulence fields of great forecast significance. From the last chapter, it is further known that these quantities can be readily located as part of an operational forecast routine.

6.7. Characteristics of Kelvin-Helmholtz Waves. This summary of characteristics follows from hydrodynamic theory and the verifications of many reports, including some referenced in the last section.

a. Kelvin-Helmholtz waves are transverse, oriented normal to the prevailing flow within which they are embedded. This is consistent with all families of waves of greater length and clouds within this flow may be arranged as transverse bands that detail the particular wavelength of the waves. Such clouds may be called billow or wave clouds.

b. Kelvin-Helmholtz waves which have dimension equal to or smaller than the thickness of the active part of the vertical-shear zone are unstable as long as energy available for amplification is greater than that energy lost through stabilization, friction, and turbulence. It is mentioned in Section 6.5. that a relationship between vertical speed shear and stability called the Richardson Number was derived to be applied to turbulence observations. This number may be described as:

$$R_1 = \frac{\text{Energy lost by stabilization}}{\text{Energy gained by vertical speed shear}}$$

Turbulence potential seems to be great, according to both theory and observational evidence, when the energy gain exceeds the loss by at least a factor of four:

$$R_1 \leq 1/4$$

The number must be greater than zero. Defant [7] has found an array of very low Richardson numbers about the jet front and tropopause in a pattern very much like the area of high turbulence potential in Figure 60 in the jet cross section. Kao [19] also verified the relationship between low Richardson number and turbulence by taking wind velocity measurements from an aircraft penetration of a jet streak and using numerical techniques to separate the mesoscale turbulent flow from the smooth mean flow. Suitably low numbers were found in the jet front and tropopause in particular.

c. Kelvin-Helmholtz waves theoretically move at a rate between the velocities of the air layers on either side. Specifically,

$$V_{kh} = \frac{1}{2} [V_{\text{upper layer}} + V_{\text{lower layer}}]$$

According to theory, waves moving at a speed much different than the average of the two layers cannot possess vorticity (centers) and would be unable to become unstable and amplify. This does not mean that stable waves cannot exist in the shear zone, but that Kelvin-Helmholtz waves and associated turbulence will not be significant. Several studies, including Reed and Hardy [36], have found the waves observed by radar to be moving at rates very close to the mean speed of the shear zone, the average of the speeds of the two layers.

d. According to theory, the fastest-growing Kelvin-Helmholtz waves have wavelengths about 7-1/2 times the thickness of the active part of the shear zone. Thus, if billow clouds are present, wavelengths can be determined and the thickness of the shear zone estimated. A simple calculation would show that shear-zone thicknesses of 300 to 2000 meters should be associated with waves of 2 to 5 km in length. This is the size range of waves with billow clouds but perhaps much too large for turbulence-scale waves. The very small Kelvin-Helmholtz waves associated with turbulence and seen to be of vastly varied wavelengths on radar may owe part of their existence to local concentrations of vertical-speed shear too small to be detectable by conventional means.

e. The cyclic nature of Kelvin-Helmholtz waves has been observed and documented in a variety of studies and manifests itself to pilots as an intermittent field of turbulence. There are a variety of ways in which turbulence fields might become patchy in nature and three will be presented here.

First, if the amount of kinetic energy available for waves is modest (that is, if the prevailing flow is weak), Kelvin-Helmholtz waves might dissipate this energy faster than it can be replenished. Atlas [1] and Gossard [13] noted this possibility in their studies. It is not possible for a forecaster to determine whether or not a particular turbulence field is outstripping its energy supply, but the fields in moderate or strong jet-stream flow probably have little chance of bringing jet flow to a halt. This phenomenon is probably significant in turbulence fields of marginal forecast interest.

A second possible cause of intermittency was touched upon in the last section, when it was said that turbulence-scale waves might be developed when the shear zone was undulating because of larger, stable gravity waves and was forced against one or another of the air layers on either side. Figure 62 diagrams such a process. In this case, it is assumed that some moisture exists in the flow so that ascending turbulent waves are visible as cloud, a possible explanation of the wave picture described by Colson [6]. These waves would be more easily seen by radar. Note that the waves appear where vertical-speed shearing is greatest, near the crests and troughs of the undulating gravity waves. Also shown are terms for portions of the breaking waves, according to Scorer [42].

Atlas [1] noted in his studies that the small Kelvin-Helmholtz waves had from a tenth to half the wavelength of the stable waves and suggested local processes that might lower the Richardson number to permit the development of these small waves. He noted a formation and dissipation cycle of about 20 minutes. Ludlam [23] noted a 30-minute cycle in his observations of Kelvin-Helmholtz waves in jet flow using radar. He attributed the cycle partly to the availability of kinetic energy.

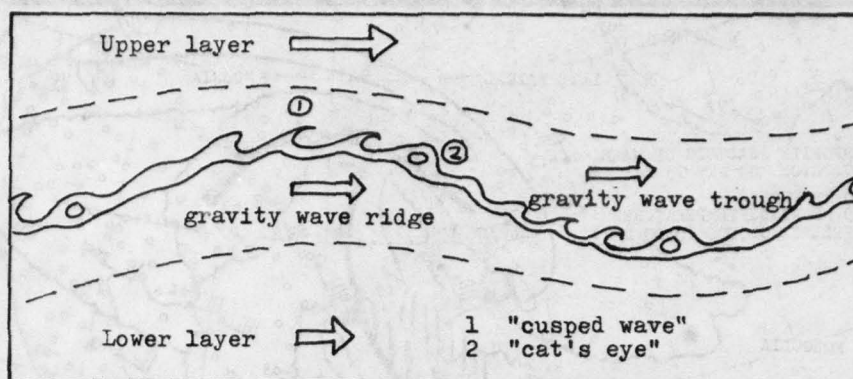


Figure 62. Kelvin-Helmholtz Waves Superimposed on Stable Gravity Waves in a Shear Zone.

A third cause of the intermittency of turbulence fields may come about from the tendency of jet flow to "finger" into a large ridge with weak flow, or when the jet is forced sharply northward upon approaching this ridge. There are often secondary flow maxima detectable on upper-air analyses but satellite pictures of cloud streaks suggest that this process is mesoscale. Kao [19], among others, has noted waves paralleling the flow with a spacing within a range of 20 to 40 km. Though they are of little direct importance to forecasting they may limit the extent of turbulence fields or subdivide a major field hundreds of kilometers in extent.

6.8. Billow Clouds on Satellite Pictures. A sampling of wave clouds from DMSP satellite data is provided in this section to show how billows appear from satellite pictures.



Figure 63. Warm Occlusion in Northeast China.

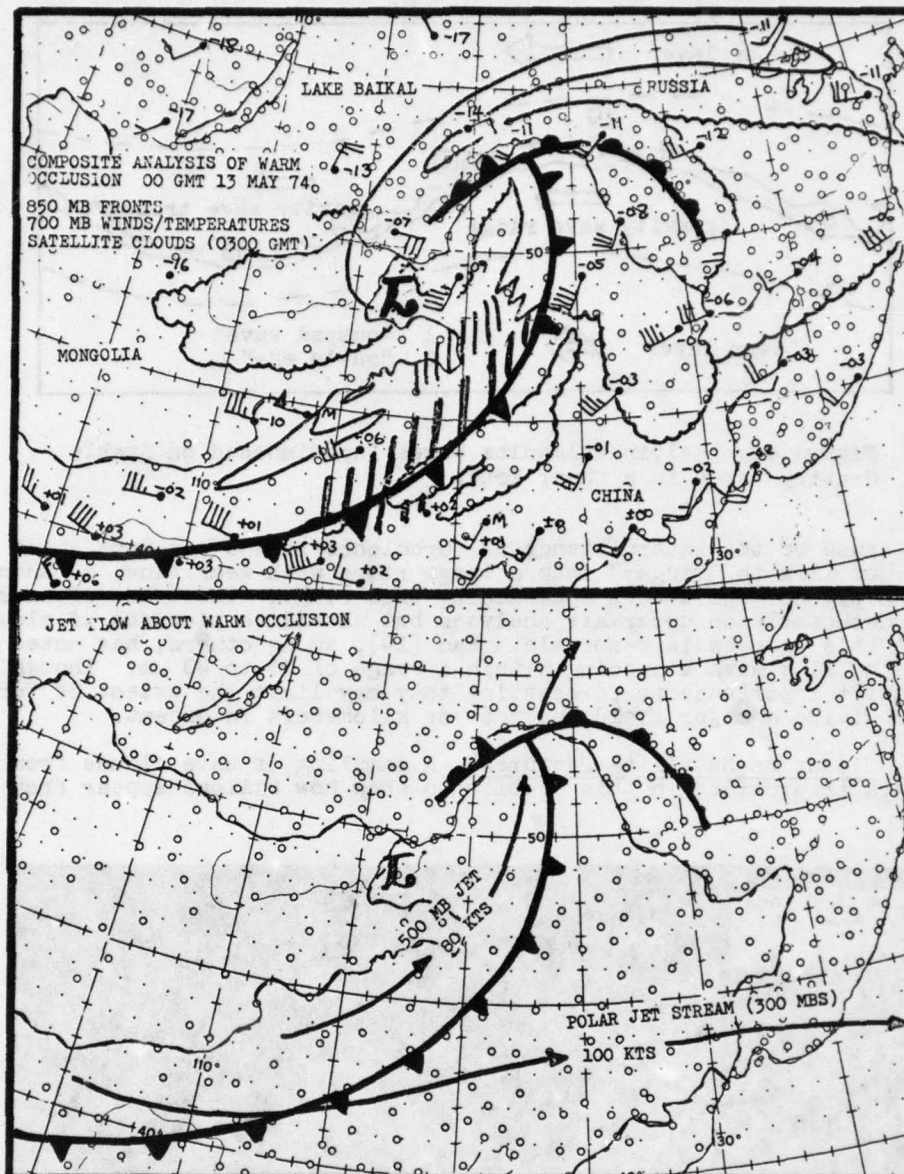


Figure 64. Two Schematics of the Northeast China Occlusion.

The first case is that of a small warm occlusion that was moving out of Northeast China into Eastern Siberia on 13 May 1974, shown in Figure 63. Lake Baikal can be seen (ice-covered) on the extreme left-center portion of the picture. There are two billow cloud types in these scene. The herringbone pattern well south of the low comprises low-level clouds associated with the weak cold front stalled in a mountain complex west and north of Peking. The second group of billows is detectable near the occlusion's "dry tongue," where clouds above the cold front near the triple point show transverse banding where they taper off. These billows are not low-level clouds, though they are probably not high enough to be cirrus, either.

Figure 64 shows two upper-level schemes superimposed on the surface fronts in order to place the billows more definitively within the system. The 850-mb frontal positions were easy to place since a good temperature wind field was possible at that

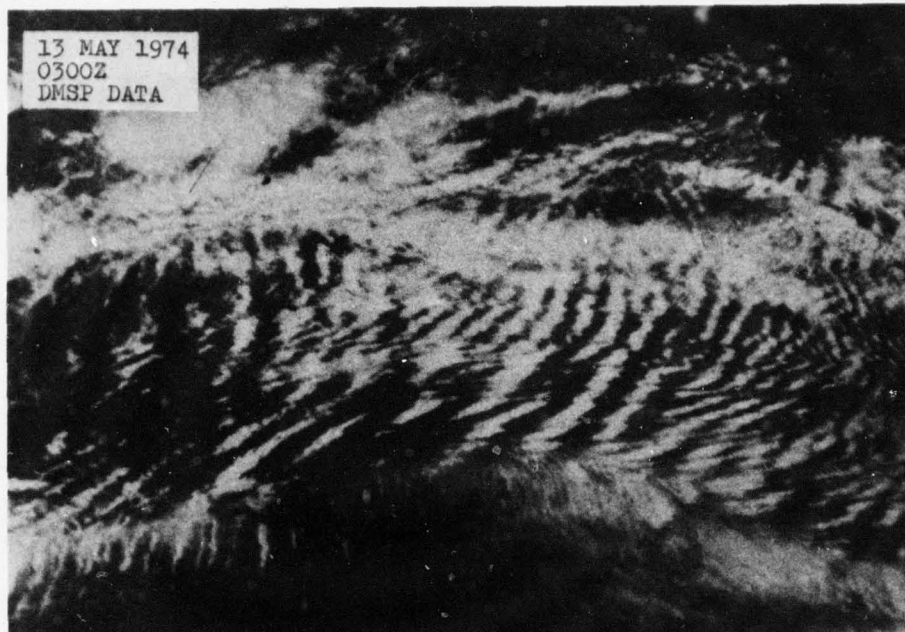


Figure 65. Detail of Billow Clouds in the Northeast China Occlusion.

level. The low-level billows result from the frontal band being disturbed by their southwest trajectory over the mountain range. Though most peaks are under 4000 feet, there are two peaks as high as 10,000 feet. The range is oriented in the direction of flow and the enlargement (Figure 65) shows a blurring of the wave pattern caused by the complex layout of this range.

The higher billows appear to be caught up in a jet segment at 500 mb shown in panel B of Figure 64. Turbulence might exist in such disturbed flow, though the billows are large Kelvin-Helmholtz waves spaced about 15 km apart.

The second case shows a jet cirrus and middle-cloud shield ahead of a deep trough over the East Coast on 8 December 1973. This particular trough has been used in the discussion of divergence and vorticity fields earlier in this chapter and will be used again in the next chapter as turbulence fields are treated in case studies. It also was the "Picture of the Month" in the Monthly Weather Review [10]. The series of figures (Figures 66 through 68) show different portions of the cloud shield and its transverse banding at the tropopause. The first picture (Figure 66) shows seldom-seen banding in the area of cold advection east and southeast of the upper-level low (see Figure 52 for a 500-mb analysis). The second picture (Figure 67) is a classic example of transverse banding in anticyclonically-curved flow, which will be shown in the next chapter to be primarily due to horizontal speed shearing at the tropopause on the anticyclonic side of the jet axis. The center of the picture is over the Virginias. The last picture (Figure 68) shows more transverse banding in this cirrus from New England eastward into the Atlantic. All three pictures show the effects of strong vertical speed shear at the tropopause (plus horizontal speed shear in anticyclonic curvature in at least one case). All wavelengths average 15 km.

The third case in this section shows small Kelvin-Helmholtz waves in a jet cirrus shield (Figure 69) over Japan on 27 March 1974. These billows are near the limits of detection on conventional satellite pictures and are too small to be caused by horizontal speed shear. The wavelengths of these billows, caused by vertical speed shear at the tropopause is from 5 to 10 km, small enough to comprise the gravity waves upon which turbulence-scale waves might be superimposed. Through pilot reports are lacking in the area, these billows may very well comprise a satellite picture of a turbulence field.

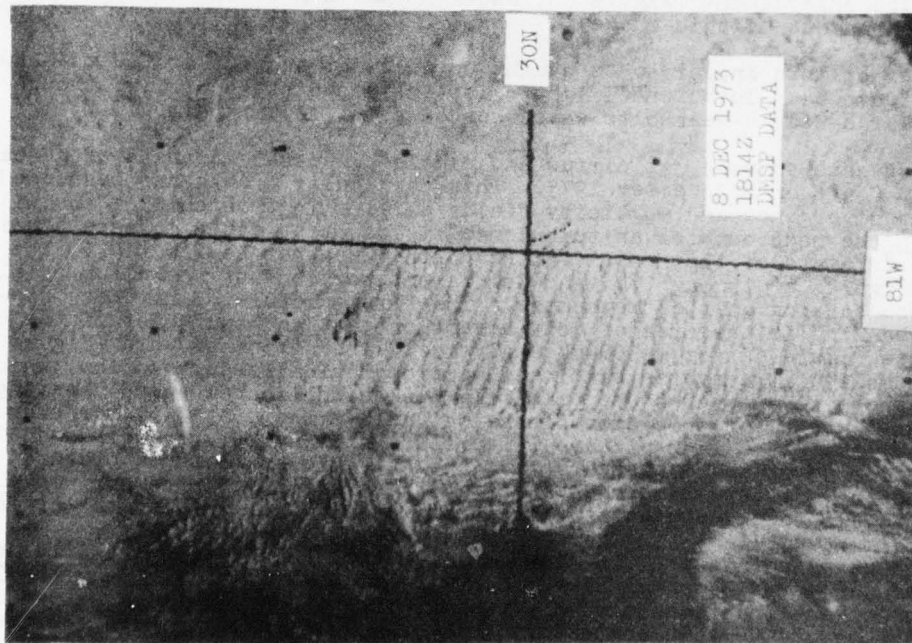


Figure 66. Cloud Billows East of an Upper-Level Low.

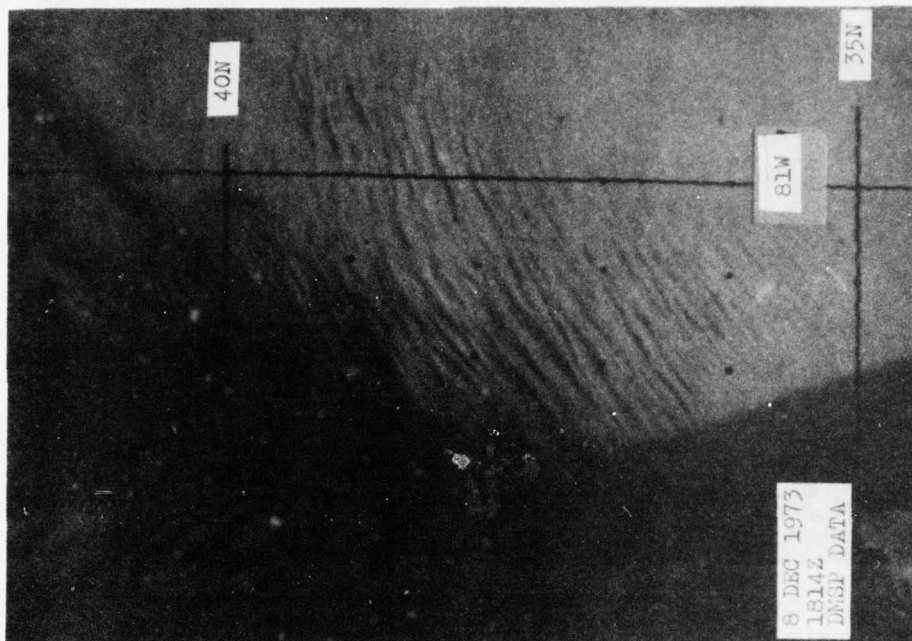


Figure 67. Cloud Billows in an Anticyclonically-Curved Cirrus Middle-Cloud Shield.

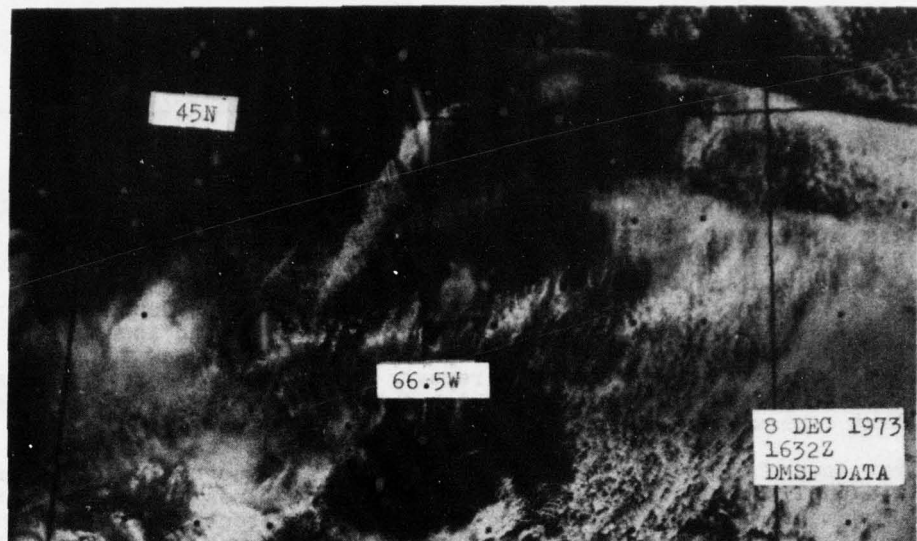


Figure 68. Transverse Banding in Thin Cirrus.

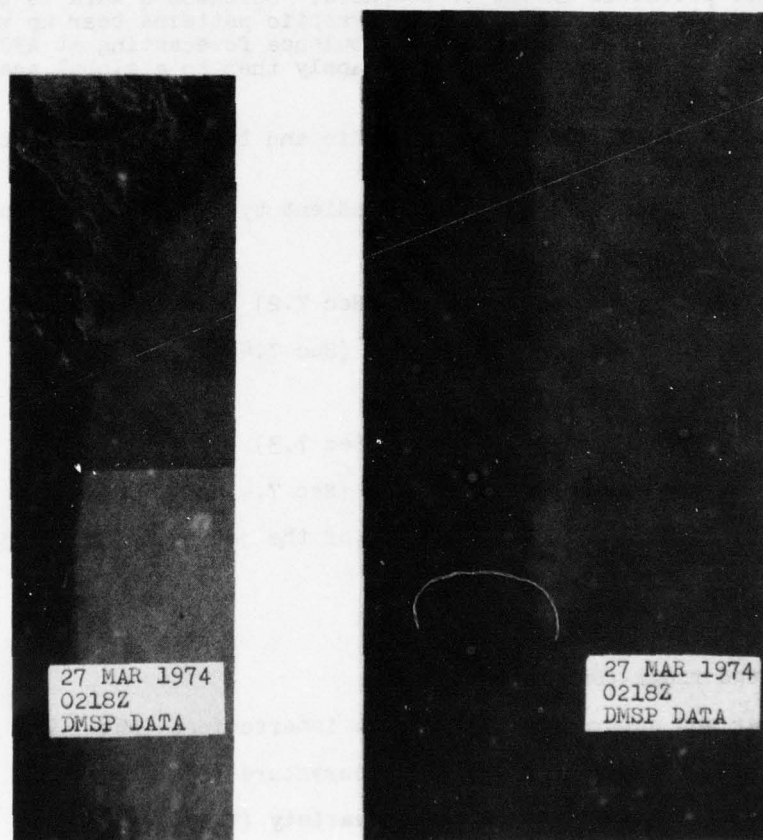


Figure 69. Jet Cirrus Shield Over Japan with a Magnified View Showing Small Kelvin-Helmholtz Waves.

SYNOPTIC PATTERNS WITH HIGH TURBULENCE POTENTIAL

7.1. Introduction. Turbulence prediction has generally lagged behind many of the major topics of operational forecasting because, as with severe weather forecasting, breakthroughs in research tend to come slowly and grudgingly after much effort and expense. However, unlike severe weather forecasting, it lacks glamor because it is but one of many phenomena of interest to flying and it is of little interest to the public. The earliest reports relating turbulence fields to synoptic patterns date from the 1950's and early 1960's. They tend to be sketchy and incomplete, reflecting the imperfect knowledge of the upper atmosphere at that time and the great difficulties of data sampling. Such well-known reports as a study by George [12] are largely collections of promising relationships which fall short of being comprehensive, however excellent otherwise.

The first comprehensive collection of synoptic features having high turbulence potential was published by Sorenson [44] of United Air Lines in 1964. He took 254 reports of moderate or greater turbulence that were apparently unrelated to terrain influences and linked them to well-defined synoptic patterns, adding analyses and justifications to strengthen the correlations. Sorenson added to this wealth of knowledge with a second report on additional features, and a third on mountain waves [45][46] which, taken together, almost certainly cover all major synoptic patterns of high turbulence potential in the troposphere. Sorenson's work is the foundation of this report and his classifications and synoptic patterns bear up very well under the severe testing of operational global turbulence forecasting at AFGWC. This report does alter some patterns in order to apply them to a global scale and to fit special needs of forecasters at AFGWC.

The following is the list of major synoptic and terrain features to be associated with turbulence fields:

- a. Increasing horizontal temperature gradient by thermal advections:
 - (1) Cold-air advection:
 - (a) With cyclone-scale waves (Sec 7.2)
 - (b) With traveling short waves (Sec 7.4)
 - (2) Warm-air advection:
 - (a) With cyclone-scale waves (Sec 7.3)
 - (b) With traveling short waves (Sec 7.4)
- b. Decreasing stability in the vicinity of the jet exit (Sec 7.5)
- c. Vertical directional shear:
 - (1) Tilted trough (Sec 7.6)
 - (2) Tilted ridge (Sec 7.7)
 - (3) Polar and subtropical jet-stream interactions (Sec 7.7)
 - (4) Ridges with sharp anticyclonic curvature (Sec 7.8)
- d. Lee waves, not of the mountain-wave variety (7.9).

7.2. Increasing Horizontal Temperature Gradient Through Cold-Air Advection in Cyclone-Scale Waves. It has already been established that because of the thermal wind relationship, strong horizontal temperature gradients (typified by "thermal packing") indicate turbulence potential. Below the jet core, such gradients are found in the jet front, a region of high potential because of vertical speed shearing in a stable stratification that promotes wave generation. Above the jet core lies another temperature gradient across the tropopause, which approximately separates cold upper tropospheric air in ridges from warmer stratospheric air. The tropopause is also marked by vertical speed shear and stable stratification and therefore has a high turbulence potential. However, the thermal wind relationship cannot be established in this latter case because temperature advections separated by the tropopause fail to increase flow above them. In fact, since the jet core is below this region, the flow decreases with height, sometimes drastically. It appears that the thermal wind relationship holds only in the area of the jet front and in the middle troposphere. If turbulence reports over such areas are received, a different cause may have to be ascribed to them.

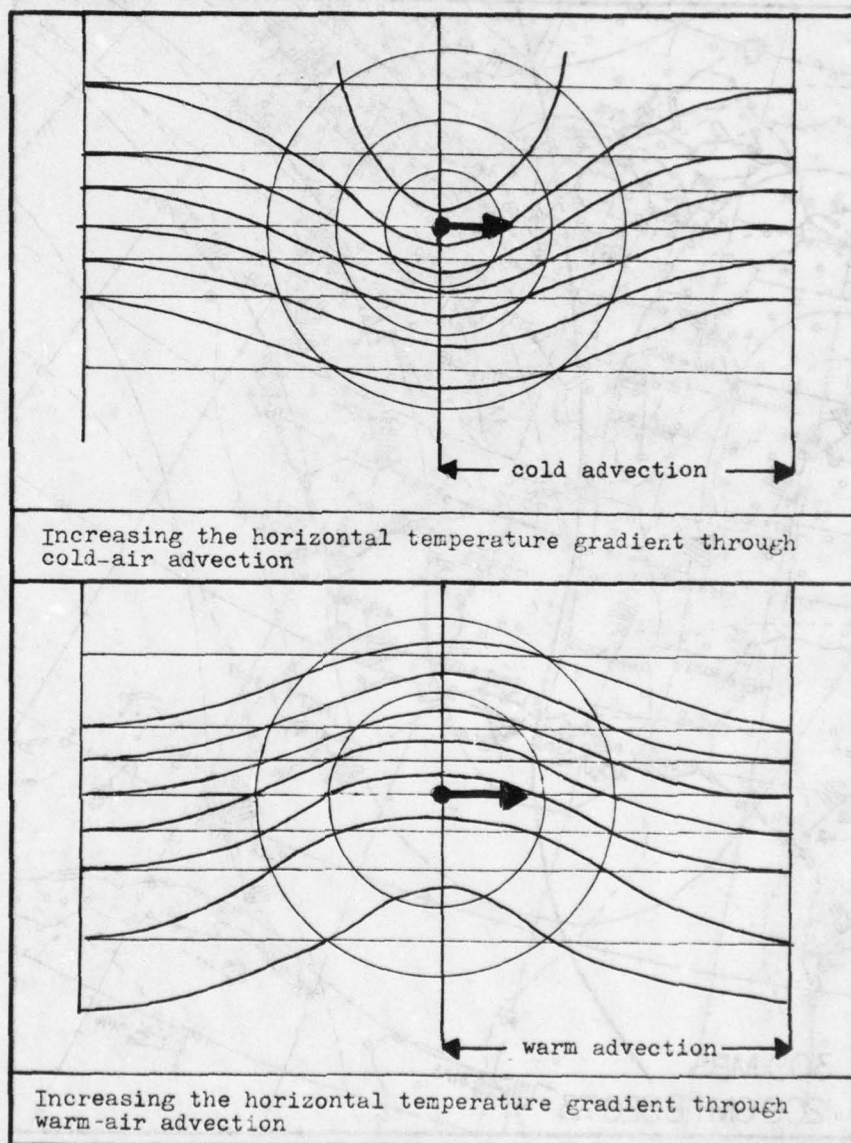


Figure 70. The Effect of Superimposing a Warm or Cold Pool of Air on a Zonal Temperature Gradient.

Figure 70 shows how the imposition of a cold or warm pool of air upon a horizontal temperature gradient creates a thermal trough or ridge and compresses the gradient. These "pools" might be part of a short-wave or cyclone-scale perturbation that moves through the westerlies. Since the usual area of highest turbulence potential in jet flow in the middle troposphere is at the jet front, it might be intensified as the perturbation approaches and the thermal gradient tightens. This is in the area of cold-air advection ahead of a trough or in warm-air advection ahead of a ridge. The cold advection case is by far the most common producer of jet-associated turbulence since it is both common and well-developed. Ridges are just as common but are usually too weak to produce extensive turbulence fields unless they are cyclone scale in size. One forecast problem in either case is that the jet front may already be capable of generating extensive turbulence fields apart from the influences of the perturbations. In such cases, more severe turbulence might be expected ahead of these features and much less in the decreasing gradients behind them.

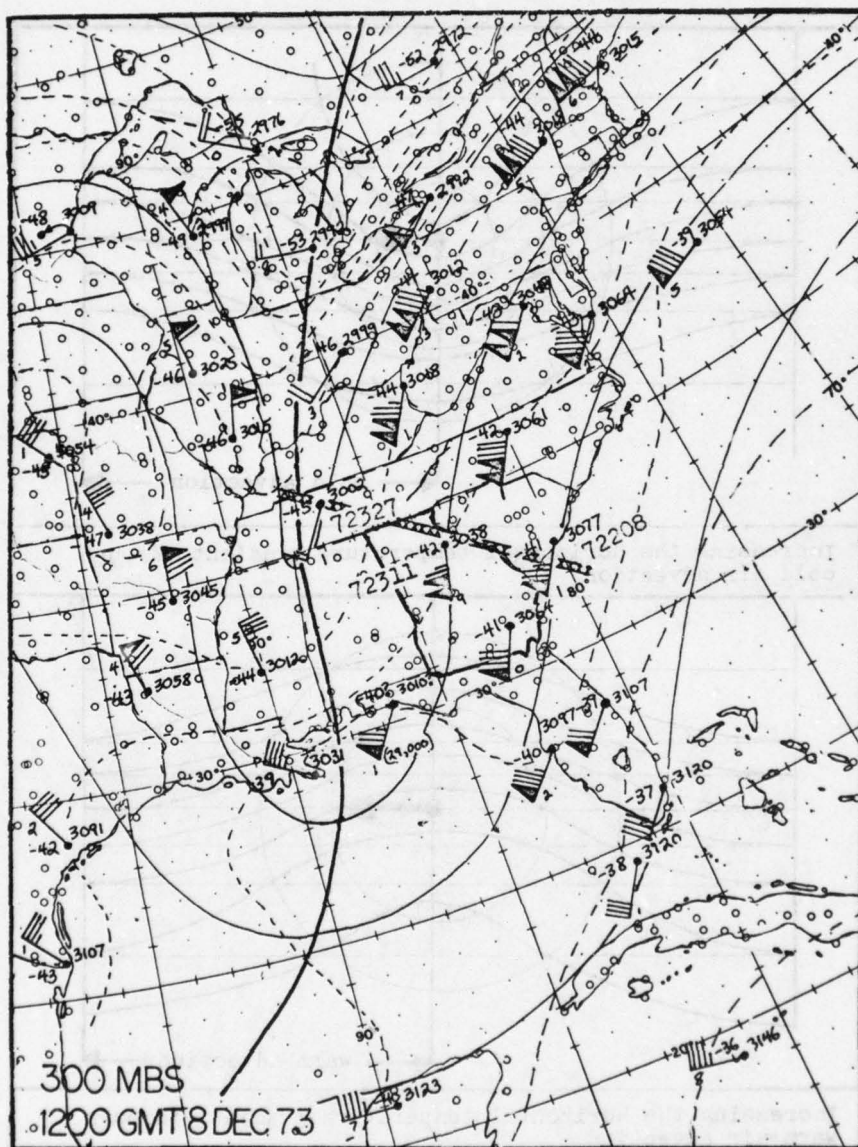


Figure 71. 300-mb Analysis of Trough with Turbulence in Georgia Associated with Cold-Air Advection.

Because of the complexity of this topic, only the case of cyclone scale cold-air advection will be discussed in this section. One synoptic pattern will, however, be used for both cyclone scale cases, the same pattern used in the divergence and vorticity fields in Sections 6.2 and 6.3, and the discussions of satellite pictures in Section 6.8.

Figure 71 is a 300-mb analysis of cold-air advection ahead of a trough over the Southeastern United States. A concentration of strong turbulence reports over Georgia appears to have been the result of the strong jet front influenced by a decreasing thermal gradient. Figure 72 is a composite of four levels of temperature fields over Georgia, designed to show that this is indeed a middle tropospheric phenomenon. Both the 500- and 400-mb analyses show a tight thermal gradient that far exceeds that of the 700- and 300-mb levels. Although it is not possible to show a clearly increasing thermal gradient with so coarse a data field, the existence of cold advection

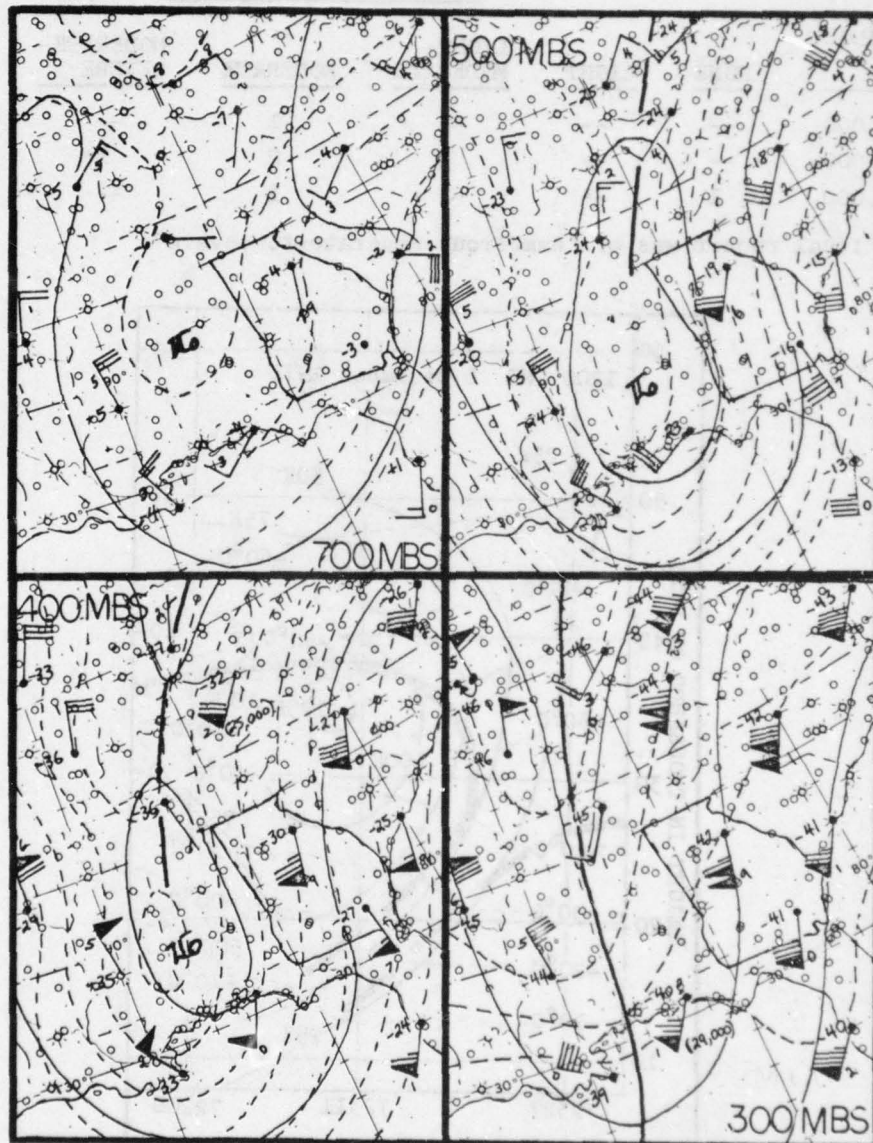


Figure 72. Composite of Horizontal Temperature Gradient Over Georgia.

suffices to show that packing must exist. It appears further from the figure that the highest turbulence potential must be from above 15,000 feet (just below the 500-mb level) to near 27,000 feet (just above 400 mb). The cross section of Figure 73 shows the jet front to lie over northern Georgia between these levels. Only the sounding of Athens, Georgia (72311) penetrates any part of the jet front, and it indicates a potential by the Millergram of 5 to 7 knots per thousand feet, which is at best, light-to-moderate in intensity. However, from Table 2 it appears that the jet front is stronger (or is aided by other factors) further west over Atlanta, where most pilot reports were received. Note that most reports lie within an altitude range very near the jet front.

Table 2. Turbulence Reports Over Georgia from 0900 GMT 8 December 1973 to 0300 GMT 9 December 1973.

ALTITUDE RANGE (feet)	TURBULENCE INTENSITIES					
	NONE	LIGHT	LIGHT-MODERATE	MODERATE	MODERATE-SEVERE	SEVERE
10,000-14,000	--	--	--	1	--	--
15,000-25,000	--	--	3	2	1*	--
Above 25,000	1	--	--	1	--	--

* An additional report was of "numerous moderate-to-severe"

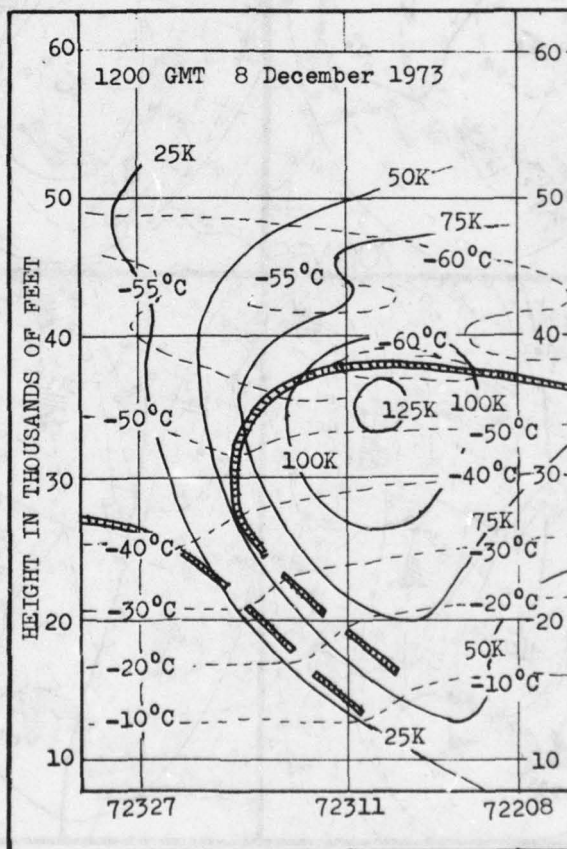


Figure 73. Cross Section of Polar Jet Stream in Cold-Air Advection.

7.3. Increasing Horizontal Temperature Gradient Through Warm-Air Advection in Cyclone-Scale Waves. In Figure 74, the area of interest includes all of the United States from Ohio, eastern Kentucky, and Virginia northeastward into New England. Turbulence reports were so numerous here that they had to be grouped by states and combined as shown in Table 3. Turbulence fields northeast of strong troughs may be caused by a variety of triggers that are hard to separate. In this case, the presence of the jet streak over the area of reports suffices to allow one to choose the warm ridge in the Carolinas as the primary cause of turbulence reports in the middle trough west of the jet streak (to be identified later).

Figure 75 is a composite of temperature fields at four levels over the Northeastern United States. It follows the same trend as in the cold advection case previously discussed. It should be expected that the gradients might lie at generally higher levels because both the jet core and jet front are higher in a ridge than in a trough. The 400-mb gradient is greater than that at the level below and even the 300-mb level shows packing where the tropopause intersects the level near the area where the jet front begins. The two cross sections of Figures 76 and 77 intersect the northeast area of reports and show the jet front extending from above 15,000 feet to approximately 30,000 feet. Vertical speed shears in the jet front were 8 to 10 knots per thousand feet at Charleston, West Virginia (72425) and 10 to 12 knots per thousand feet at Albany, New York (72518), sufficient for moderate turbulence according to the Millergram. Reports received are shown in Table 3.

One complication in warm ridges is that anticyclonically-curved flow at the jet core increases turbulence potential in both the jet front and tropopause. While this serves to reinforce turbulence potentials in the middle troposphere, it also may make it necessary to extend forecast areas into the tropopause to account for the scattered reports above the jet core.

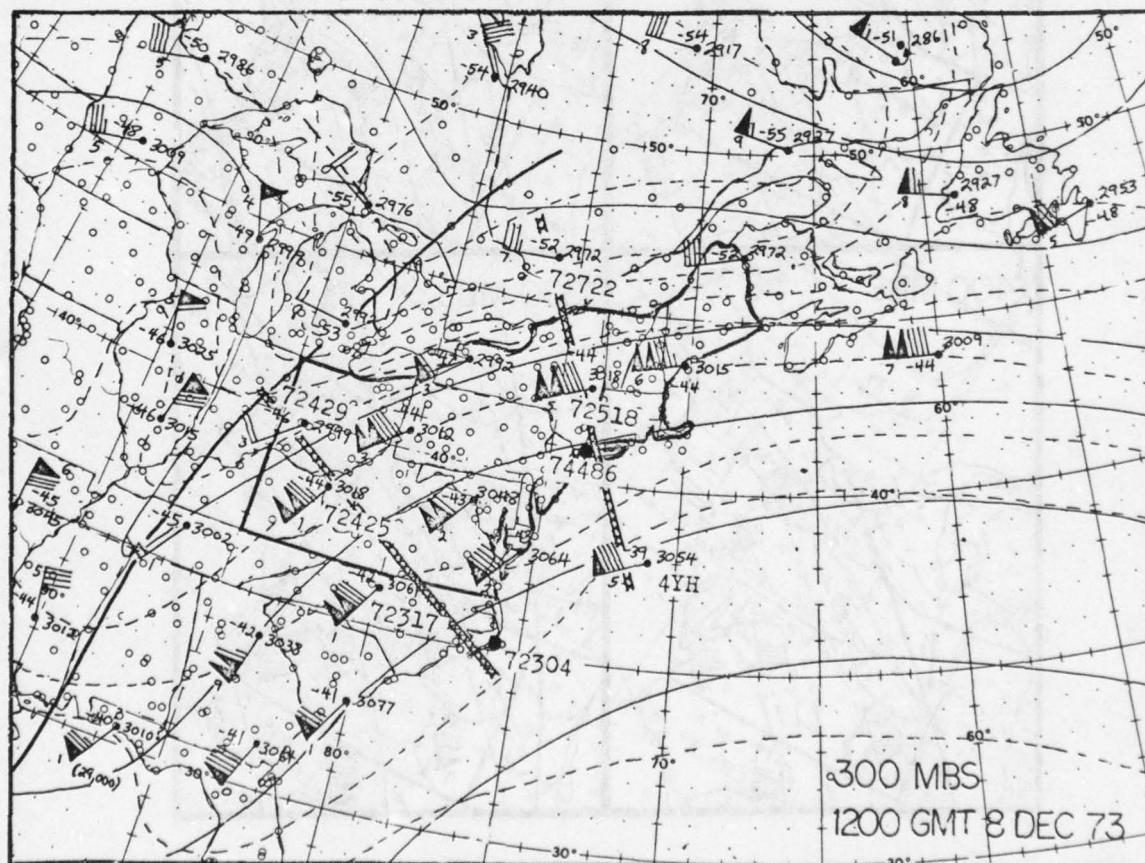


Figure 74. 300-mb Analysis of Ridge with Turbulence Over the Northeast Associated with Warm-Air Advection.

Table 3. Turbulence Reports Over the Northeast from 0900 GMT
8 December 1973 to 0300 GMT 9 December 1973.

ALTITUDE RANGE (feet)	TURBULENCE INTENSITIES					
	NONE	LIGHT	LIGHT- MODERATE	MODERATE	MODERATE- SEVERE	SEVERE
15,000-30,000	1	2	9	17	3	4
Above 30,000	1	4	2	--	--	--



Figure 75. Composite of Horizontal Temperature Gradient Over
the Northeast.

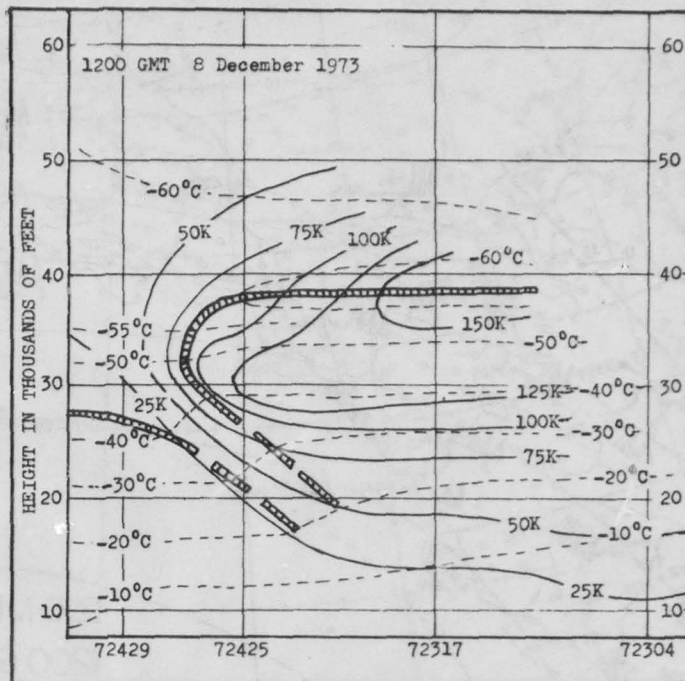


Figure 76. Cross Section of Polar Jet Stream in Warm-Air Advection (Dayton, OH to Cape Hatteras, NC).

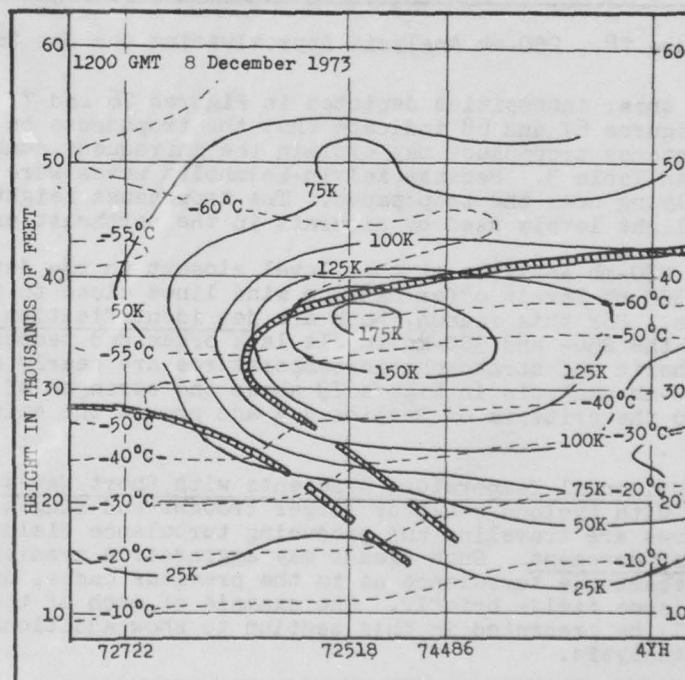


Figure 77. Cross Section of Polar Jet Stream in Warm-Air Advection (Maniwaki, Quebec to Ocean Station Vessel Hotel).

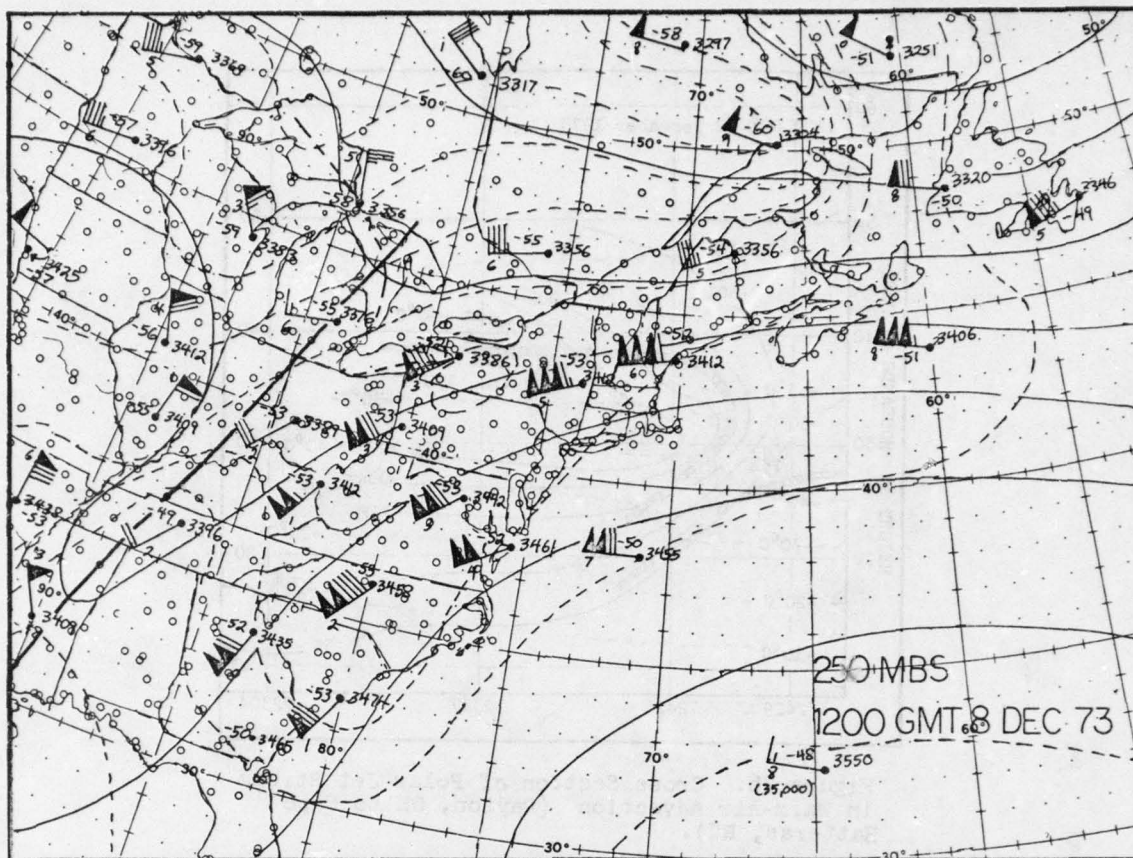


Figure 78. 250-mb Analysis Approximating the Jet Core.

The wind speed shear intensities depicted in Figures 76 and 77 and the transverse banding shown in Figures 67 and 68 indicate that the tropopause on 8 December 1973 was intense. An intense tropopause may explain the infrequent number of flights above 30,000 feet in Table 3. Because Kelvin-Helmholtz waves were visible, pilots may have avoided flying near the tropopause. The tropopause height was also higher than most of the flight levels used by aircraft in the northeast area.

Figure 78 is a 250-mb analysis at that level closest to the jet-streak core. Both the 250- and 300-mb levels offer maximum wind lines close to the jet axis in macroscale analyses. For this reason, both are jet identification levels. Note, however, that both the 250- and 300-mb levels lack organized temperature fields because both tropospheric and stratospheric temperatures are nearly equal. On the other hand, the 200-mb analysis in Figure 79 shows the strength of the ridge and trough according to the criteria of Section 4.3 and proves the existence of a strong polar jet streak.

7.4. Increasing Horizontal Temperature Gradients with Short Waves. Sections 7.2 and 7.3 have dealt with cyclone scale or larger troughs and ridges. Throughout such features, short waves are traveling and producing turbulence fields sharing their small scope and fast movement. Such fields may aggravate a gradient of already high potential into forecastable turbulence as in the previous cases, or they can augment larger-scale turbulence fields briefly. One example of each of the cold and warm advection cases will be presented in this section to show additional features best seen under closer analysis.

Figures 80 through 82 show a very interesting cold-air advection case that occurred over northern Wisconsin and Michigan during a military aircraft refueling exercise. Table 4 shows that most aircraft experienced moderate turbulence and analysis shows

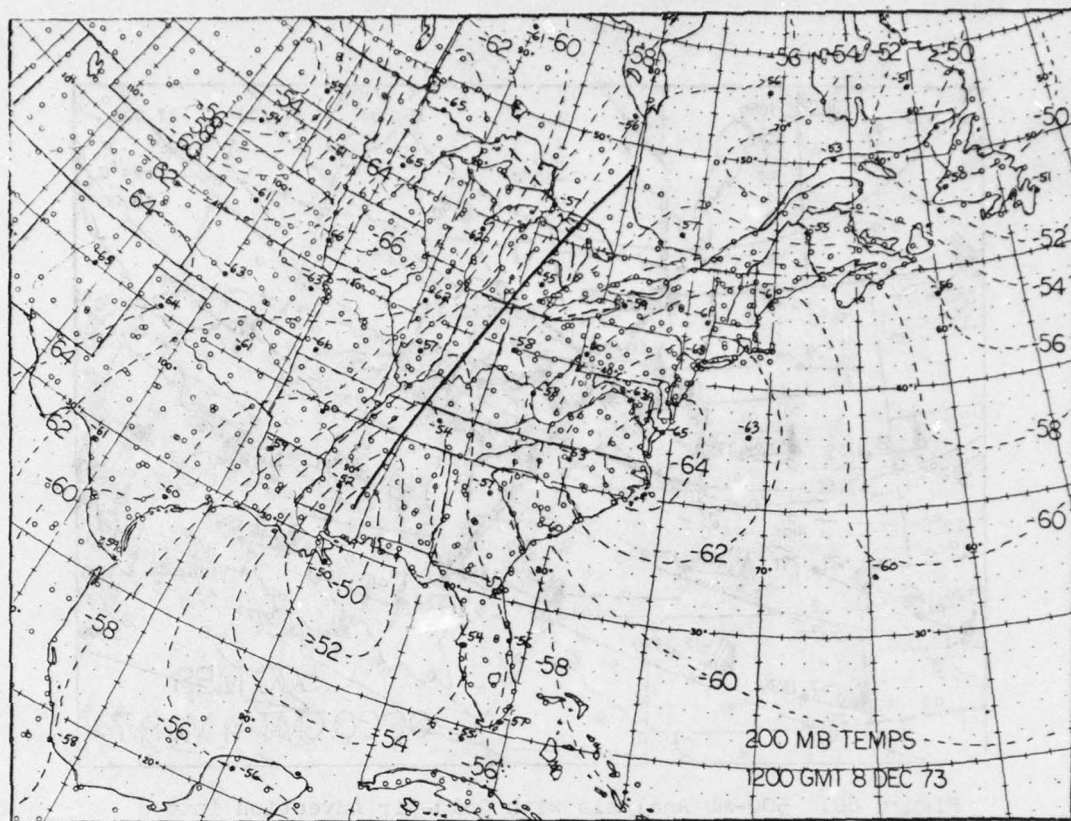


Figure 79. 200-mb Thermal Field.

that this occurred not only in an increasing horizontal temperature gradient (Figure 80) and under the jet-stream maximum wind line (Figure 81), but also within the jet front where turbulence potential is highest (Figure 82). This example constitutes powerful evidence that cold advection in the middle tropopause is a common and reliable source of turbulence in jet flow.

Table 4. Reports of Turbulence Within a Jet Front. "Light-to-moderate" turbulence is reported as "light" and "moderate-to-severe" as "moderate." Military aircraft refueled flying westward from 3 March, 2035 GMT to 4 March, 0400 GMT at levels from 21,000 to 19,000 feet. "Other" reports are various civil and private aircraft of unknown type.

AIRCRAFT TYPE	TURBULENCE REPORTS				% REPORTS MODERATE-SEVERE
	NONE	LIGHT	MODERATE	SEVERE	
B-52	7	7	11	0	44
KC-135	1	1	8	0	80
Other	0	6	1	0	--

Figures 83 through 86 show the warm short-wave ridge counterpart, one usually incapable of sustaining persistent forecastable turbulence fields unless jet flow is strong, that is, unless the jet front is very well-developed with strong vertical speed shearing. The reports in Figure 85 show intermittently significant turbulence in the ridge with enough moderate or greater reports to justify a forecast. Note that a following short-wave trough also has accumulated reports upwind. The 500-mb analysis (Figure 83) shows no clear indication of a decreasing temperature gradient (though one must exist), typical of this relatively subtle mechanism. The 300-mb analysis following shows very strong jet flow, however, so that the cross section

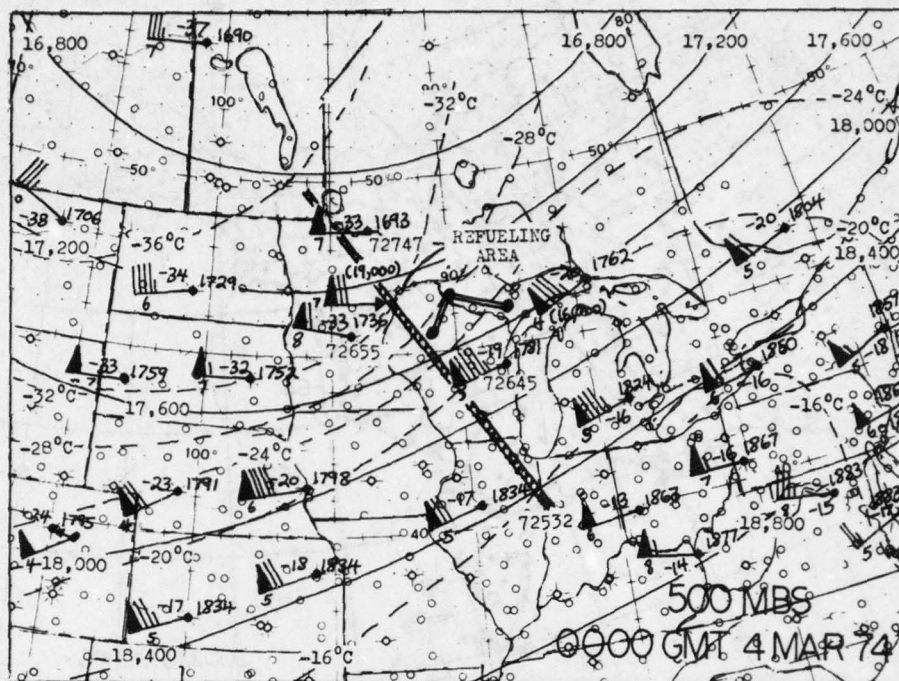


Figure 80. 500-mb Analysis with Cold-Air Advection into a Refueling Area.

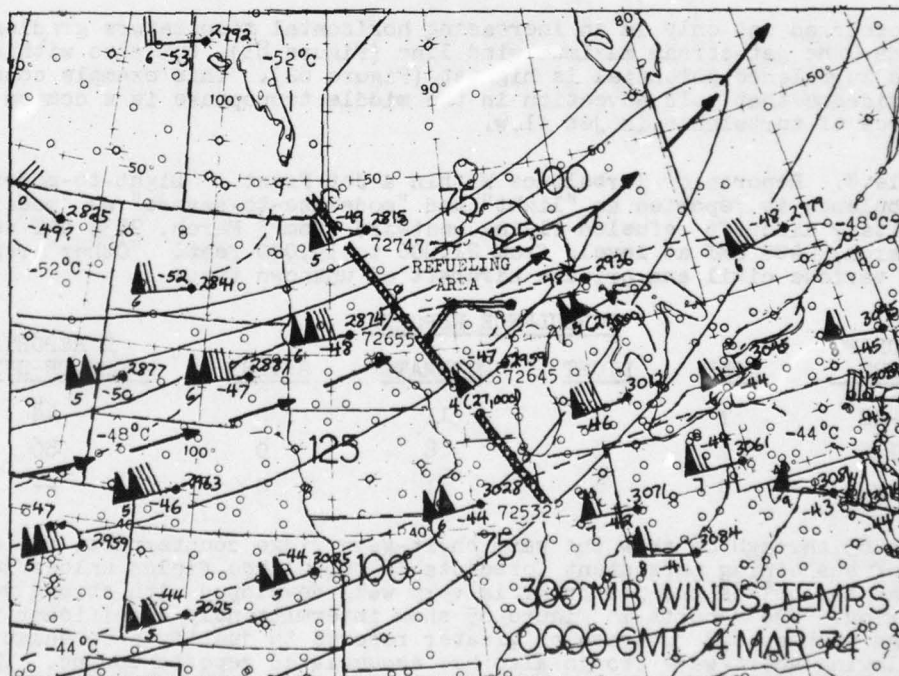


Figure 81. 300-mb Analysis Showing Maximum Wind Line Over Refueling Area.

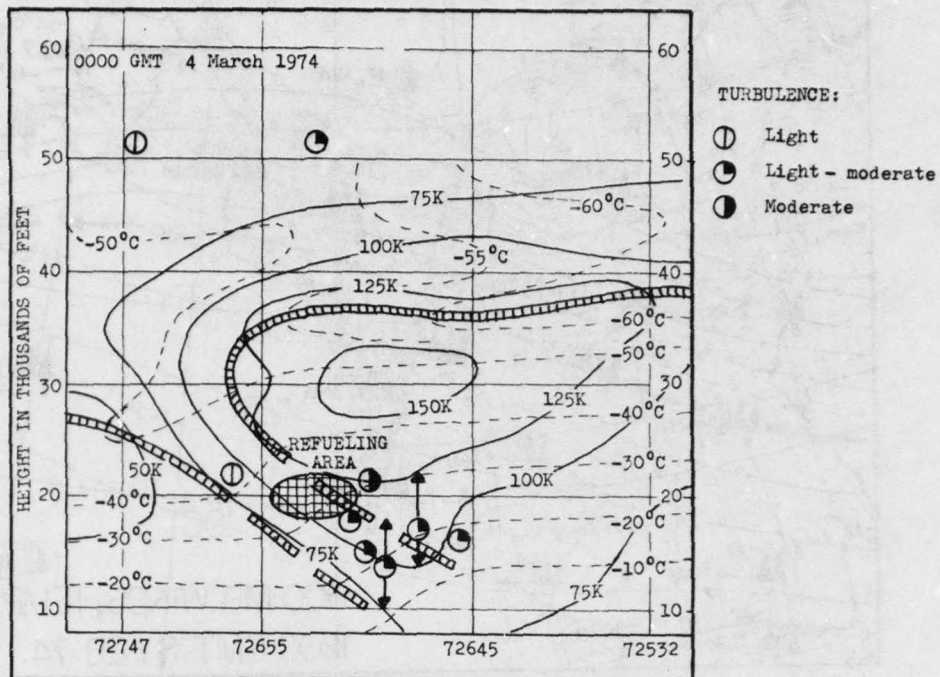


Figure 82. Cross Section Through Refueling Area.

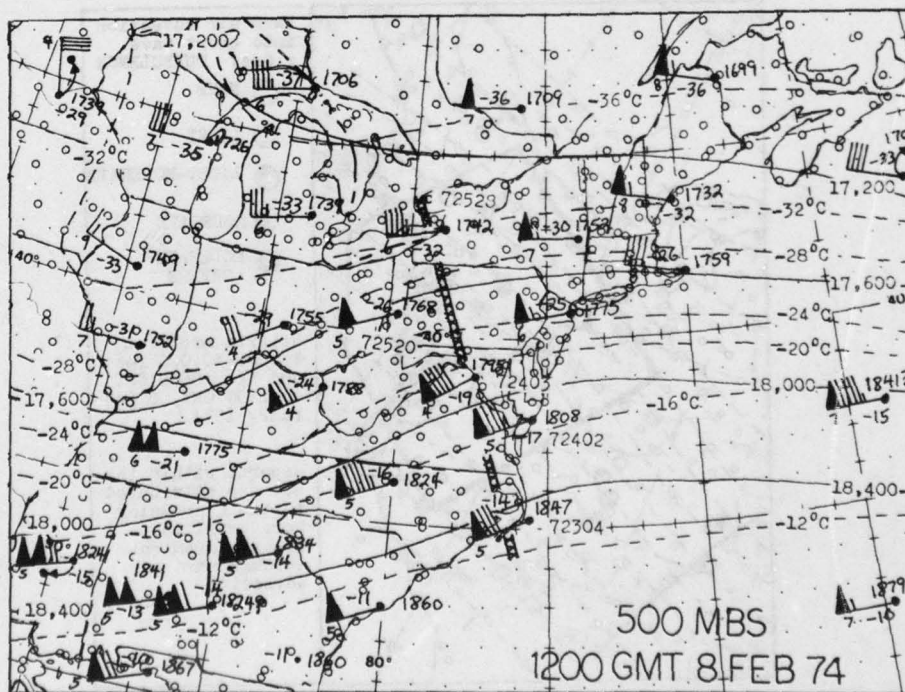


Figure 83. 500-mb Analysis of Warm-Air Advection with a Short-Wave Ridge.

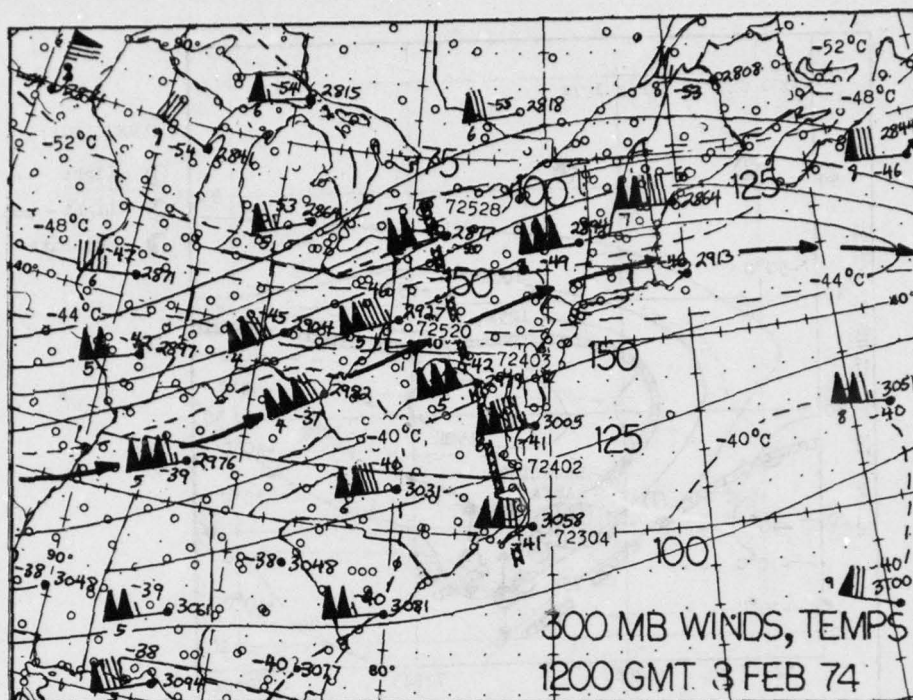


Figure 84. 300-mb Maximum Wind Analysis.

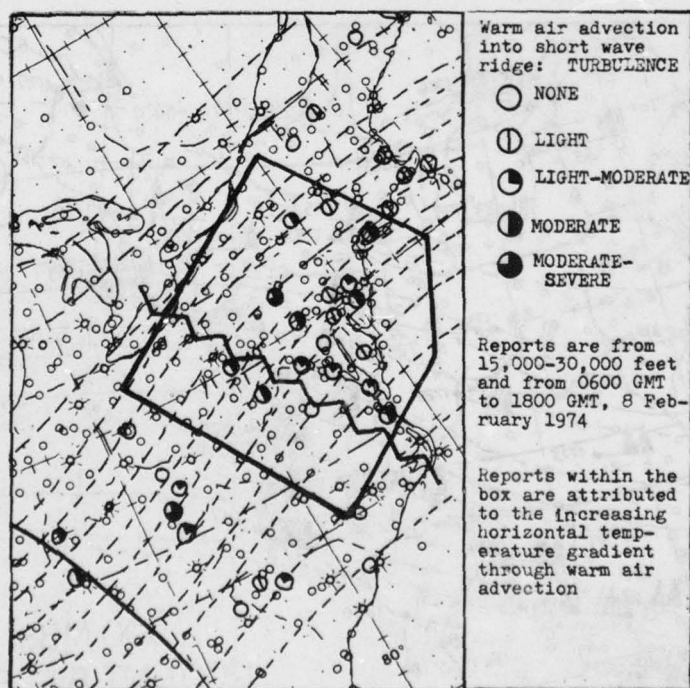


Figure 85. Reports of Turbulence in a Short-Wave Ridge.

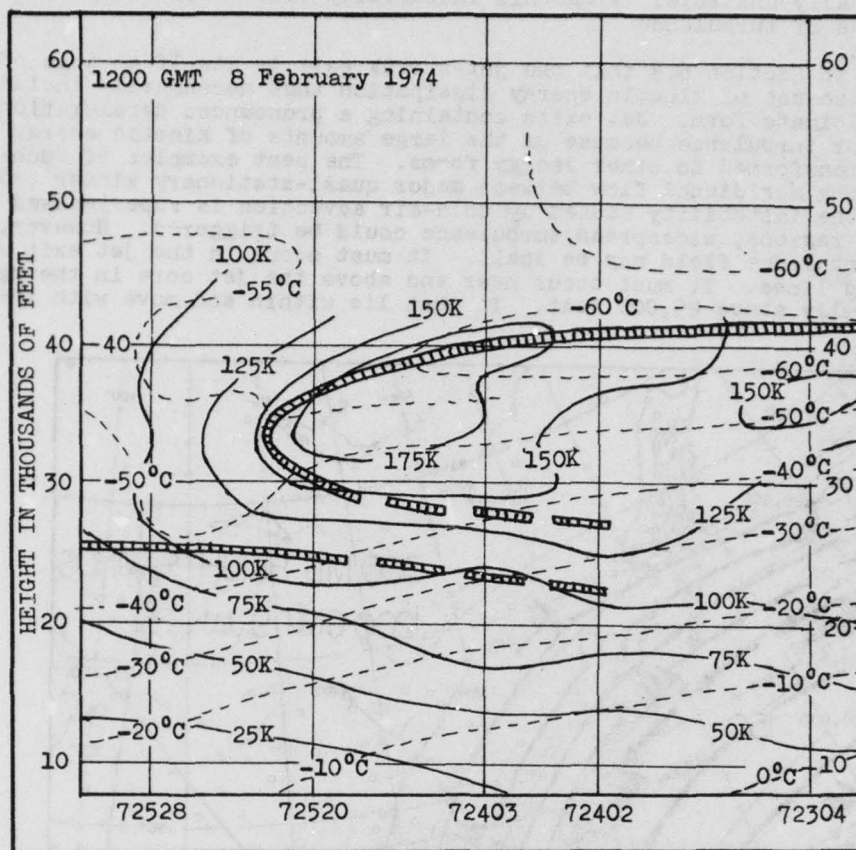


Figure 86. Cross Section Through Short-Wave Ridge.

(Figure 86) shows a well-developed jet front. This cross section lies almost over the ridge line so reports from 15,000 to 30,000 feet lie within or reasonably near the jet front. In general, forecasts are seldom made of fields generated by short-wave ridges.

7.5. Decreasing Stability in the Vicinity of the Jet Exit. All of the previously discussed turbulence patterns have been caused by thermal advections which increase horizontal temperature gradients, thereby increasing wind flow according to the thermal wind relationship. There is another important turbulence generating process that appears to apply thermal advections in a different fashion to a portion of the jet stream relatively unaffected by the other processes - the jet exit region. Furthermore, it acts above the jet-stream core near the tropopause, thereby invalidating the thermal wind relationship (see Section 7.2). These unique conditions make the process readily distinguishable from all others.

The rationale for jet exit turbulence has been provided again by Sorenson [45] in his second work on turbulent synoptic features, calling the phenomenon "cold cell CAT" after the upper-level cold pool of air over mid-latitude warm-core ridges that appears to trigger instability. The upper portions of the jet-streak exit lie between the relatively warm air of the trough downstream and the cold pool just upstream, such as over Nevada at 200 mb in Figure 89. Most major jet streaks lie within slowly-moving long wave or cyclone scale ridges, so neither the cold pool nor the jet exit are likely to move much in relation to each other unless vigorous traveling short waves are superimposed on the flow which bring cold air with them. In such cases, cold air will be advected near the tropopause over the jet exit as the traveling ridges move in, decreasing the vertical temperature lapse rate and making the atmos-

phere hydrostatically unstable. From this instability come vertical motions and an unspecified degree of turbulence.

It was shown in Section 6.4 that the jet-streak exit is itself an area of turbulence potential because of kinetic energy dissipation that necessarily includes turbulence in its ultimate form. Jet exits containing a pronounced deceleration have high potential for turbulence because of the large amounts of kinetic energy which can be rapidly transformed to other energy forms. The best examples of such jet exits lie in strong meridional flow between major quasi-stationary winter troughs and ridges. If the instability caused by cold-air advection is superimposed on these already unstable regions, widespread turbulence could be triggered. However, the extent of the turbulence field may be small. It must occur in the jet exit and thus near maximum wind lines. It must occur near and above the jet core in the upper troposphere, usually above 25,000 feet. It must lie within and move with the cold-

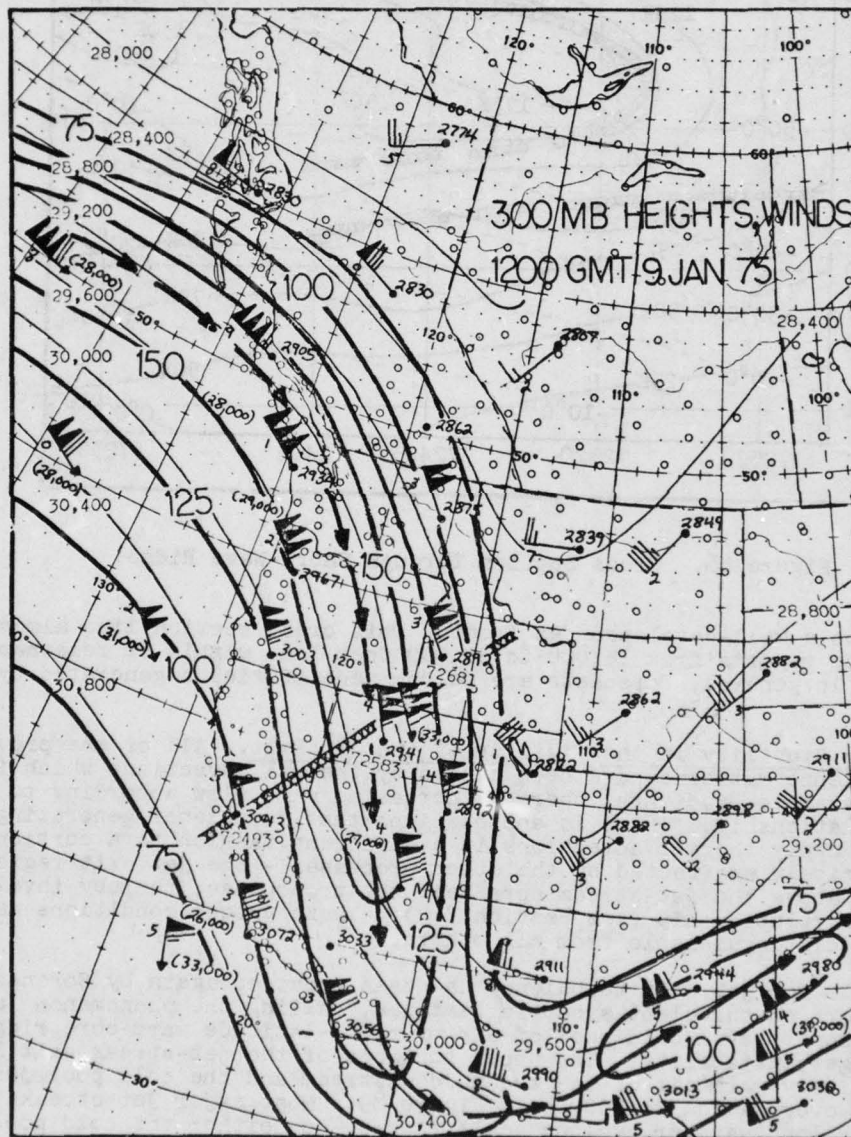


Figure 87. 300-mb Analysis of Jet-Exit Region.

air advection, but since the traveling wave damps in the major trough, turbulence will not likely move out of the back side of any trough in this form.

Before discussing a case of this "cold cell CAT," the general Northern Hemisphere environment for this phenomenon will be explored using some of the analyses in Chapter 5. First, the 300-mb analysis (Figure 34) shows a typical winter pattern with weakly organized flow over Central Asia, multiple ridges over the North Pacific, one broad ridge over the Atlantic, and pronounced ridging over Western North America and Europe. Jet-stream exits behind major troughs are of interest here.

Figure 36 shows the upper tropospheric cold pools over all warm-core ridges with 300-mb maximum wind lines added. Of special interest are five ridges, two in the Western Pacific, the Western North American ridge, the broad Central Atlantic ridge, and the European blocking high, all having 200-mb temperatures colder than -60°C .

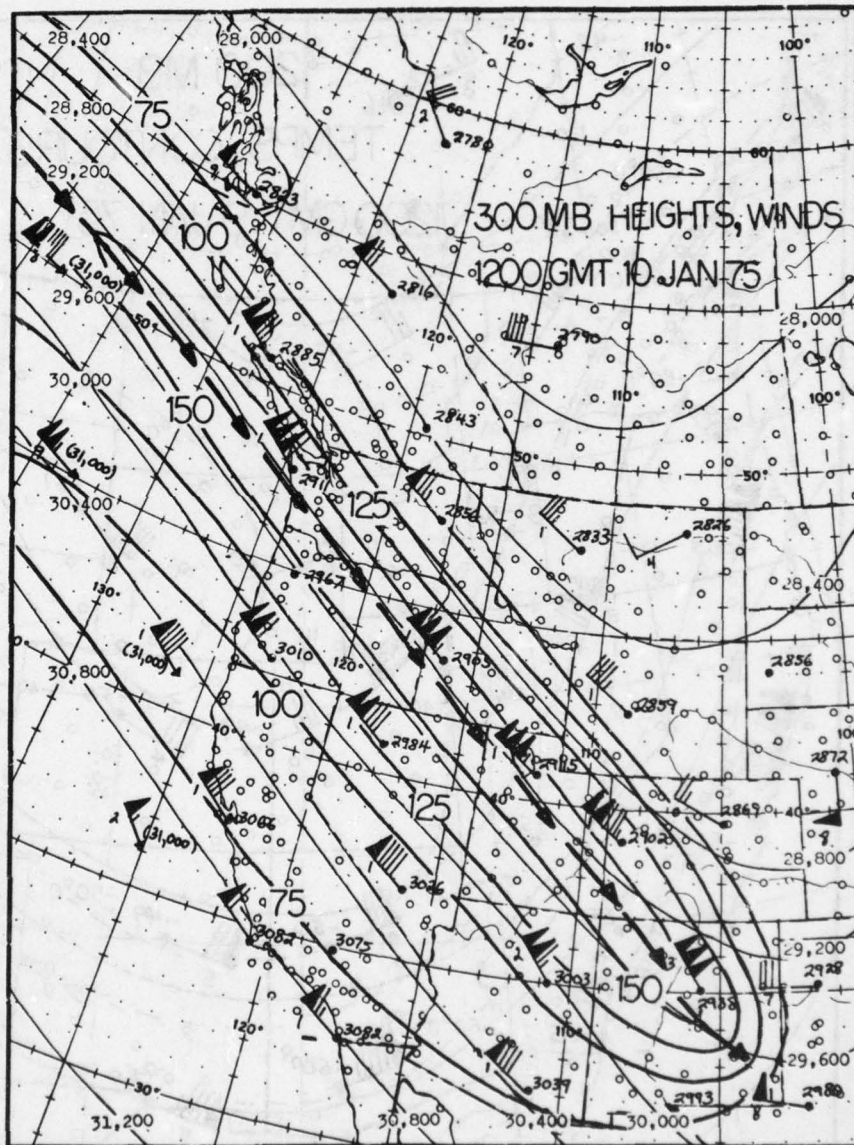


Figure 88. 300-mb Analysis of Jet Exit 24 Hours Later.

Maximum wind lines cut through the larger amplitude ridges, invalidating the thermal wind relationship by being almost normal to thermal gradients. If the cold pools are moving into the jet exits, turbulence potential is strongly implied. The meridional flow patterns suggest that cold-air advections may be substantial contributors to turbulence because jet flow may be variable in strength in both space and time in this unstable situation. On the other hand, broad ridges, such as that over the Atlantic, tend to be associated with strong jet flow and short waves are not prominent. Thus, temperature advections are relatively ineffective in comparison to the massive decelerating flow at the jet exit. This enhances the desirability for meridional flow before cold-air advections trigger turbulence fields.

In summarizing the favorable environments for "cold cell CAT," it should be noted that the major ridges and jet exits are partially linked to geography. Ridging is typical along the west coasts of both North America and Europe with jet exits

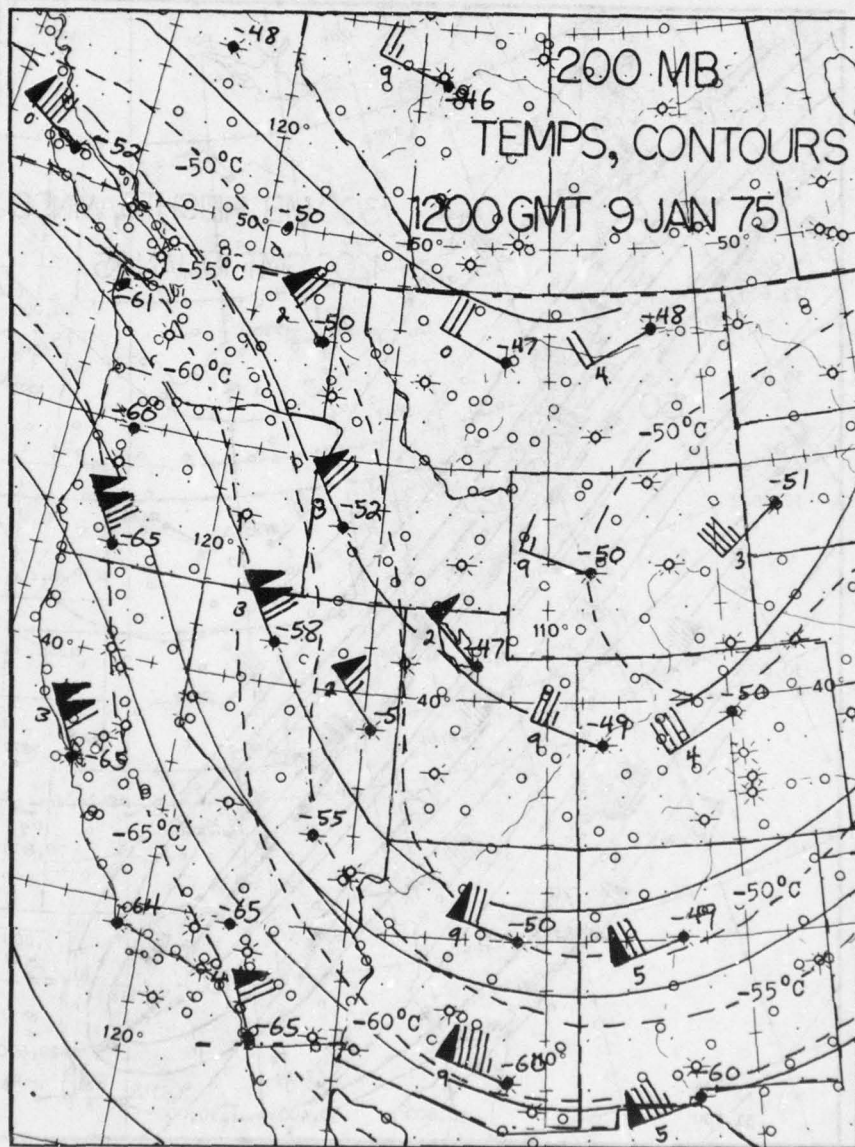


Figure 39. 200-mb Analysis of Jet-Exit Region.

often just inland. Mid-oceanic troughs are also common, so exits may be significant in the North Pacific near Hawaii or Midway, and again in the Central Atlantic near the Azores. Particularly noteworthy are intense upper-level lows that may develop near Hawaii or the Azores. On the other hand, turbulence fields are less commonly observed on the back side of the Aleutian and Icelandic Troughs, covering areas near Japan and the Eastern United States, respectively. They tend to be too broad and the flow too zonal.

The series of figures, Figures 87 through 92, detail a case of "cold cell CAT." Figures 87 and 88 show 300-mb analyses 24 hours apart in which a strong traveling short-wave ridge pushes into the Far West from the Pacific Northwest to Texas. A major ridge lies off the coast, while the trough is in the Midwest. Figure 89 shows cold-air advection at 200 mb at the time of the first 300-mb analysis. Both the cold-air advection and jet exit overlies Nevada at that time and these areas may be

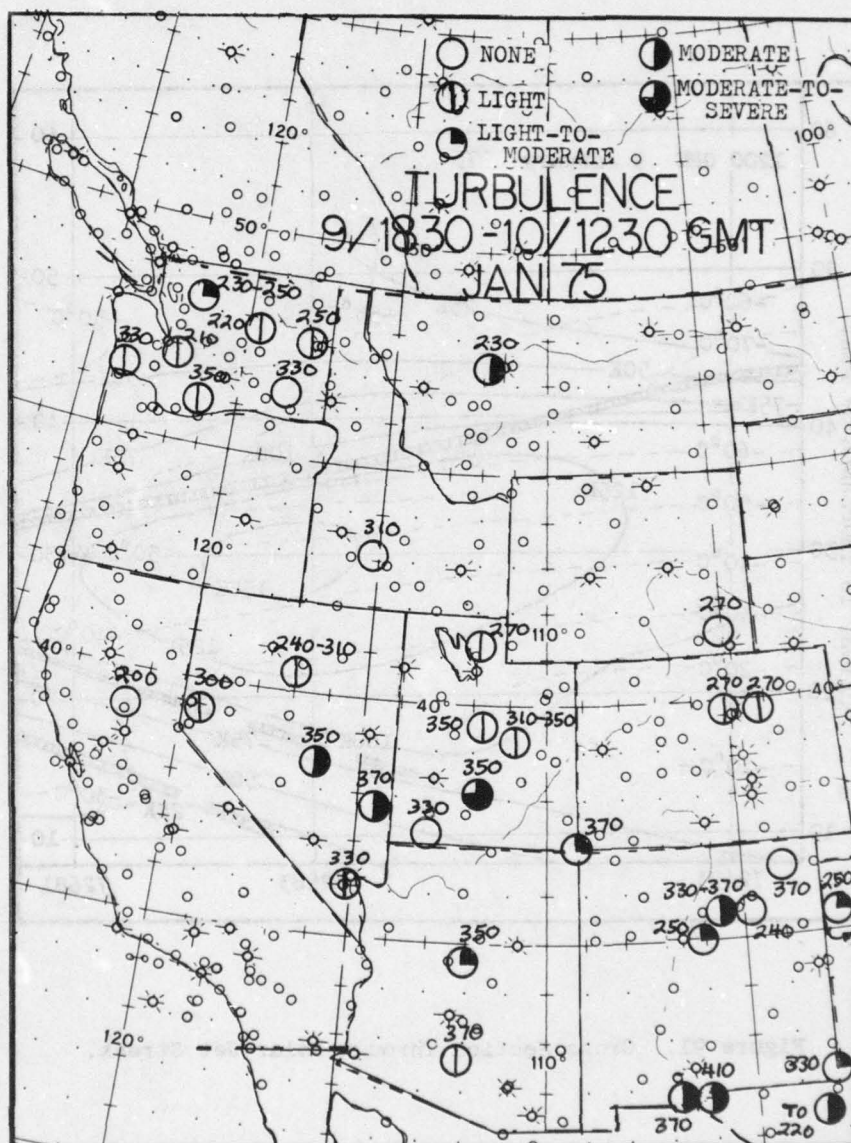


Figure 90. Turbulence Reports Near the Tropopause and Jet Exit.

expected to move through New Mexico in 24 hours, judging from Figure 88. Figure 90 verifies this with later turbulence reports ending at the 24-hour period. The most important reports appear to have occurred where the jet exit and advection must have traveled.

The intensity of the jet exit and its need to dissipate kinetic energy through methods involving turbulence can be inferred through the cross section and sounding within the jet exit in Figures 91 and 92. Substantial inversions and vertical speed shear can be found in both the jet front and tropopause. In the latter case, perhaps only cold-air advection was needed to trigger the observed turbulence.

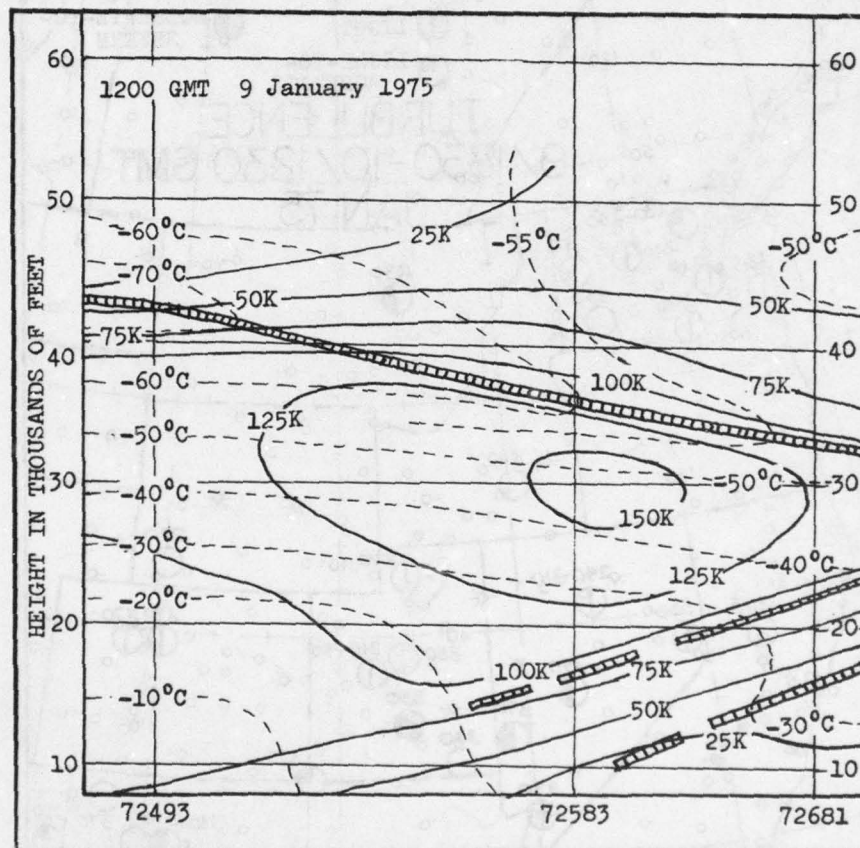


Figure 91. Cross Section Through Polar Jet Streak.

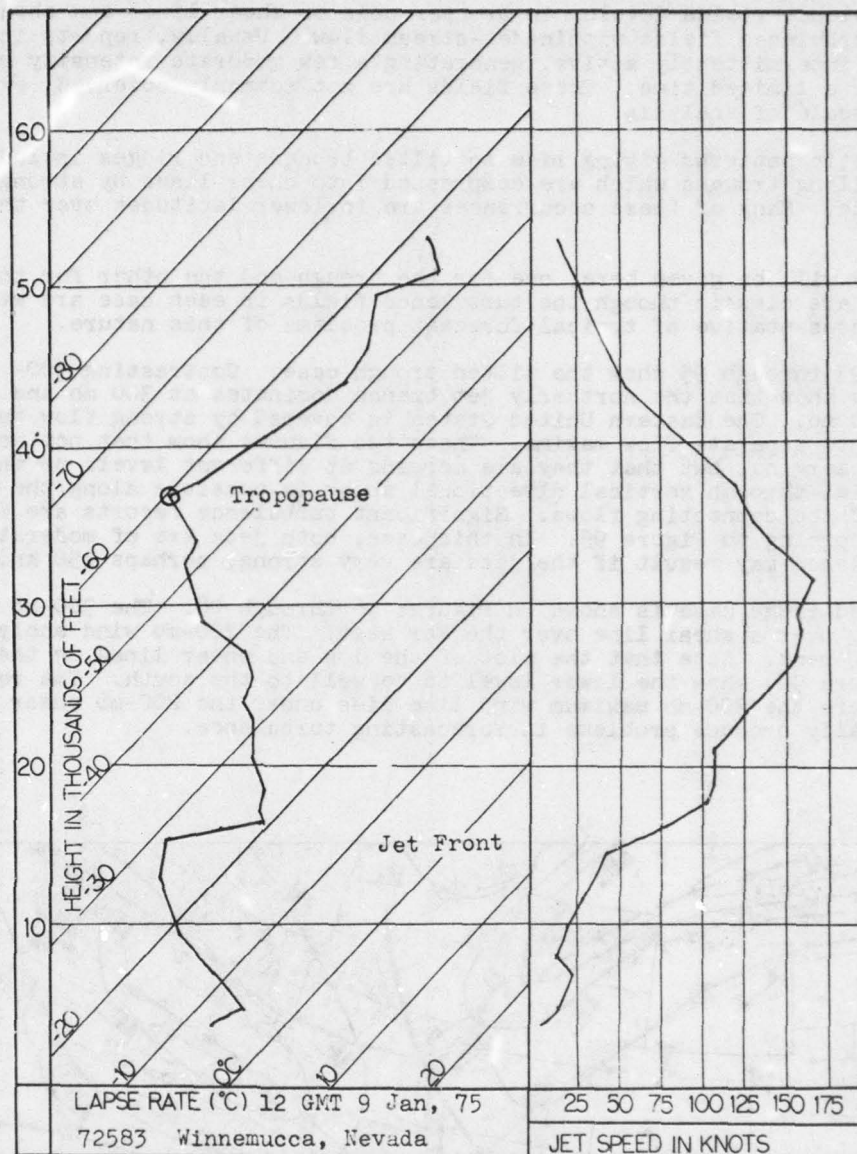


Figure 92. Sounding Through Strong Jet Streak.

7.6. Turbulence Potential Within Tilting Troughs and Ridges. Although most turbulence reports near troughs lie in jet flow, sizeable turbulence fields may be uncovered elsewhere, particularly in cols and shear zones. These fields may develop from several causes and Sorenson [44] ascribed them mainly to synoptic features that were tilted in the vertical, resulting in vertical directional shear that can be shown to increase turbulence potential. The following are several characteristics of these phenomena:

a. Tilted troughs are those which usually move faster at lower levels, so that wind speeds and directions may change greatly in the vertical. It is possible that opposing jets might partially merge or overlap. Tilted ridges also may move faster at lower levels so that similar speed and directional changes may occur.

b. Turbulence fields develop in or near cols or shear lines and should be distinct from turbulence fields within jet-stream flow. Usually, reports indicate that the field is intermittently active, generating a few moderate intensity reports, and then only for a limited time. These fields are not commonly observed, except in the hemispheric scale of analysis.

c. Synoptic patterns giving rise to tilted troughs and ridges include cut-off lows and trailing troughs which are compressed into shear lines by strong ridging on the north side. Many of these occurrences are in lower latitudes over the data-poor oceans.

Two cases will be given here, one for the trough and the other for the ridge. The patterns are classic though the turbulence fields in each case are weak. Both cases are representative of typical forecast problems of this nature.

Figures 93 through 95 show the tilted trough case. Contrasting 300- and 200-mb wind analyses show that the northerly jet branch dominates at 300 mb and the south branch at 200 mb. The Eastern United States is covered by strong flow that cannot be divided into separate flow maxima. These two figures show that not only are the jet branches merging, but that they are merging at different levels so that turbulence potential through vertical directional shear is possible along the trough at the "fork" of the connecting flows. Significant turbulence reports are centered in this area according to Figure 95. In this case, both jets are of moderate strength. Severe turbulence may result if the jets are very strong, perhaps 150 knots in speed.

The tilted ridge case is shown in Figures 96 through 98. The 300-mb analysis shows ridging over a shear line over the Far West. The 200-mb wind analysis is markedly different. Note that the plot of the low and shear lines on the turbulence reports (Figure 98) show the lower level to be well to the south. The reports are occurring where the 300-mb maximum wind line lies under the 200-mb shear line. Such patterns usually produce problems in forecasting turbulence.

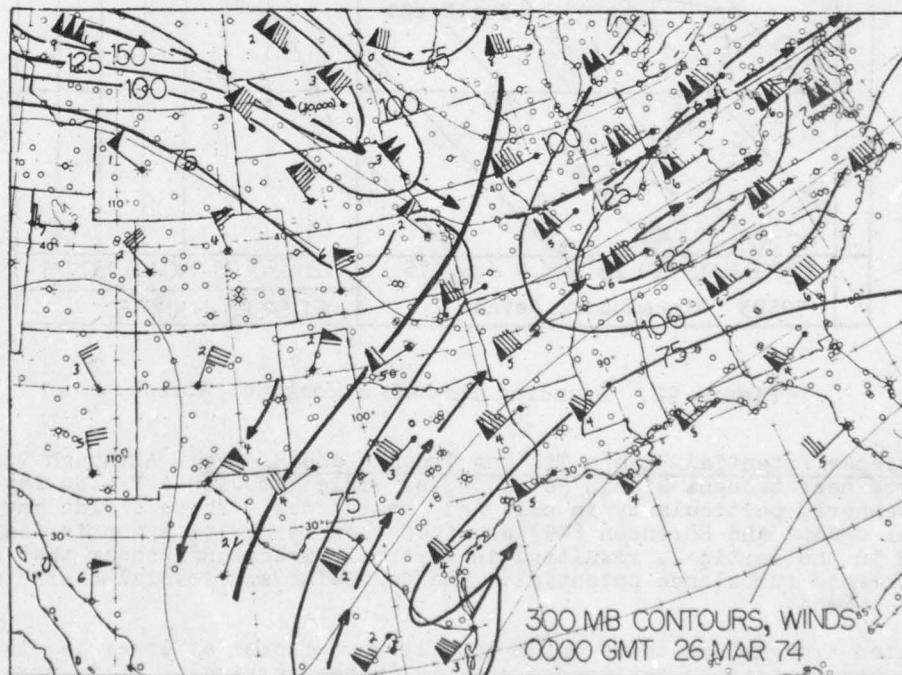


Figure 93. 300-mb Analysis of Tilted Trough Case.

AD-A062 344

AIR FORCE GLOBAL WEATHER CENTRAL OFFUTT AFB NEBR
JET-STREAM ANALYSIS AND TURBULENCE FORECASTING.(U)
MAR 76 M C HOLCOMB
AFGWC-TM-76-1

F/G 4/2

UNCLASSIFIED

2 OF 2

AD
A062344



END
DATE
FILMED

3-79

DDC

NL



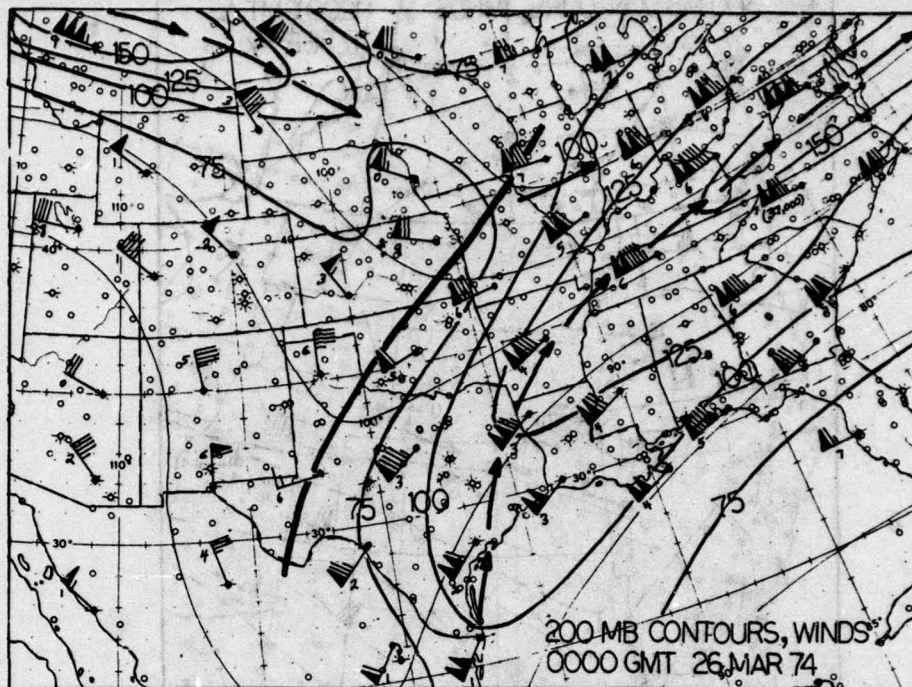


Figure 94. 200-mb Analysis of Tilted Trough Case.

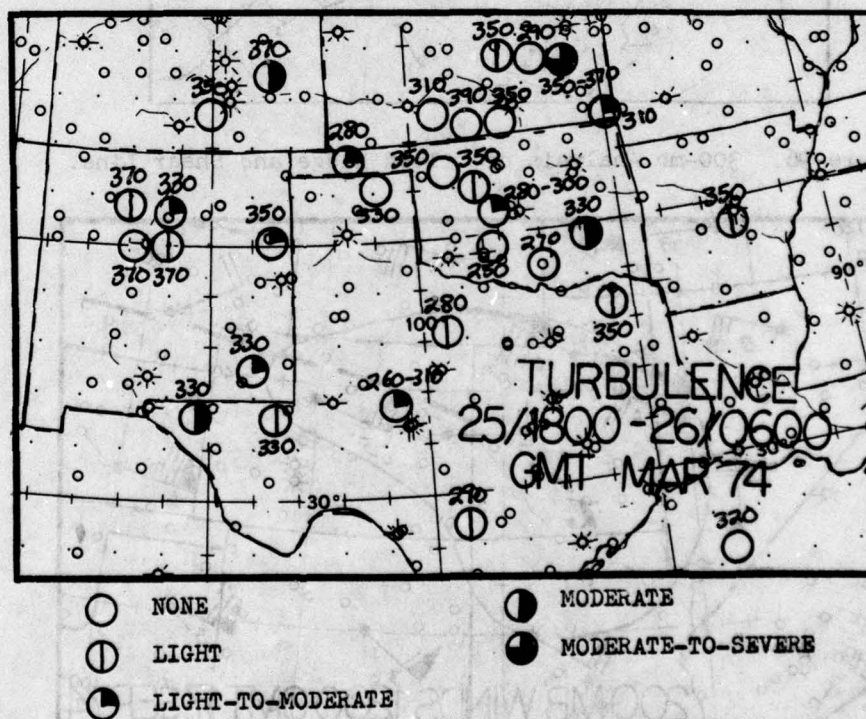


Figure 95. Turbulence Reports Above 26,000 Feet Near the Confluence of Two Jet Streams.

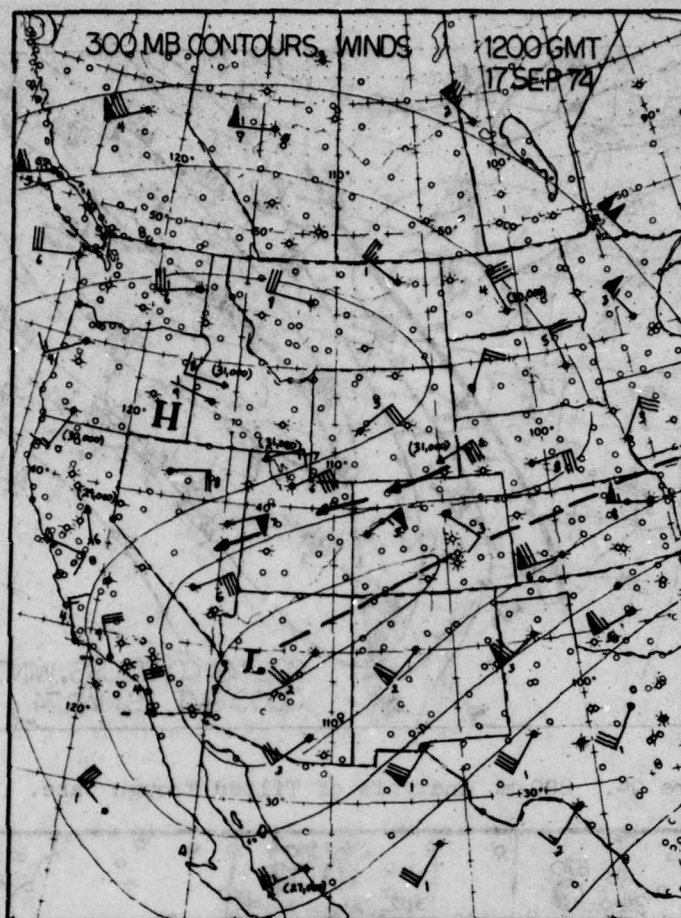


Figure 96. 300-mb Analysis of Tilted Ridge and Shear Line.

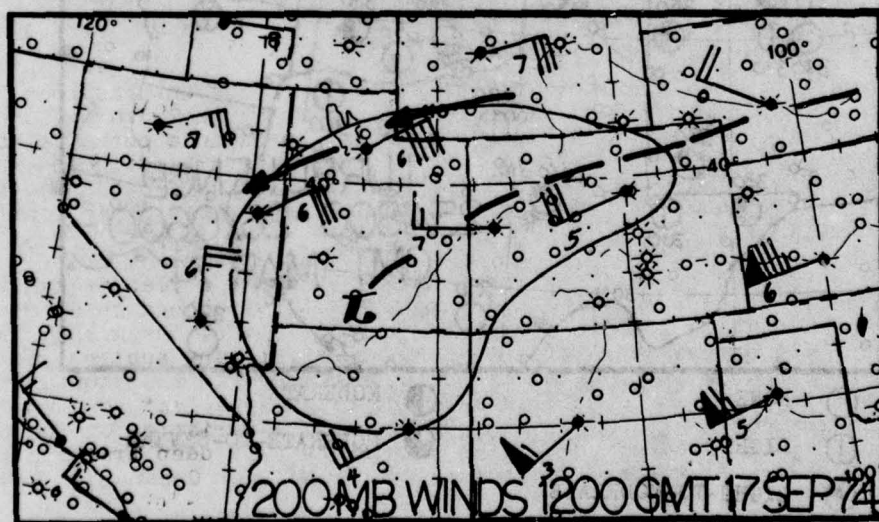


Figure 97. 200-mb Analysis of Tilted Ridge Case.

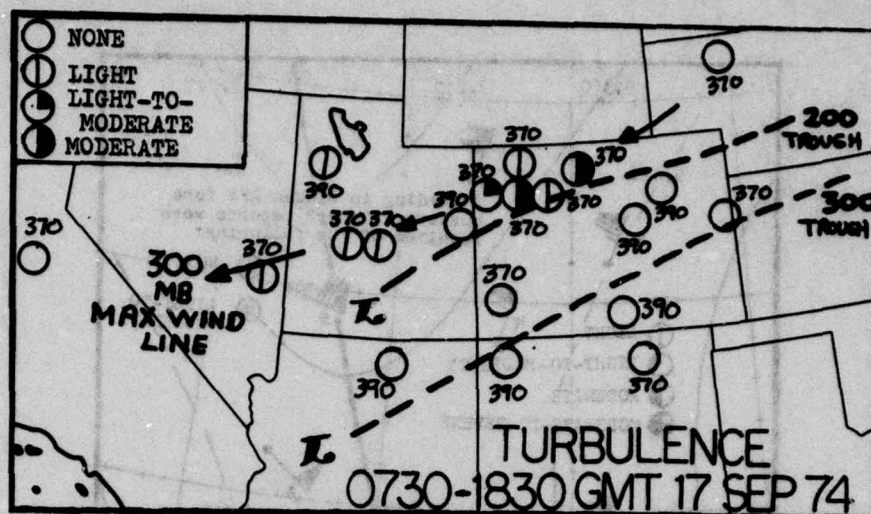


Figure 98. Turbulence Reports in a Tilted Ridge Case.

7.7. Turbulence in Polar and Subtropical Jet-Stream Interactions. It has long been surmised that the subtropical jet stream is a feature with turbulence potential comparable to the polar jet stream. However, unlike the latter, the subtropical jet stream is far less accessible to both pilot and forecaster. Its activity is intermittent, even in winter when it is most commonly observed. It is found over data-poor oceans at high altitudes. Even when subtropical flow crosses well-traveled routes reports may be lacking. Nevertheless, there are three clues as to the real effectiveness of this jet stream in producing turbulence fields:

- a. Satellite pictures (especially infrared), often show cirrus as a moderate or strong subtropical jet streak flows across a ridge. Transverse banding sometimes is present and it indicates turbulence potential because of the Kelvin-Helmholtz waves generated.
- b. The subtropical jet stream may have jet fronts and a tropopause with vertical speed shears and stability entirely as pronounced and (therefore) as effective as any in polar jet streaks of equivalent intensity. The subtropical jet front is shown in Figures 16 and 23, cross-sectional analyses which place this feature within the altitude range of 27,000 to 35,000 feet in its most active portions. The tropopause is very near 50,000 feet, too high to be of forecast interest.
- c. What few reports that are received appear to implicate interactions between the polar and subtropical jet streams. The two basic jet-stream interactions were shown in Section 4.4 (Figure 18). The area of highest turbulence potential should be over and southeast of the trough, where the two flows are closest. The vertical area would be from 27,000 to 35,000 feet in the subtropical jet front. Not only is there stability and vertical speed shear there, but also vertical directional shearing between the conflicting flows.

Two cases are discussed in this section. Figure 99 shows a deep trough in low latitudes over Hawaii and several reports of significant turbulence relayed to AFGWC from Hickam AFB forecasters. Reports are at high levels and either within or southeast of the trough. It cannot be determined just how strong the subtropical jet stream is. It may be that a major factor in this turbulence is the damping out of the trough that should occur above the mid-latitude tropopause level, one way in which vertical directional shear might occur. This pattern is a variation of the one seen in Figure 18, panel A, the case of converging jets ahead of a deep trailing trough. Such troughs and lows are occasionally observed in the Pacific Ocean near Hawaii and in the Atlantic near the Azores.

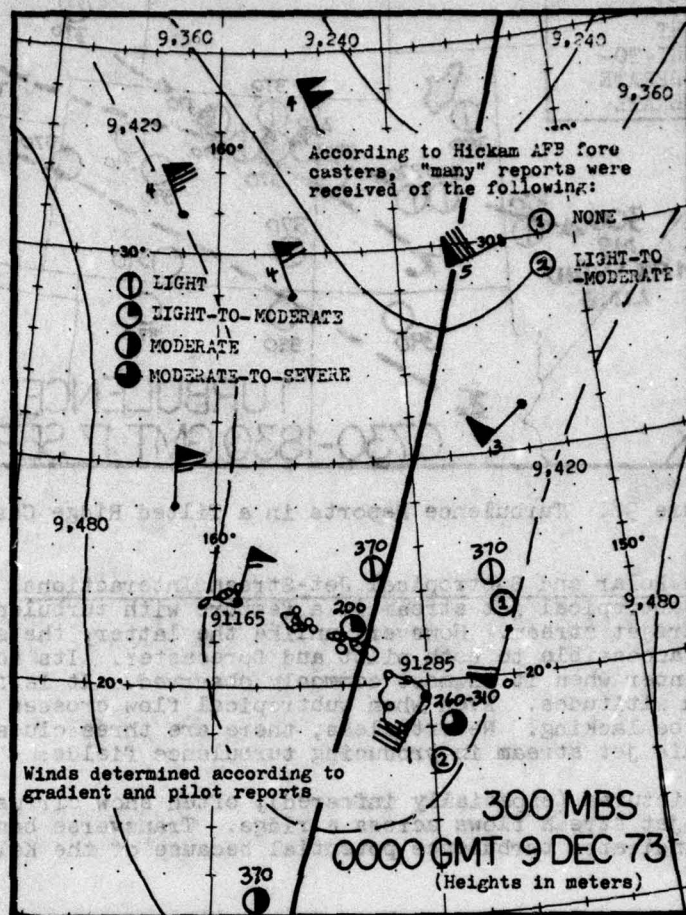


Figure 99. Turbulence Reports in an Area of Polar-Subtropical Jet Stream Intersection Near Hawaii.

Data in the analysis has been determined from aircraft reports and from gradient wind scales as part of the analysis routine of upper-air analysts at AFGWC. This is supplemented by soundings at Lihue (91165) and Hilo (91285), Hawaii.

The second case is again one of a trailing trough with possibly converging jets ahead. Figures 100 and 101 show this trough in the Caribbean north of the Dominican Republic at 33,000 feet with very significant reports. It is interesting that the aircraft reports winds much higher than nearby soundings. There is some thermal packing at 300 mb which suggests an air-mass change in the area of the turbulence. The 200-mb temperature field is warming towards the south and is well above -60°C , indicating that this flow is primarily subtropical. Strong winds are also indicated at this level south of Bermuda and northeast of Puerto Rico. It appears that the aircraft penetrated a local field of turbulence marked by a narrow band of stronger flow and a well-developed jet front, but this cannot be determined analytically from the data field.

Turbulence reports from this cause are infrequent due to factors already mentioned. When pilot reports indicate significantly strong winds, when the aforementioned synoptic features are present, and when winds between 300 and 200 mb are different in characteristics, the forecaster must investigate this area for potential turbulence.

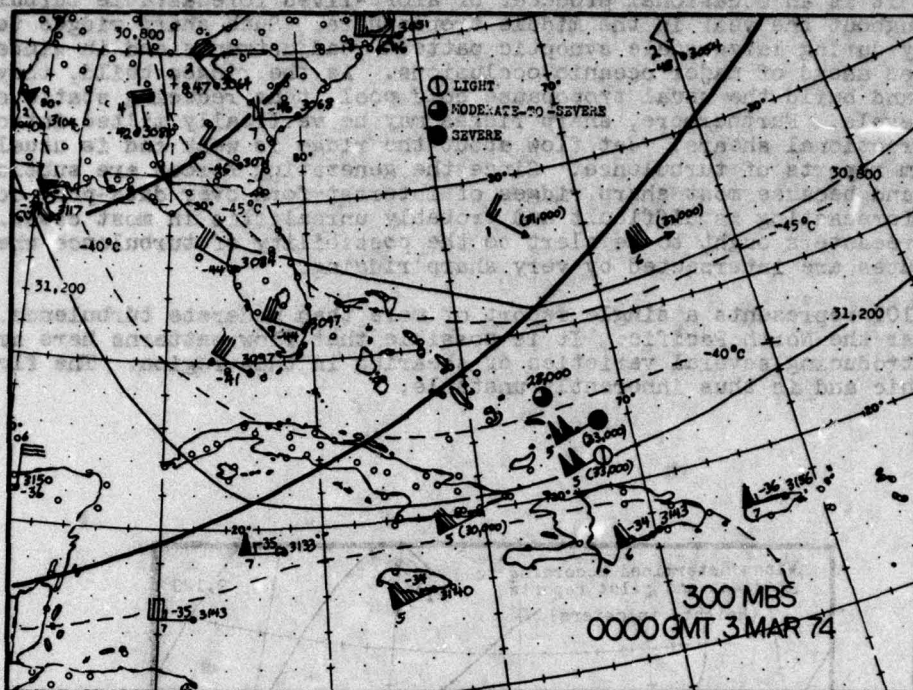


Figure 100. 300-mb Analysis of Polar-Subtropical Jet Stream Intersection in the Caribbean.

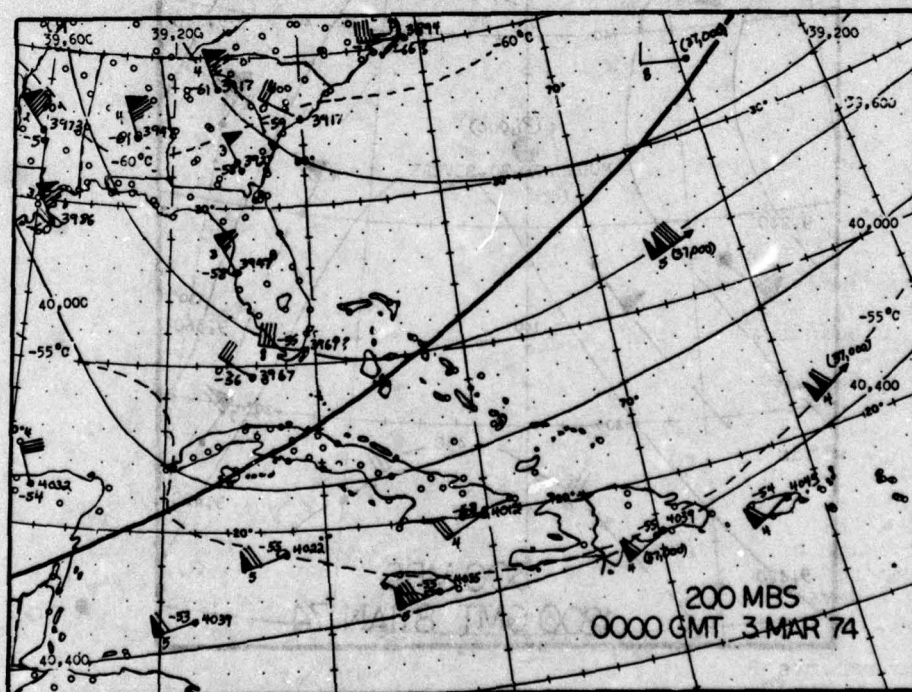


Figure 101. 200-mb Analysis of Polar-Subtropical Jet Stream Intersection in the Caribbean.

7.8. Turbulence in Sharp Anticyclonic Curvature. Sorenson [44] discussed this case, noting that it is an occasional producer of short-lived forecastable turbulence fields throughout the year in the middle troposphere. Such sharp ridges tend to form briefly during large-scale synoptic pattern readjustments and in winter are chiefly noted ahead of major oceanic occlusions. As the ridges build, they warm at low levels and build the usual tropopause cold pool, thus reducing static stability at higher levels. Furthermore, sharp ridges may be vertically tilted introducing vertical directional shears. Jet flow about the ridge is weak and is usually far removed from reports of turbulence. Since the generating forces are subtle and temporary, and because most sharp ridges of interest form over data-poor oceans, turbulence forecasting is difficult and probably unrealistic in most cases. Nevertheless, forecasters ought to be alert to the possibility of turbulence wherever aircraft routes are intersected by very sharp ridging.

Figure 102 represents a single report of more than moderate turbulence. This occurred over the North Pacific. It is possible that flow patterns here are very complex, introducing several varieties of shearing in this region. The flow cannot be geostrophic and is thus inherently unstable.

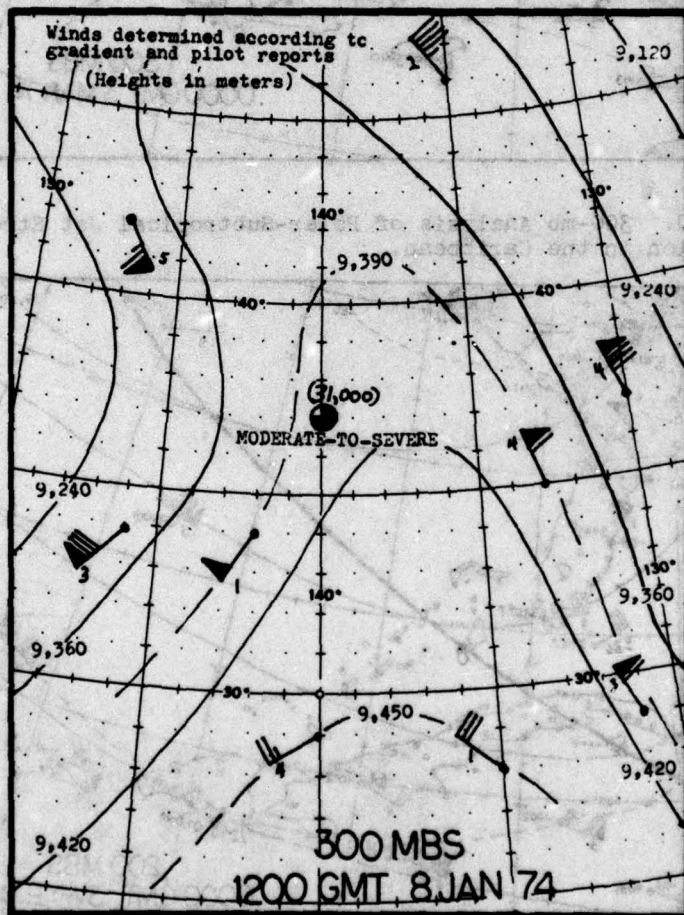
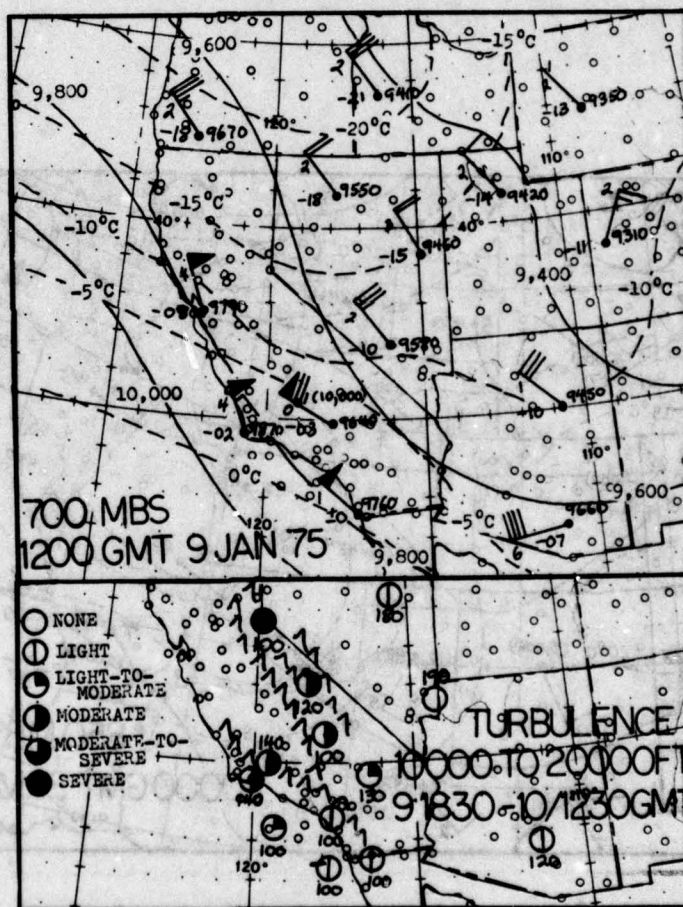


Figure 102. An Example of Turbulence in a Ridge with Sharp Anticyclonic Curvature.

7.9. Examples of Low-Level Turbulence in Possible Lee Waves. In Section 2.1 it was mentioned that forecasters must differentiate between mountain waves and those processes that merely generate low-level turbulence, particularly lee waves. At AFGWC the decision is made according to Standard Operating Procedures. This section assumes that a decision against mountain waves has been made.

a. Frontal Systems and Anticyclones. In the winter half of the year, fast-moving (and usually dry) cold fronts and migratory anticyclones may push aggressively through the more mountainous parts of the continents generating many reports of low-level turbulence. Reports suggesting lee-wave regimes, may often be received from the vicinity of mountains ranging in height from 10,000 to 20,000 feet. One area notorious for such phenomena is the Far West of the United States. Forecasters should look for flow greater than 50 knots if lee waves are anticipated. In the absence of such flow they should look for strong surface pressure gradients indicative of the potential of these migratory systems for turbulence.

b. Warm-Air Advection at Low Levels. In Section 7.5 it was shown how approaching ridges could generate turbulence at high levels in the jet exit. In the Far Western United States, the jet exit tends to overlies mountainous country which, in turn, stimulates terrain-induced turbulence. In strong northwesterly jet flow, the jet front may be as low as 15,000 feet and is a well-known source of turbulence in itself. This can be seen in the cross-section (Figure 91). In this section, Figure 103 shows low-level turbulence generated in this very case. Winds over 50 knots



c. Turbulence on the Lee of Major Ranges in the Absence of Strong Flow. Figures 104 and 105 show low-level analyses of the lee side of the Rockies during a period when several significant turbulence reports were received. Sorenson [45][46] notes a high correlation between mountain waves and the superimposition of an 850-mb warm tongue, a basic condition not met here. Instead, southerly warm flow on the lee of the Rockies with troughing indicated at 850 mb is countered by zonal flow at 700 mb. Possible aids to the development of turbulence in this case might lie in the following speculations:

-

96

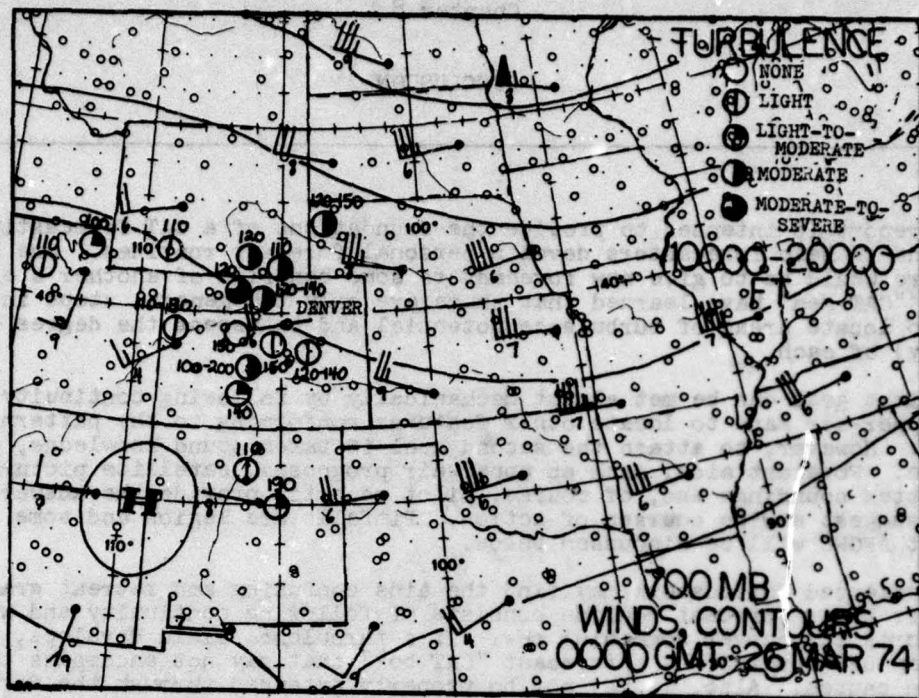


Figure 105. 700-mb Analysis of Turbulence in the Lee of the Rockies.

CONCLUSION

This report is intended to provide the foundations of a CAT forecasting training program and to help forecasters develop personal forecast routines. One last contribution here would be to give new forecasters some benefits of another's experience. Long-time "CAT Men" have learned that there are only two general steps in CAT forecasting to locate areas of turbulence potential and to assess the degree of potential (intensity) of each.

The first goal can be met almost mechanically by following continuity and consulting upper-air maps to locate other features conforming to the patterns in Chapter 7. However, to attain the second goal it takes sound knowledge, skill, and experience. Forecast aids, such as upper-air prognoses, satellite pictures, computer-plotted soundings and, of course, pilot reports, provide the answer, but they can also suggest unwise courses of action. Pitfalls are legion and some of the most popular at AFGWC will be discussed below.

Inexperienced forecasters may find the aids confusing and retreat gradually to a point where their forecast routine consists of following continuity and waiting for pilot reports to uncover something new. If a turbulence field develops, pilot reports may be "covered" by a forecast "CAT box" that may not encompass the upper-air or terrain causes. Also, it may not be properly extended through the forecast period. The point to be made is that the act of "covering" pilot reports is not forecasting, but the mere acknowledgement of what already exists. The only answer is to learn what features cause turbulence and to forecast from them, following the suggestions of the above aids.

A second fault, when pilot reports are widespread, is the tendency to "overforecast." Researchers sometimes say that CAT is less frequent than forecasters think. The conclusion is not to reduce the number of forecasts but to limit the size of the forecast areas to the extent of the triggering features. During certain widespread winter CAT outbreaks over the continental United States, CAT boxes were once produced that were 6 miles deep, 500 miles wide, and extended from the Gulf of Mexico to Canada. This amalgamation of many independent causes cannot maintain itself for long and it threatens Air Force operations over half of the country as well. The answer here is like that before, though plural: Forecast all features separately and retain their dimensions. It is not necessary to use all of the available pilot reports. Each feature has characteristic intensity and allotted life span.

A third fault is the tendency to use data-rich areas and to neglect all others. It is not unusual to find half of the Northern Hemisphere CAT boxes in the continental United States, nor is it unusual to find nothing covering high-potential features over data voids. This aversion to data voids shows up in boxes using the borders of the United States as boundaries so that boxes vanish as they leave the country. One hazard here is that analyses over data voids appear "smoothed" and the high potential features appear harmless. In this case the forecaster must discuss the matter with upper-air analysts in addition to using the usual aids. Some of these such as the weather satellite will be unaffected by the lack of upper-air data. The basic answer to these pitfalls is again to forecast the feature and not cover pilot reports.

With this report supplementing a good training program, pitfalls such as those mentioned may become unfamiliar. Also, the well-trained forecaster will find that it is actually easy to forecast many turbulent areas after gaining experience. He will then have more time to devote to other forecasting goals and can prepare his products well ahead of the deadline, the practical goal of all forecast routines.

REFERENCES AND BIBLIOGRAPHY

- [1] Atlas, D., et al.: "The Birth of 'CAT' and Microscale Turbulence," J. Atmospheric Sci., Vol. 27, No. 6, September 1970, pp. 903-913.
- [2] Batchelor, G. K.: The Theory of Homogeneous Turbulence, Cambridge University Press, 1960, 195 p.
- [3] Browning, K. A.: "Structure of the Atmosphere in the Vicinity of Large-Amplitude Kelvin-Helmholtz Billows," Quart. J. Roy. Meteorol. Soc., Vol. 97, No. 413, July 1971, pp. 283-299.
- [4] Burnett, P. T.: "Turbulence Forecasting Procedures," AFGWC Tech. Memo. 70-7, Air Force Global Weather Central, 1970, 83 p.
- [5] Clem, L. H.: "Clear-Air Turbulence from 25,000 to 45,000 Feet Over the United States," AWS TR 105-147, Air Weather Service, July 1957, 13 p.
- [6] Colson, D.: "Wave-Cloud Formation at Denver," Weatherwise, Vol. 7, No. 2, April 1954, pp. 34-35.
- [7] Defant, F.: "On Hydrodynamic Instability Caused by an Approach of Subtropical and Polarfront Jet Streams in Northern Latitudes Before the Onset of Strong Cyclogenesis," in: The Atmosphere and the Sea in Motion, Rockefeller Inst. Press, New York, 1959, pp. 305-332.
- [8] Dreyling, H.: "An Airline's Experience on Turbulence," Deutsche Lufthansa Ag., 1973, 17 p.
- [9] Dutton, J. A.: "Clear-Air Turbulence, Aviation, and Atmospheric Science," Rev. Geophys. Space Phys., Vol. 9, No. 3, August 1971, pp. 613-657.
- [10] Erickson, C. O.: "Picture of the Month: 'A Jet Stream Cirrus Shield,'" Monthly Weather Rev., Vol. 102, No. 3, March 1974, pp. 260-261.
- [11] Foltz, H. P.: "Prediction of Clear Air Turbulence," Atmospheric Sci. Paper No. 106, Dept. of Atmospheric Sci., Colorado State University, January 1967, 145 p.
- [12] George, J. J.: Weather Forecasting for Aeronautics, Academic Press, New York, 1960, 673 p.
- [13] Gossard, E. E., Richter, J. H., and Atlas, D.: "Internal Waves in the Atmosphere from High-Resolution Radar Measurements," J. Geophys. Res., Vol. 75, No. 18, June 1970, pp. 3523-3536.
- [14] Graham, R. D.: "A New Method of Computing Vorticity and Divergence," Bull. Am. Meteorol. Soc., Vol. 34, No. 2, February 1953, pp. 68-74.
- [15] Haltiner, G. J. and Martin, F. L.: Dynamical and Physical Meteorology, McGraw-Hill Book Company, Inc., New York, 1957, 470 p.
- [16] Hess, S. L.: Introduction to Theoretical Meteorology, Holt, Rinehart, and Winston, New York, 1959, 355 p.
- [17] Hoskins, B. J.: "Atmospheric Frontogenesis Models: Some Solutions," Quart. J. Roy. Meteorol. Soc., Vol. 97, No. 412, April 1971, pp. 139-153.
- [18] Hushke, R. (Ed.): Glossary of Meteorology, American Meteorological Society, Boston, 1959, 638 p.
- [19] Kao, S.-K. and Woods, H. D.: "Energy Spectra of Meso-Scale Turbulence Along and Across the Jet Stream," J. Atmospheric Sci., Vol. 21, No. 5, September 1964, pp. 513-519.
- [20] Krishnamurti, T. N.: "The Subtropical Jet Streams of Winter," J. Meteorol., Vol. 18, No. 2, April 1961, pp. 172-191.

- [21] Landsberg, H., et al.: World Maps of Climatology, Springer-Verlag, New York, 1965, 28 p.
- [22] Lass, P. and Dreyling, H.: "An Airline's Experience on Turbulence in South America," Deutsche Lufthansa Ag., 1973, 12 p.
- [23] Ludlam, F. H.: "Characteristics of Billow Clouds and Their Relation to Clear-Air Turbulence," Quart. J. Roy. Meteorol. Soc., Vol. 93, No. 398, October 1967, pp. 419-435.
- [24] Lumley, J. L. and Panofsky, H. A.: The Structure of Atmospheric Turbulence, Vol. XII of Interscience Monographs and Texts in Physics and Astronomy, Interscience Publishers, J. Wiley and Sons, New York, 1964, 239 p.
- [25] Miles, J. W. and Howard, L. N.: "Note on a Heterogeneous Shear Flow," J. Fluid Mech., Vol. 20, 1964, 331.
- [26] Mohri, K.: "Jet Streams and Upper Fronts in the General Circulation and Their Characteristics Over the Far East (Part II)," Geophys. Mag., Vol. 29, 1959, pp. 333-412.
- [27] Namias, J. and Clapp, P. F.: "Observational Studies of General Circulation Patterns," in: Compendium of Meteorology, American Meteorological Society, Boston, 1951, pp. 551-567.
- [28] Palmén, E. and Newton, C. W.: "A Study of the Mean Wind and Temperature Distributions in the Vicinity of a Polar Front in Winter," J. Meteorol., Vol. 5, No. 5, October 1948, pp. 220-226.
- [29] Palmén, E. and Newton, C. W.: Atmospheric Circulation Systems, Vol. 11, International Geophysics Series, Academic Press, New York, 1969, 603 p.
- [30] Panofsky, H. A.: "Internal Atmospheric Turbulence," Bull. Am. Meteorol. Soc., Vol. 50, No. 7, July 1969, pp. 539-543.
- [31] Panofsky, H. A., Hinkelman, J. W., and Somervall, W. L. Jr.: "An Introduction to Atmospheric Turbulence," US Navy Weather Research Facility, NAVAER 50-IP-546, May 1958.
- [32] Petterssen, S.: Weather Analysis and Forecasting, Vol. I, McGraw-Hill Book Company, Inc., New York, 1956, 428 p.
- [33] Pinus, N. Z., et al.: "Power Spectra of Turbulence in the Free Atmosphere," Tellus, Vol. 19, No. 2, 1967, pp. 206-213.
- [34] Pogosian, K. P.: "Jet Streams in the Atmosphere," Hydrometeorological Publishing House, Moscow, 1960, 188 p.
- [35] Proceedings of the Symposium at the Royal Aircraft Establishment, Farnborough, 1961: "Atmospheric Turbulence and Its Relation to Aircraft," Her Majesty's Stationary Office, London, 1963, 287 p.
- [36] Reed, R. J. and Hardy, K. R.: "A Case Study of Persistent, Intense, Clear Air Turbulence in an Upper Level Frontal Zone," J. Appl. Meteorol., Vol. 11, No. 3, April 1972, pp. 541-549.
- [37] Reed, R. J. and Sanders, F.: "An Investigation of the Development of a Mid-Troposphere Frontal Zone and Its Associated Vorticity Field," Vol. 10, No. 5, October 1953, pp. 338-349.
- [38] Riehl, H., Lea, D. A., and Hinkelman, J. W.: "Jet Streams of the Atmosphere," US Navy Weather Research Facility, NAVAER 50-IP-549, 1959.
- [39] Riehl, H.: "Jet Streams of the Atmosphere," Tech. Paper No. 32, Dept. of Atmospheric Sci., Colorado State University, May 1962, 117 p.
- [40] Reiter, E. R.: Atmospheric Transport Processes, Part 3, US Atomic Energy Commission, Office of Information Services, 1972, 212 p.

- [41] Reiter, E. R.: Jet-Stream Meteorology, University of Chicago Press, Chicago, 1963, 515 p.
- [42] Scorer, R. S.: Clouds of the World, Stackpole Books, Harrisburg, PA, 1972, 171 p.
- [43] Scorer, R. S.: Natural Aerodynamics, Pergamon Press, New York, 1958, 312 p.
- [44] Sorenson, J. E.: "Synoptic Patterns of Clear Air Turbulence," UAL Meteorol. Circ. No. 56, United Air Lines, December 21, 1964, 64 p.
- [45] Sorenson, J. E.: "Thermal Patterns and Clear Air Turbulence," UAL Meteorol. Circ. No. 62, United Air Lines, 1968, 88 p.
- [46] Sorenson, J. E.: "Mountains and Clear Air Turbulence," UAL Meteorol Circ. No. 63, 1976, 22 p.
- [47] Stanton, T. E.: "Wind Shear Turbulence," 3WWP 105-7, USAF, 3d Weather Wing, 1964.
- [48] Starr, V. P.: "Applications of Energy Principles to the General Circulation," in: Compendium of Meteorology, American Meteorological Society, Boston, 1951, pp. 568-574.
- [49] Sutcliffe, R. C.: "A Contribution to the Problem of Development," Quart. J. Roy. Meteorol. Soc., Vol. 73, Nos. 317-318, July-October 1947, pp. 370-383.
- [50] Veazey, D. R.: "A Literature Survey of Clear Air Turbulence," NASA CR-0106211, Texas A and M University Report, 1970, 101 p.
- [51] Webb, W. L.: Structure of the Stratosphere and Mesosphere, Vol. 9, International Geophysics Series, Academic Press, New York, 1966, 382 p.
- [52] Zbrozek, J. K.: "Aircraft and Atmospheric Turbulence," Proc. Symp. Roy. Acft. Estab., 1961, 1963.